

Optimization of the in-vitro model equipment for future heart-valve studies

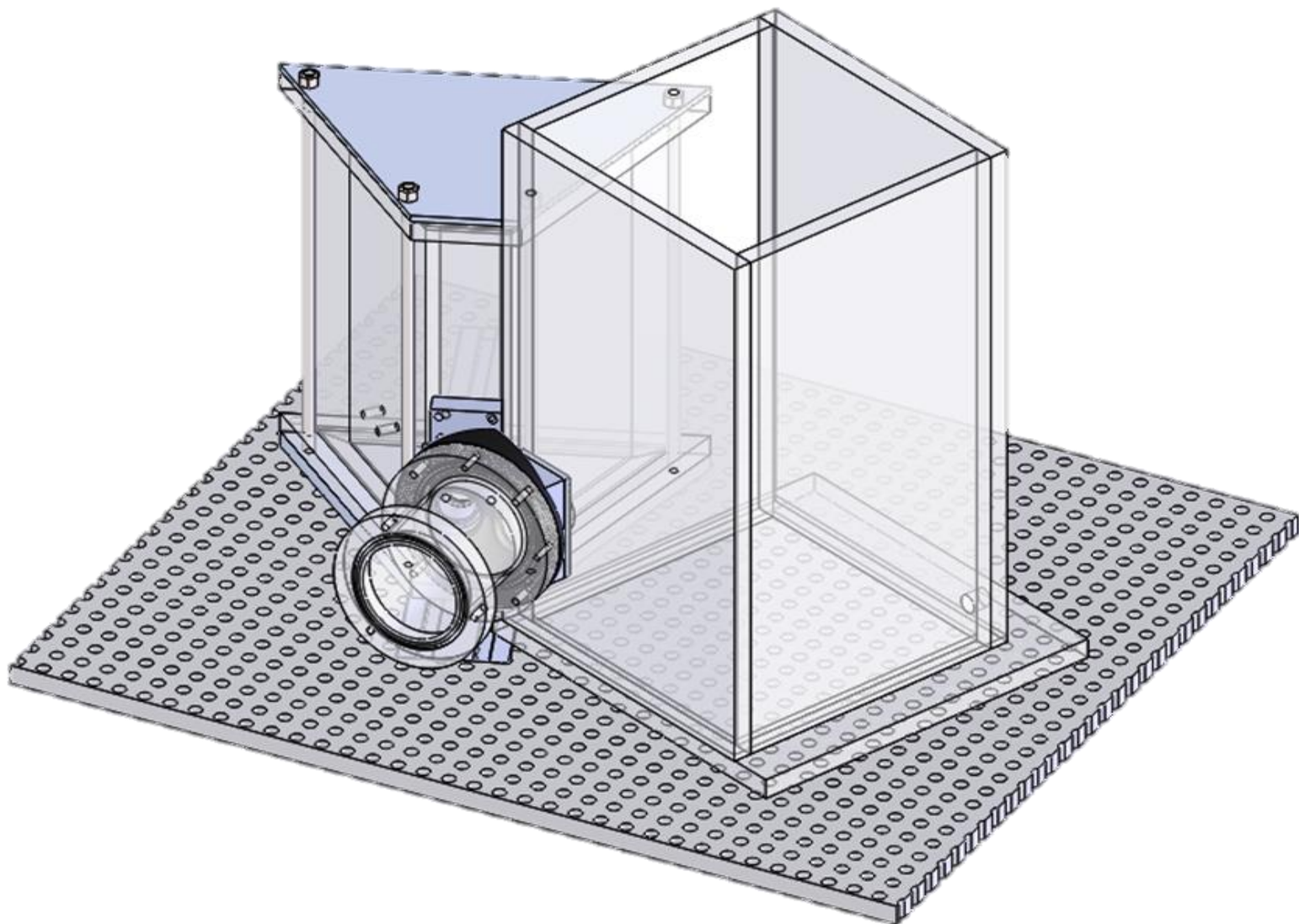
BACHELOR'S PROJECT - APPENDIX

Author: Ana Ochotorena Portales

Student number: 201301955

Spring semester 2014

Mechanical Engineering Department



Index

1- Structure of the report and briefly explanation of each section	3
2- Requirement for the new in vitro model	8
3- Images from Solid-Works (Compliance chamber and aortic root)	13
4- Real images (Compliance chamber and aortic root)	24
5- Drawings (Compliance chamber and aortic root)	27
6- Images and drawings of the mould for the silicone rings	62
7- Equipment	63
8- Fluid mechanics theory to achieve Bernoulli equation	65
9- Compliance chamber pressure calculation	67
10- Compliance chamber's wall force calculations	68
11- Compliance chamber screws force and stress theoretical calculations	71
12- Compliance chamber screw's stress simulations	79
13- Pressure drops in the entire model	89
14- Fluid passing through the new model	99
15- Silicone	100
16- List of materials	102
17- Transonic flow sensor specifications	105
18- Glue options for the wall's connection	107
19- Tests	
19.1. Signal processing	109
19.2. Comparison of results – Analysis methods	110
19.3. Tests results	115
20- Project management planning's tools. FMEA and Fishbone analysis	
20.1. FMEA	128
20.2. Ishikawa diagram or Fishbone analysis	134
21- List of figures, tables and equations	135

1- Structure of the report and briefly explanation of each section

1- Introduction

1.1. General description

A general view of the model is presented in this section

1.2. Project specification

The abstract of the project is written in this section, not only the part done MIBAC4 group but also the part done by M7BACH.

2- Background

In this section are presented different some theoretical concepts around the heart and the prosthesis valves, due to the purpose of the designed model is to analyse them

2.1. Heart

2.2. Blood

2.3. Cardiac cycle

2.4. Diseases

2.5. Overall about the kind of valves

3- Previous in-vitro model – Description

3.1. List of the parts of the current model

A list of the different parts in the previous model is presented in this section, and its explanation in the next one.

3.2. Description of each parts of the current model

3.3. Aramis

Some concepts around Aramis which may affect the design are explained in this section.

3.4. Discussion of the current in-vitro model

Here are described the problems seen by the previous groups working on the model. There is also a list of requirements added in the appendix.

4- Updates in the in-vitro model

In this section is presented a view of the changes done in each part of the model, not only the ones done by myself but also, briefly, the ones made by the other group

4.1. Compliance chamber

4.1.1. Requirements

In this section are explained briefly the requirements to be fulfilled.

4.1.2. Versions of the new compliance chamber

Here are described the final chambers designed – square and trapezoidal. There are also going to be described the previous options, explaining briefly how the process was to achieve the final result. Also are going to be shown the Solid-works graphs and some photos (In the appendix are the drawings attached)

4.1.3. Pressure calculations inside the chamber

Explained the results achieved for pressure calculations inside the chamber

4.1.4. Calculation of forces and stress in the screws

A force analysis and stress analysis is done theoretically in order to compare the results with the one done by simulations. By this calculation is possible to know if the model is an improvement or not of the previous one. This calculation has been done for the square and trapezoidal chambers

4.1.5. Forces inside the compliance chamber

Calculations to achieve the forces that the walls and therefore the connections inside the compliance chamber

4.2. Aortic root

4.2.1. Requirements

In this section are explained briefly the requirements to be fulfilled.

4.2.2 Versions of the fittings

Here is described the final fittings for the aortic roots designed. There are also going to be described the previous options, explaining briefly how the process was to achieve the final result. Also are going to be shown the Solid-works graphs and some photos (In the appendix are the drawings attached)

4.2.3. Flow meter

Here is going to be described the flow meter chosen and the requirements to be fulfilled for its usage.

4.3. Ventricle chamber and atrium chamber

Here is described the final ventricle and atrium chamber designed by the other group.

4.3.1. Ventricle chamber

4.3.2. Ventricle module

4.3.3. Atrium chamber

4.4. Analysis of the new model

Some analysis done to the new model designed

4.4.1. Pressure drops

It has been calculated different kinds of pressure drops in the model, due to different agents.

4.4.2. Fluid passing through the entire model

It has been calculated the flow passing through the model, this value should be reduced in comparison with the old model

5- Connection test

Due to problems seen in the bolt connections, some test were done in order to find an improvement of them. Reducing the time to break or avoiding it, by the usage of quickserts or helicoils

5.1. Expected results – Theoretically

The expected results are described in this section.

5.2. Test procedure

The procedure explanation and things to take into account are explained in this section.

5.3. Diverse connections – Results of the test and explanation

In this part all the test done are explained and the results achieved.

5.3.1. Connection 1 – Test 1

- Characteristic of this kind of connection
- Present the test notes and the results
- Discussion

5.3.2. Connection 2 – Test 2

- Characteristic of this kind of connection
- Present the test notes and the results
- Discussion

5.3.3. Connection 3 – Test 3

- Characteristic of this kind of connection
- Present the test notes and the results
- Discussion

5.4. Other relevant tests

Some other tests done are explained in this section, such as the water test and its non-success.

5.5. Discussion of the results

In this part is discussed which option is best one and also the cracking problem seen in the previous compliance chamber.

6- Mould for the silicone rings

A silicone ring was desired in order to connect some parts in the model minimizing the leakage between them. In this section it is going to be explained the procedure to achieve it.

6.1. Theoretical part

In this section is explained the chemistry and formulas given to explain the reason of the initial problems seen on the silicone bag construction, which are relevant also for the ring design, due to same material is used.

6.2. Mould design – SolidWorks

In this part is the description of the mould and Solid-works graphs (In the appendix are the drawings attached)

6.3. Silicone ring obtained

Explanation of the silicone ring obtained and how it works in the model

7- Materials

As some problems are seen in the previous material, was considered a change of it.

7.1. General description

In this section are explained the different materials evaluated, the previous and the new ones. PMMA, POM and PC are described.

7.2. Analysis of characteristics (in order to explain why the material was changed)

In this section many properties are analysed in order to choose the best material. The properties analysed are the ones connected with the fracture of the material, so as to the bolts are the critical point. Mechanical properties, optical properties, chemical properties, physical properties, thermal properties and price have been analysed.

7.3. Glue

As the walls are connected each other by glue, in this section is explained the chosen one and the other options evaluated.

8- Evaluation of the new model

8.1. Test procedure

In this part is explained how the analysis sequence was and the ideas to do the different test in the new in-vitro model

8.2. Standards that must be followed

In this section are explained briefly the standards that must be followed

8.3. Signal processing

How the signal obtained while recording have been treated and analysed

8.4. Comparison of results – Analysis

In this section is explained the way to get and analyse the data

8.5. Different tests done in the new model

In this section are defined and explained the different tests achieved. The test results are added in the appendix

8.5.1. Square compliance chamber and ventricle chamber without the bag

8.5.2. Square compliance chamber and ventricle chamber with the bag

8.5.3. Trapezoidal compliance chamber and ventricle chamber without the bag

8.5.4. Trapezoidal compliance chamber and ventricle chamber with the bag

8.5.5. Discussion of the waveforms

8.5.6. Comparison between the new model without the bag and the old model

8.5.7. Comparison between the new model with the bag and the old model

8.5.8. Addition of compliance in the ventricle chamber

8.5.9. Additional tests

8.6. Interpretation of the results

9- Conclusion

10- List of figures, tables and graphs

2- Requirements for the new in-vitro model (cave)

¹ Some requirements were provided by the people who have been working with this model before. This document was provided at the beginning of the semester in Danish, and here is attached the translation into English.

General design requirements

- The components must as far as possible be designed in order longevity. That is, the following parameters should be considered when working with:
 - Metal Parts - corrosion
 - Plastic items - cracks and internal stresses
- For the items should be used acrylic sheets with a thickness of 20 [mm].
- In collections density should be carefully assessed. Good collection (see Annex 2):
 - Small recess (immersion) of 1-2 [mm] for controlling the second party
 - O-ring or gasket at all joints
 - All surfaces must be close to each other must be ground level
- Plastic Thread is very fragile and damaged over time. Possibly alternative assemble principles can be incorporated

Atrium chamber

Atrium chamber acts as a large open reservoir before the ventricle chamber. Filling the chamber during systole, the mitral valve which is opened during diastole and ventricle chamber filled.

Design Requirements

- a. Instrumentation:
 - No
- b. Construction:
 - Atrium Comrade shall work with the mechanical mitral valve from the laboratory.
 - Mitral valve must be positioned vertically i.e. with the entrance on the side of ventricle chamber.
 - The volume of the chamber must be at least 6 [L], to ensure a more stable flow.
 - Atrium chamber must be open to the atmosphere.
 - Atrium chamber coupled with compliance buddy via 14mm [mm] silicone tube.
 - Atrium chamber must be designed so that it is able to provide a water column in ventricle chamber (at the aortic valve) during diastole between 10 and 20 [mmHg].
 - No requirements for transparency.

¹ Provided by the Cave team

Ventricle chamber

Ventricle chamber coupler the aortic section, atrium chamber and pump together.

Design Requirements

- a. Instrumentation:
 - No
- b. Construction:
 - The shape of ventricle chamber must be based on the biological left ventricle. This means that the entrance from the atrium chamber and the exit to the aortic root must be angled relative to one another.
 - The volume of ventricle chamber be sought likened the human (about 130 [mL]).
 - To ensure a more natural flow through the system is desired pump located the plunger pointing directly toward the aortic valve. For location see Annex 1
 - Well - rounded inlet to the aortic valve, so a more natural flow (laminar) is achieved before the flip.
 - During the test used a saline solution, which requires the separation between the pump and system. Encourage to using a home molded silicone bellows / diaphragm are designed and manufactured.
 - "Guide straws" to allow manual insertion, adjustment and rotation of Millar catheters into the native aortic root. These straws need to have an inner diameter very close to the outer diameter of the catheter Millar to ensure minimal leaking. Furthermore the straw needs to be pointed towards the aortic root section to allow an easy installation of the catheter.
 - A wire installation port is needed to allow for a cable ($\varnothing 2.76$ mm) to enter the ventricle chamber. / Alternatively a biological mitral valve can be used and the cable can go through here.

Aortic root # 1

Pressure Gradient: For existing aortic root respectively intact and blocked sinus Valsalva, desired to measure the transvalvular pressure gradient across the aortic root associated with the compression and then expansion of the flow. If we know pressure gradient and flow through the system we can calculate the Gorlin area is calculated and compared with the GOA.

Flow: also aims to measure the pulsatile flow before aortic valve. By placing the flow meter before aortic valve may want. We will be able to reflux recorded.

Design Requirements

- a. Instrumentation:
 - Pressure measurement must take place immediately just before and after aortic valve aortic valve.
 - Identical cross-sectional area at the measuring points.
 - Pressure measurements must Millar catheter.
 - The flow meter should be placed as pulsatile flow can be registered. Note specific requirements for flow meter.
- b. Construction:
 - Possibly well - rounded inlet to the aortic root before pressure measurement, in order to minimize disruption in the flow.
 - Hole diameter for pressure measurement with Millar catheter: 6 [mm]
 - There should be room for positioning the ultrasound transducer.
 - The location of measurement points must not collide with any. Ultrasound measurements of the aortic valve. Specific requirements for ultrasonic measurements:
 - a. Sensor : 40 [mm]
 - The material should be transparent for flow visualization.

Aortic root #2

It should be possible to implant a native aortic root section from an animal (often a pig) between the ventricular chamber and the aortic chamber. The fittings to attach a native root should be based in the same design as “aortic root #1” to enable us to use the same chambers for different experiments.

The transvalvular pressure should be measured very close to the native aortic valve by use of Millar catheters. If possible a measurement of the pulsatile blood flow would be nice but not a demand (i.e. the mean flow as measured between the aortic and atrial chamber is acceptable)

Design specifications:

- a. Instrumentation: the same as listed in “aortic root #1”.
- b. Construction:
 - The native aortic root is to be sewn onto a rubber sheet to ensure proper mounting of non-similar roots in the same model.
 - A flange-system with the same dimensions as the previously mentioned root #1 must be developed that ensures a good mechanical connection between each end of the native root and their respective attachment chambers must be developed. Maybe this could be sealed using an o-ring on top of the rubber sheet?

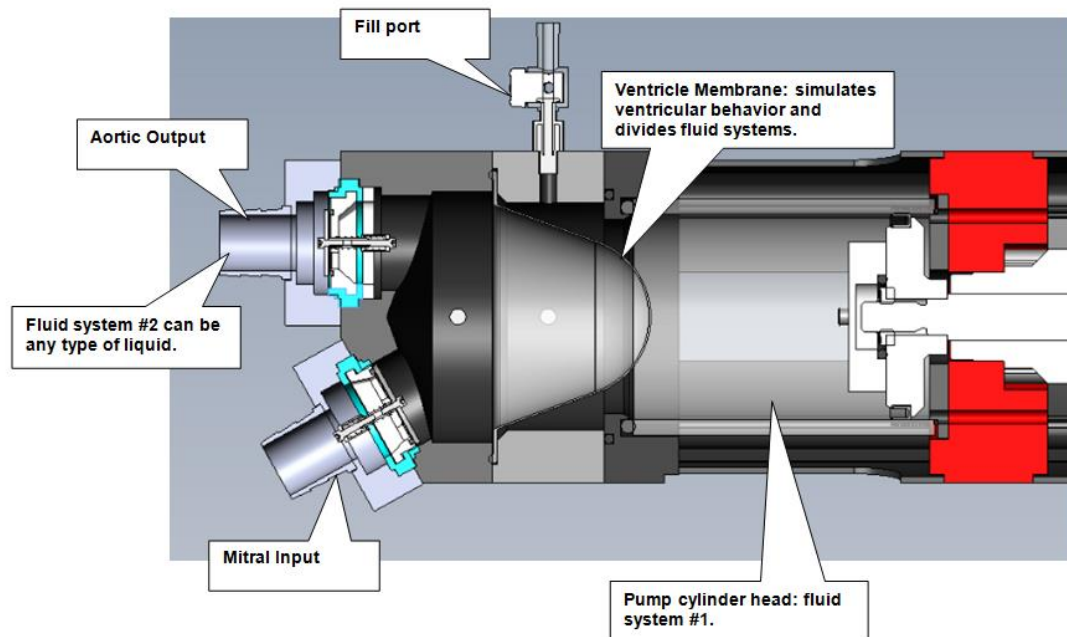
The compliance chamber

To simulate the body's elasticity (compliance) it is used a compliance chamber where compressed air is supplied.

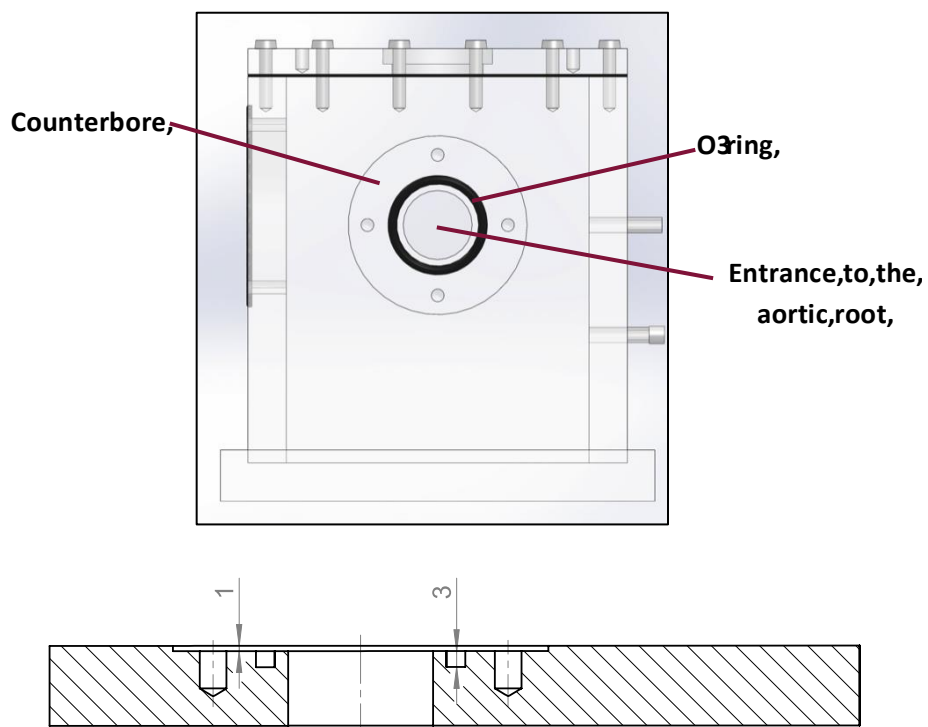
Design Requirements

- a. Instrumentation:
 - Pressure gauge for reading the actual pressure in the compliance chamber.
- b. Construction:
 - Fully sealed chamber.
 - Possibility to add 3 to 4 liters of air above the aortic valve.
 - "Guide straws" to allow manual insertion, adjustment and rotation of Millar catheters into the native aortic root. These straws need to have an inner diameter very close to the outer diameter of the catheter Millar to ensure minimal leaking. Furthermore the straw needs to be pointed towards the aortic root section to allow easy installation of the catheter.
 - Consider two avoid screws in the compliance chamber and use glue for sealing. (Avoid any Unnecessary dismantle of all chambers!)

Appendix 1 - Installation of pump



Appendix 2 - Good assembly



3- Images from Solid-Works (Compliance chamber and aortic root)

Compliance chamber

Following are presented the images of the two final compliance chambers' designs, the first is a square chamber and the second is a trapezoidal chamber. The chamber are also briefly explained and some pictures are attached to explain the steps to achieve them.

Below it is shown the square compliance chamber.

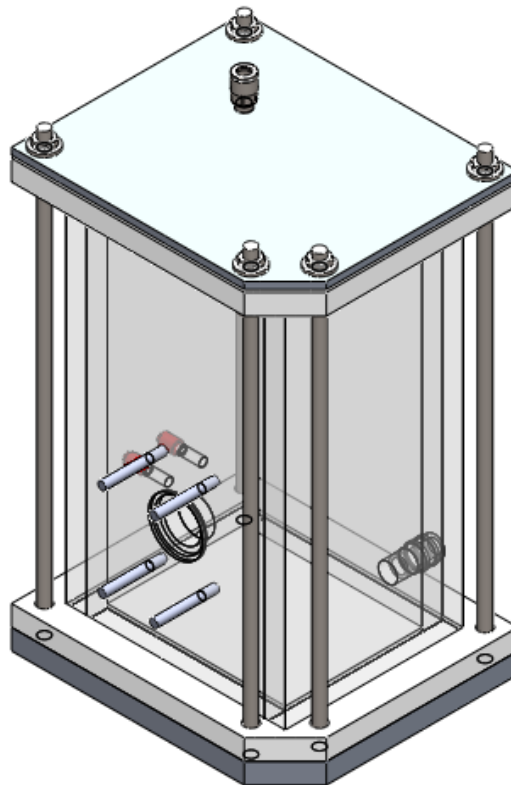


Figure 1 - Isometric view – square compliance chamber (A.O.P.)

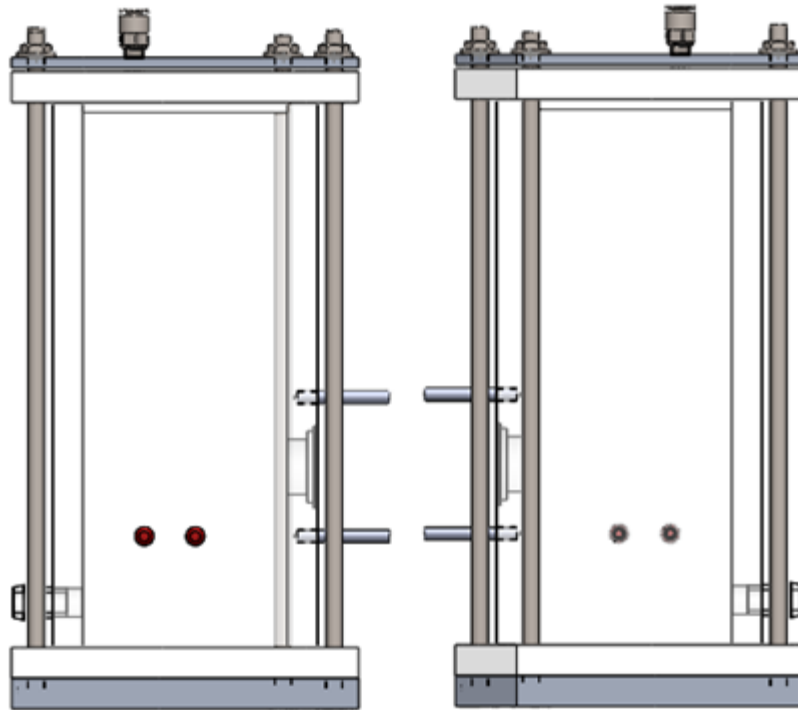


Figure 2 - Left and right view of the square compliance chamber (A.O.P.)

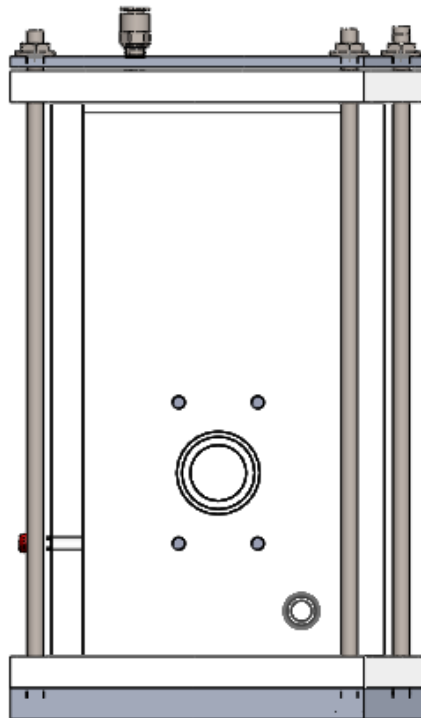


Figure 3 - Front view of the square compliance chamber (A.O.P.)

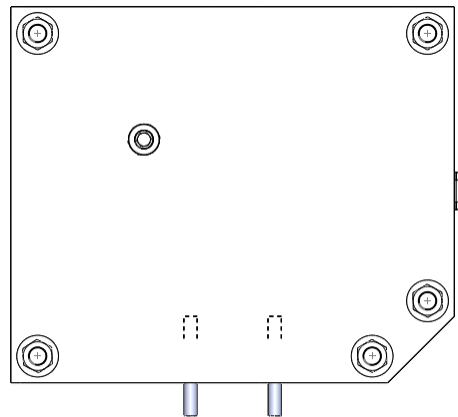


Figure 4 - Top view of the square compliance chamber (A.O.P.)

Before achieving the square chamber final design, some changes were done. The first design was bigger than the final and the connection between it and the aortic root was by using an O-ring. Then this connection was changed for a silicone ring built by using a mould. Afterwards, another big change was made, the dimensions of the chamber. Initially it was followed one of the requirements which was having 4[L] above the aortic hole, but after talking with the supervisors there was no need for it. The last change made on the chamber, was cutting one of the corners, it was needed to do it due to space problems with the atrium chambers in the assembly. Following is possible to see some pictures of the previous chambers.

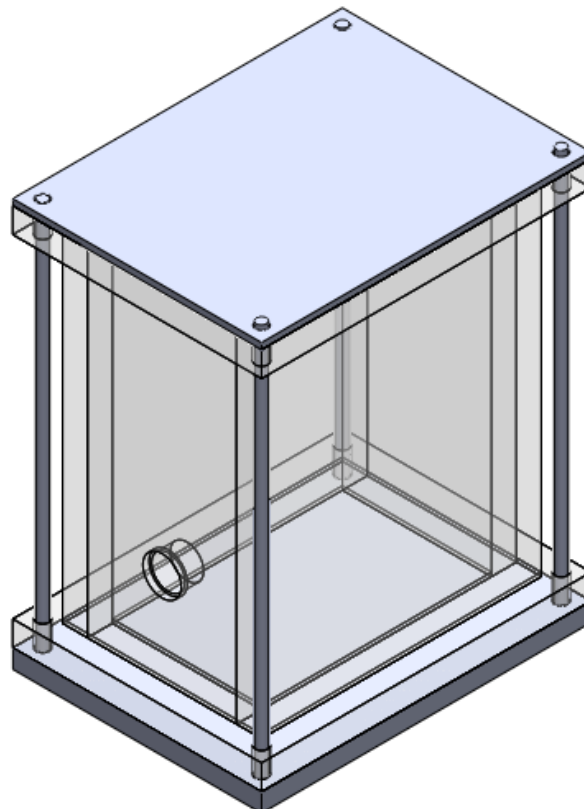


Figure 5 - Initial square compliance chamber (A.O.P.)

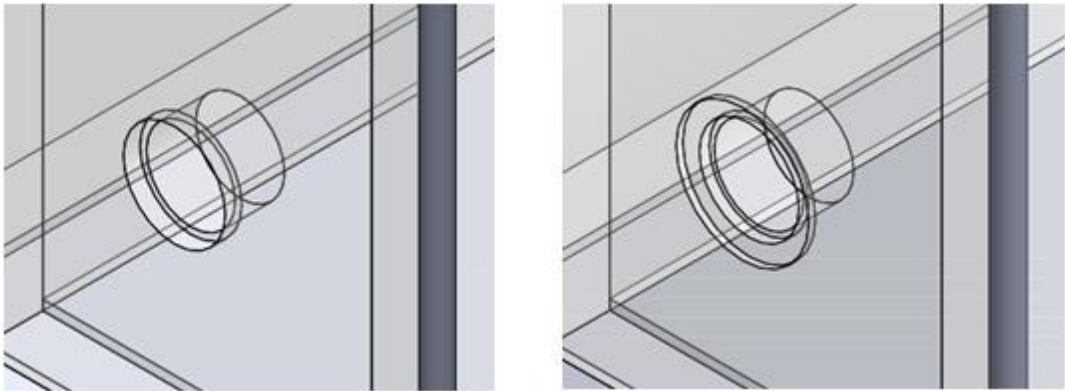


Figure 6 - O-ring connection (left) and silicone ring connection (right) (A.O.P.)

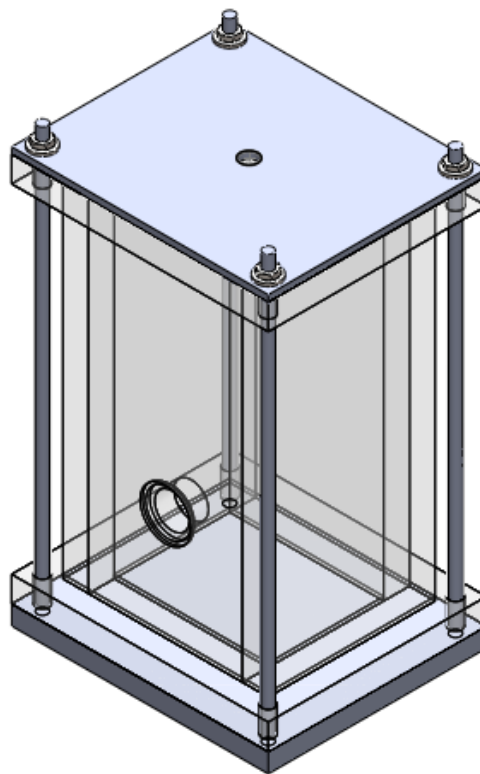


Figure 7 - Almost final square compliance chamber design – without corner cut (A.O.P.)

The second compliance chamber designed was a trapezoidal one. The entire model is also going to be used to analyse biological aortic root, which length is shorter than the acrylic ones used to test the aorta valves. So that, the chambers have to be closer, and by using a square one was not enough room for it. For that reason a trapezoidal one, with less front dimension was designed. Following is possible to see some images of the chamber.

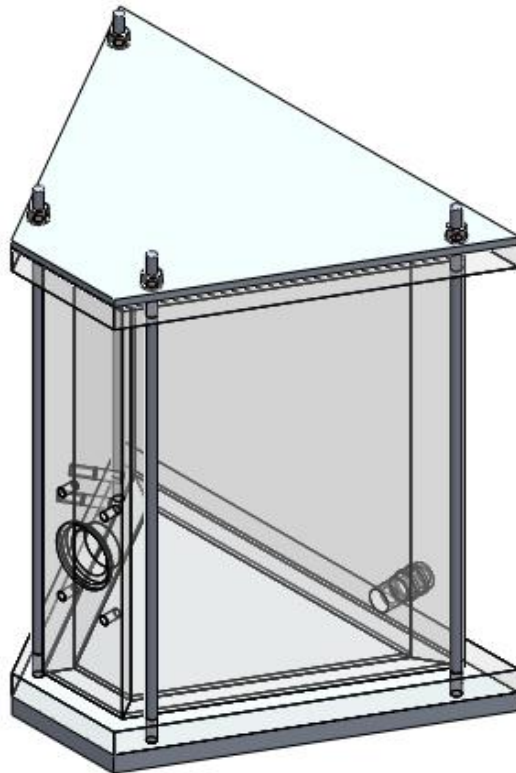


Figure 8 - Isometric view – trapezoidal compliance chamber (A.O.P.)

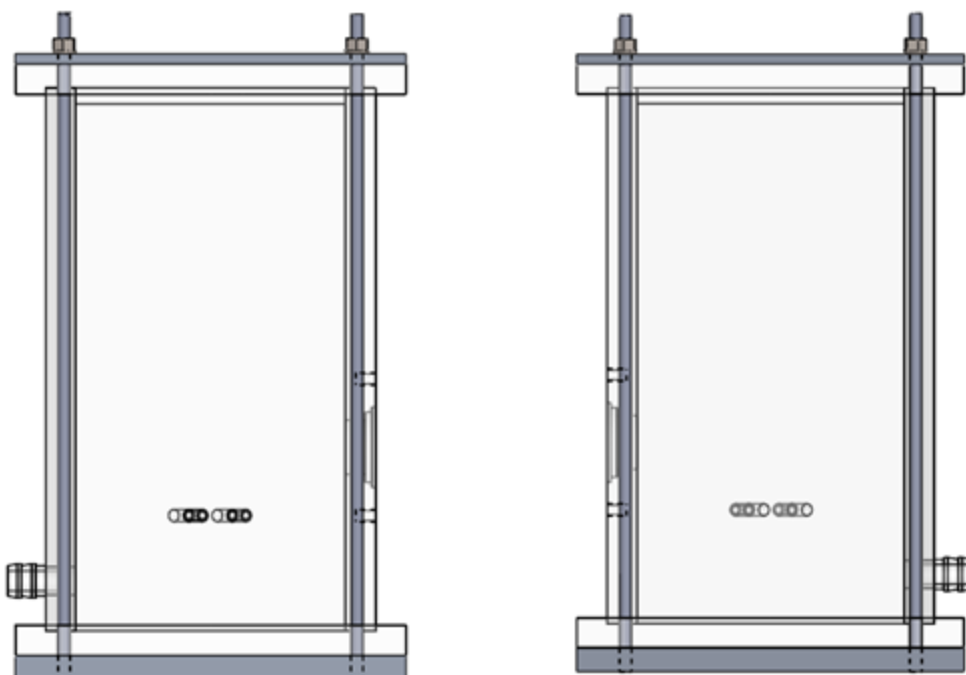


Figure 9 - Left and right side of the trapezoidal compliance chamber (A.O.P.)

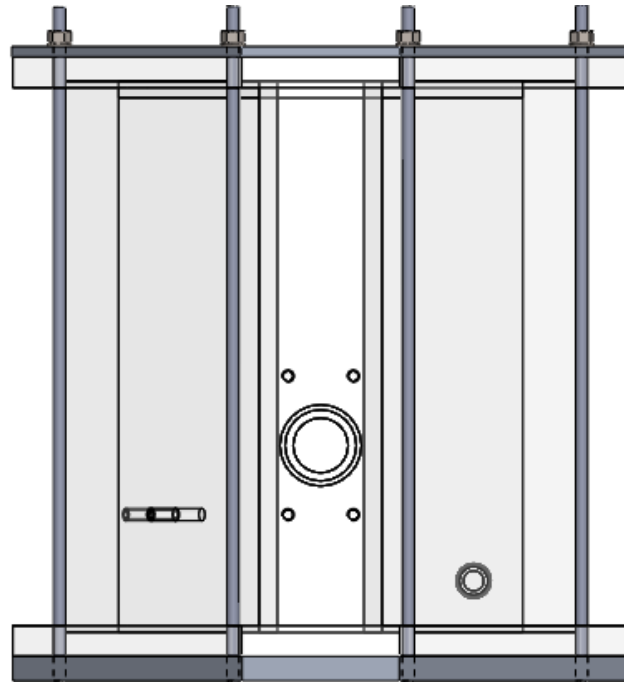


Figure 10 - Front view of the square compliance chamber (A.O.P.)

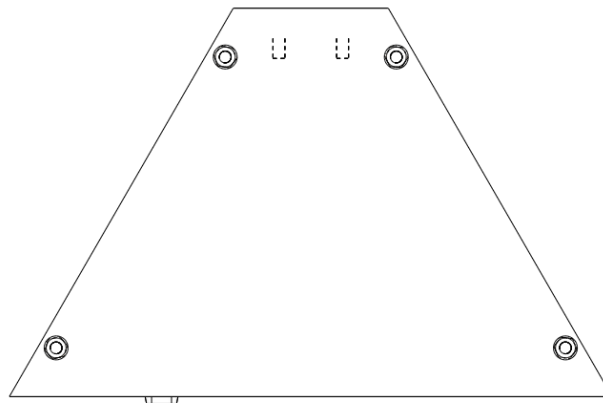


Figure 11 - Top view of the square compliance chamber (A.O.P.)

Aortic Root

For the aortic root, the main problem to focus in was the fittings in order to connect avoiding the leakage between it and the chambers. Some fittings have been developed to end in two designs. The first one is used for all the analysis which the model will be used for but for flow analysis. For this last analysis a flow meter is required. Due to the big diameter of the aortic root a big clamp flow meter is therefore required. For that reason a lot of room is needed for it. For this usage, new fittings have been designed.

The first fitting was designed to be used with an O-ring connection between them and the chambers, the first one with a circular shape and the second with a rectangular shape. But due to leakage problems seen in the previous models, was decided to attach them by a silicone ring connection designed by using a mould. In all the models was needed to add some room to insert the Millar catheters. The first idea was to insert the catheters in the sides of the fittings but later on, the holes were moved to the top area of the fittings because it was easier and more convenient for the user.

The original shaped was circular and then it was changed into rectangular, with Millar catheters in the sides of the fittings. Below are presented some images of the initial models.

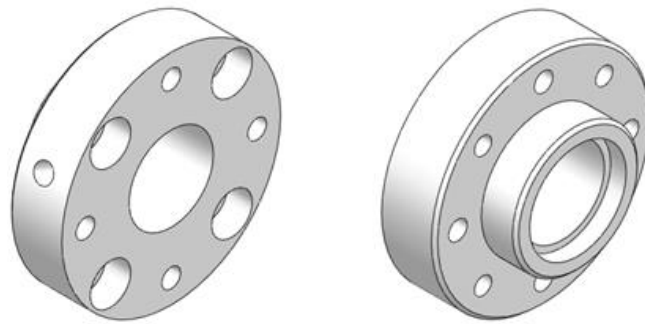


Figure 12 - Circular shaped fitting connection (A.O.P.)

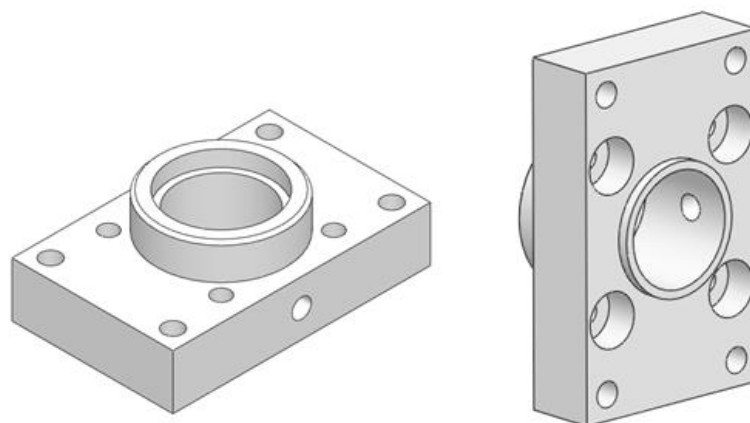


Figure 13 - Rectangular shaped fitting connection (A.O.P.)

Due to leakage problems, the connection between the fittings and the chamber was improved into a silicone ring connection. Below is possible to see the both different connections, the O-ring connection in the left and the silicone ring connection in the right.



Figure 14 - O-ring connection and silicone ring connection (A.O.P.)

Afterwards the Millar catheters were moved into another position. From the side to the top. Below are the images for both positions.

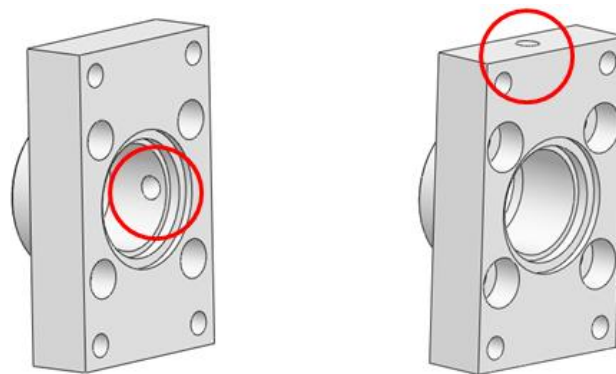


Figure 15 - Millar catheters' positions (A.O.P.)

The final assembly is possible to see below.

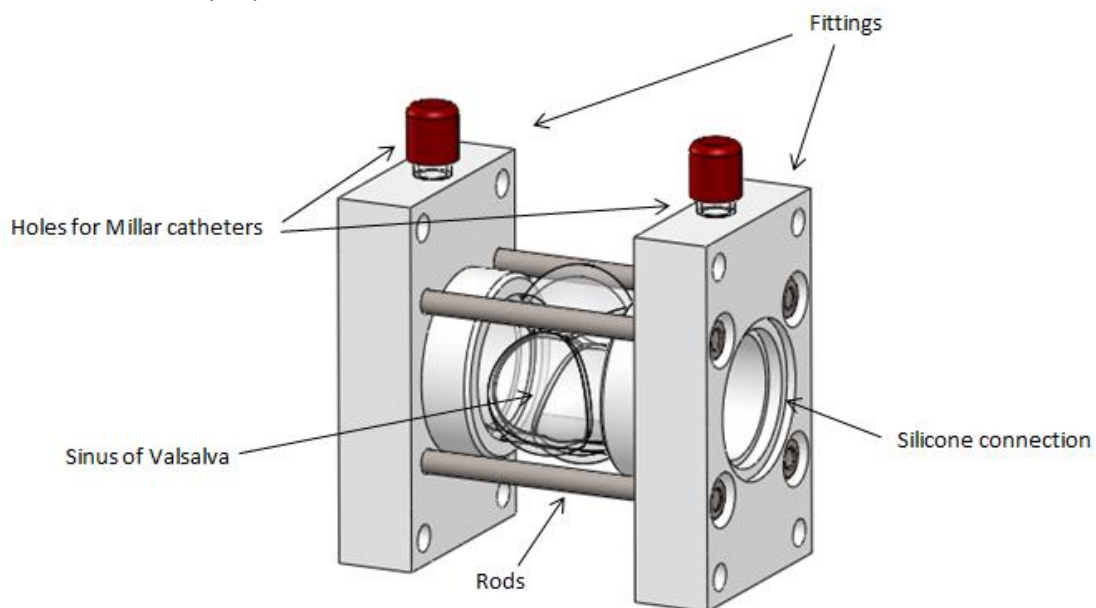


Figure 16 - Aortic root assembly (A.O.P.)

So as to be able to insert the flow meter was needed to relocate some of the rods that connect both fittings, in order to increase the required room to do it. Therefore, a new design was desired because there was not enough space in the designed fittings. This new design not only changes the rods position, but also a connector in acrylic has to be added. This acrylic connector is used to connect the aortic acrylic root with the silicone tube which will be used to attach the flow meter. Pressure drops are expected due to the length, so that it is recommend the usage of this second model only for flow calculations, more about this topic in other sections. Before achieving this solution, other ones were tough.

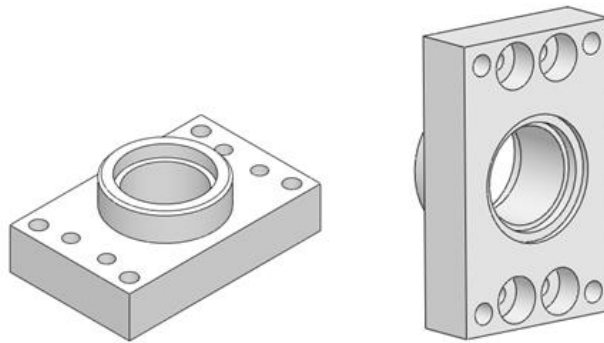


Figure 17 - Fittings – rods changed in position (A.O.P.)

Below is shown the hand-drawing and the solid works image for the connector design and the way to join it with the acrylic sinus of Valsalva. The connector is made in acrylic as well and has a silicone tube attached.

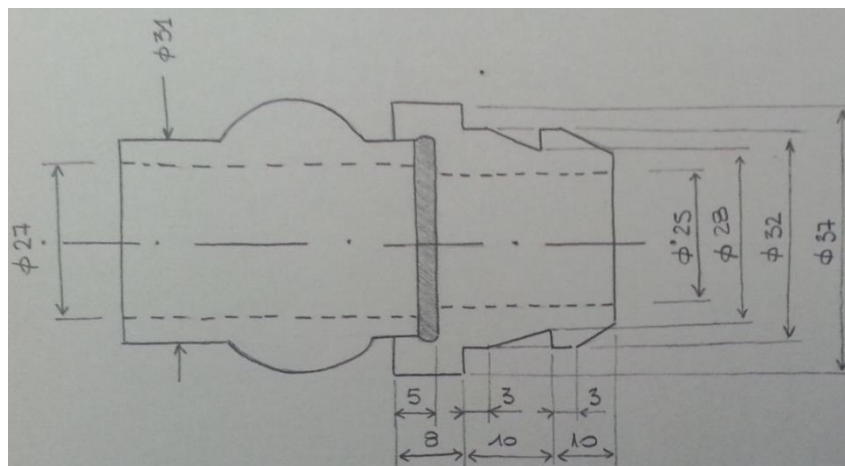


Figure 18 - Connector sinus of Valsalva and silicone tube – Hand drawing (A.O.P.)

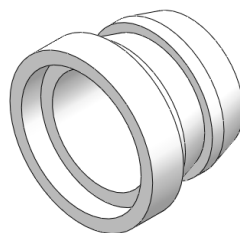


Figure 19 - Connector sinus of Valsalva and silicone tube – Solid Works (A.O.P.)

Before this design was thought another kind of connection which can be seen below. It was neglected for two reasons. The first one is because is easier and more secure to attach the silicone tube into the chosen connector, due to its conical shape. Another important reason is a construction one. Some similar pieces have been manufactured before; it will be easier and faster therefore for the workshop to produce it. In the graph below is presented a hand drawing of the previous thought connector.

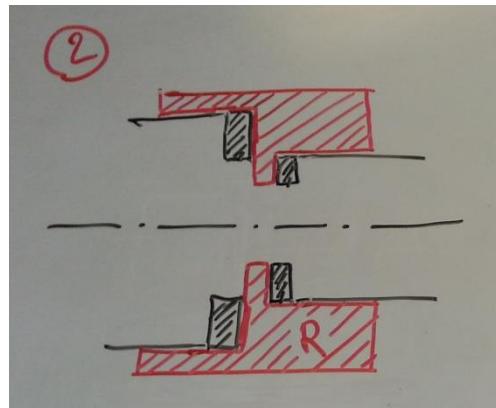


Figure 20 - Previous design for the connector - Hand drawing (A.O.P.)

It was also needed to design a connection between the silicone tube and the fitting that is connected to the compliance chamber since the tube was not big enough to be attached directly to the fitting. The design is possible to be seen below. Finally, there was no need to manufacture it since was possible to achieve a 31 [mm] diameter tube. Note 31 [mm] is the dimension which fits perfectly in the fitting connection.

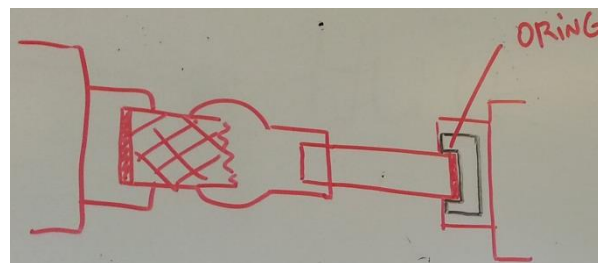


Figure 21 - Connector silicone tube and fitting – Hand drawing (A.O.P.)

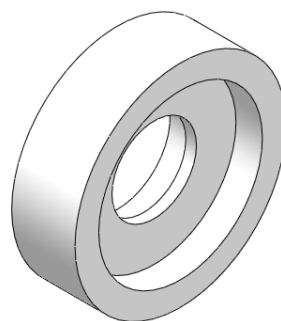


Figure 22 - Connector silicone tube and fitting – Solid Works (A.O.P.)

The final assembly of the fittings, the sinus of Valsalva, the silicone tube and the O rings are possible to be seen below. Note the rods are not drawn in the graphs.

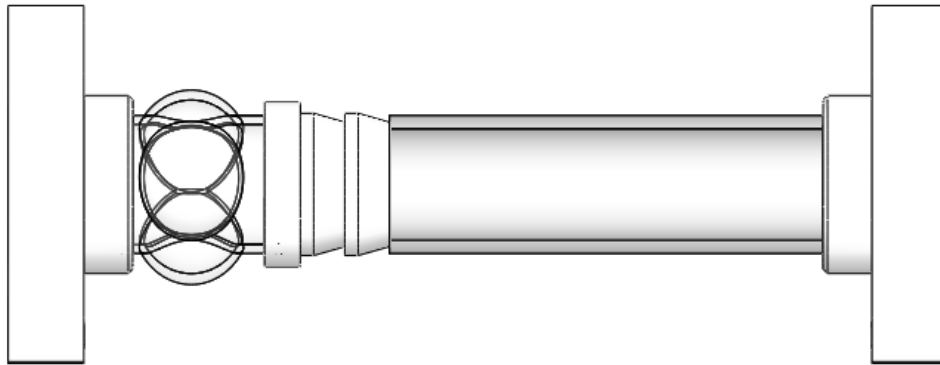


Figure 23 - Aortic root assembly for flow calculations – front view (A.O.P.)

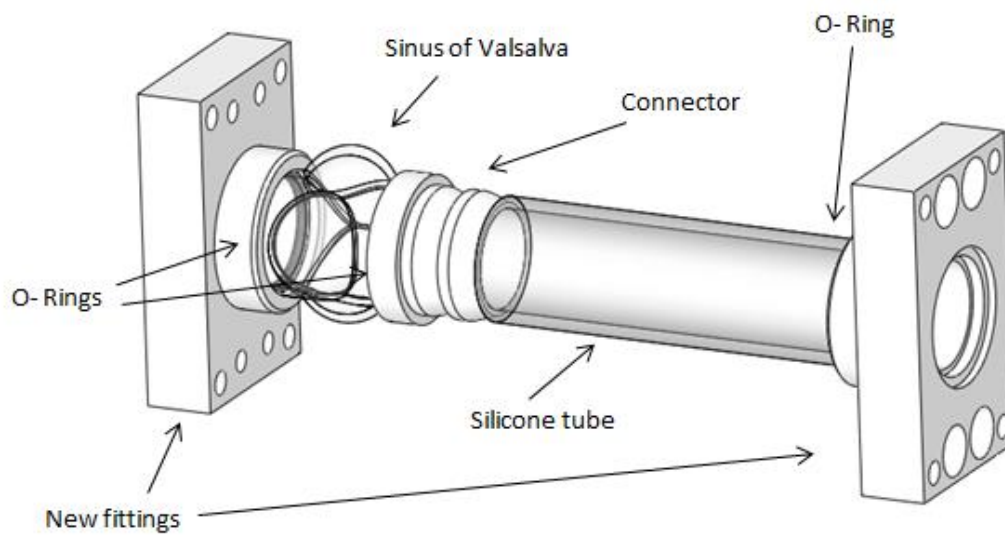


Figure 24 - Aortic root assembly for flow calculations (A.O.P.)

4- Real images (Compliance chamber and aortic root)

Square compliance chamber



Figure 25 – Square compliance chamber assembly (A.O.P.)

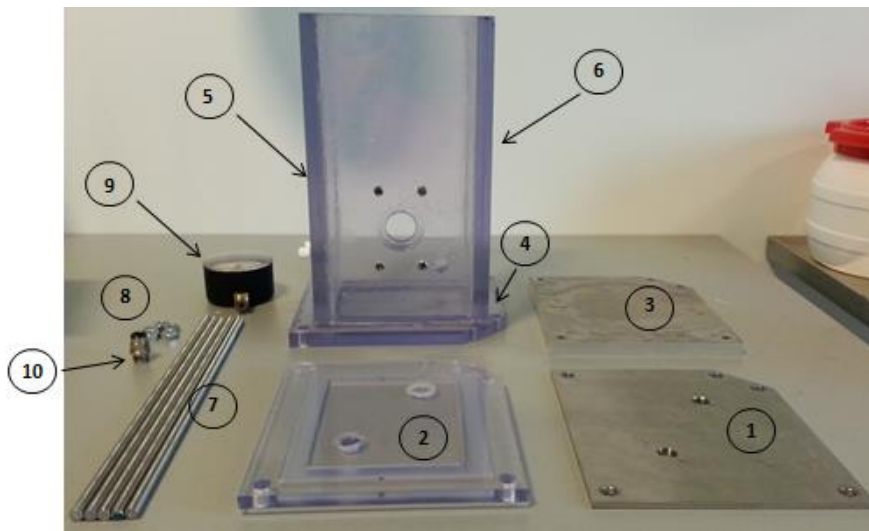


Figure 26 - Parts of the square compliance chamber (A.O.P.)

Nº	Part	Material	Quantity
1	Top plate	Steel	1
2	Top plate	Polycarbonate	1
3	Bottom plate	Steel	1
4	Bottom plate	Polycarbonate	1
5	Side plate for Millar Cth.	Polycarbonate	1
6	Side plate	Polycarbonate	1
7	M8 Bars – 335 [mm] length	Stainless stell	5
8	M8 Nuts	-	5
9	Pressure gauge	-	1
10	Compressed air inlet	-	1

Table 1 - List of parts in the square compliance chamber assembly (A.O.P.)

Trapezoidal compliance chamber



Figure 27 - Trapezoidal compliance chamber assembly (A.O.P.)

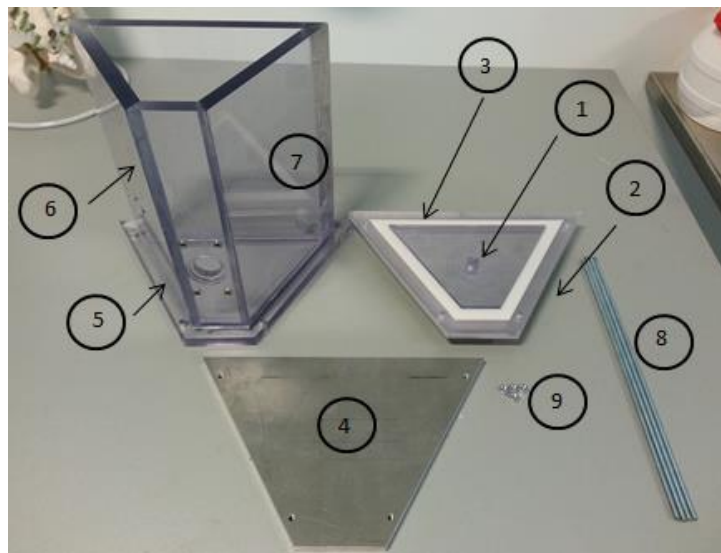


Figure 28 - Parts of the trapezoidal compliance chamber (A.O.P.)

Nº	Part	Material	Quantity
1	Top plate	Steel	1
2	Top plate	Polycarbonate	1
3	Bottom plate	Steel	1
4	Bottom plate	Polycarbonate	1
5	Side plate for Millar Cth.	Polycarbonate	1
6	Side plate	Polycarbonate	1
7	M8 Bars – 335 [mm] length	Stainless stell	5
8	M8 Nuts	-	5
9	Pressure gauge	-	1
10	Compressed air inlet	-	1

Table 2- List of parts in the trapezoidal compliance chamber assembly (A.O.P.)

Aortic root

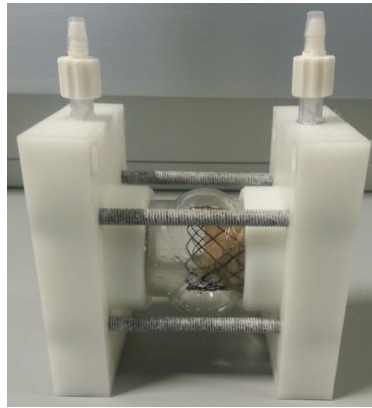


Figure 29 - Aortic root assembly (A.O.P.)

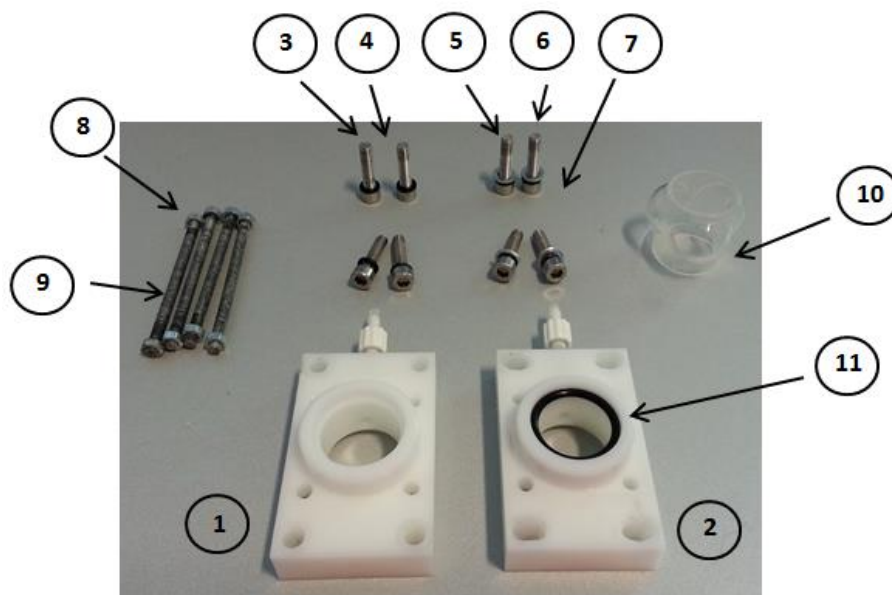


Figure 30 - Parts of the aortic root assembly (A.O.P.)

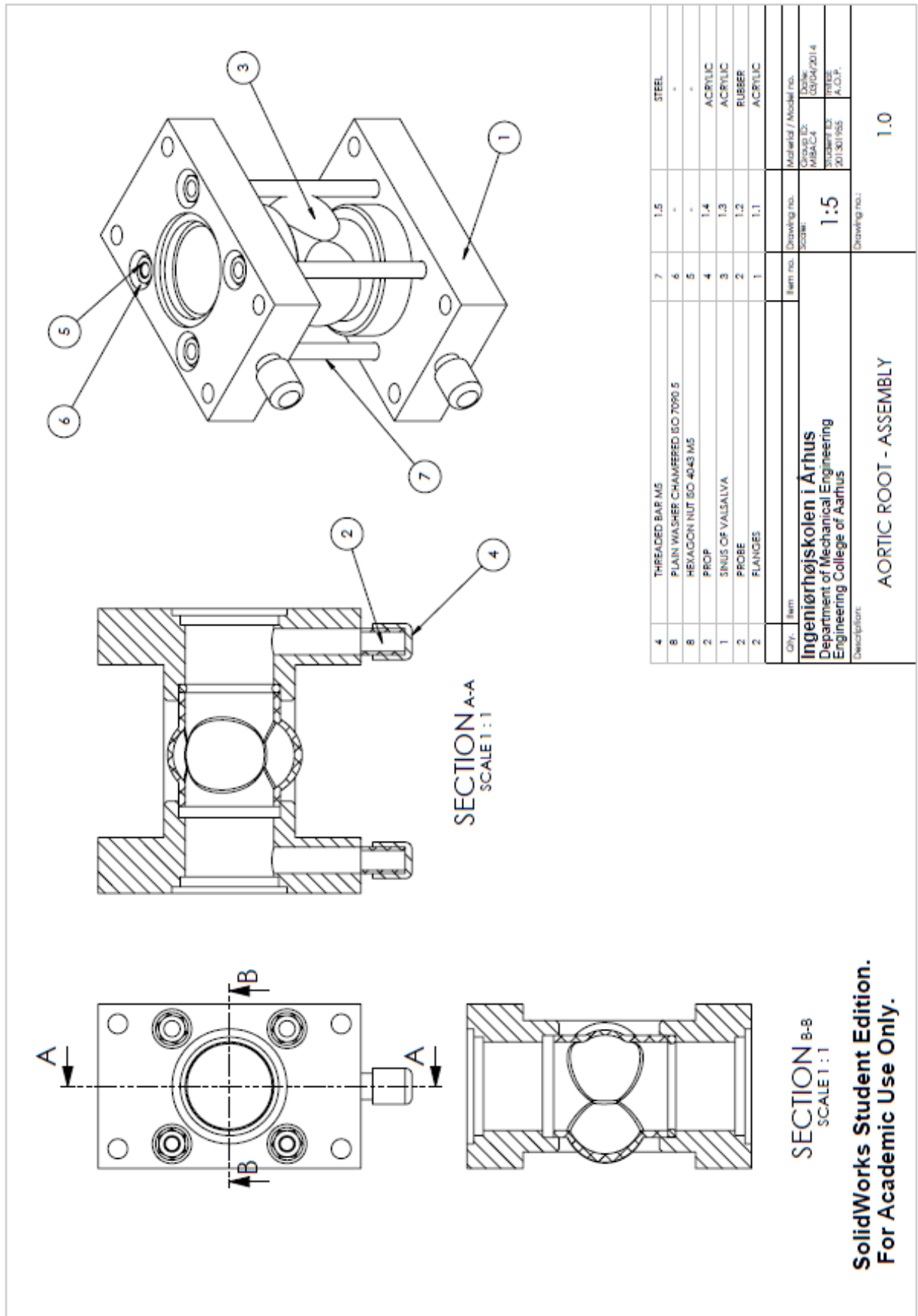
Nº	Part	Material	Quantity
1	Fitting – Ventricle chamber	POM	1
2	Fitting – Compliance chamber	POM	1
3	Screws Fitting M6 (1)	-	4
4	Washers (1)	Rubber	4
5	Screws Fitting M6 (2)	-	4
6	Washers (2)	Rubber	4
7	Washers (2)	Metal	4
8	Nuts M5	8	4
9	M5 bars – 80 [mm] lenght	Stain steel	4
10	Aortic root	Acrylic	1
11	O-ring	-	1

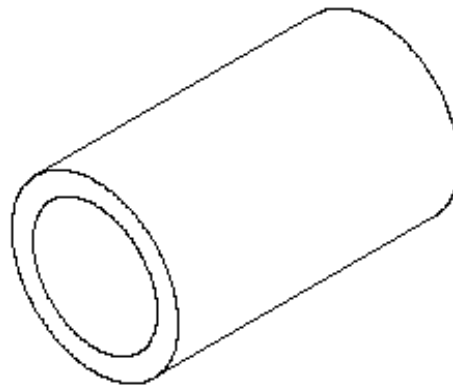
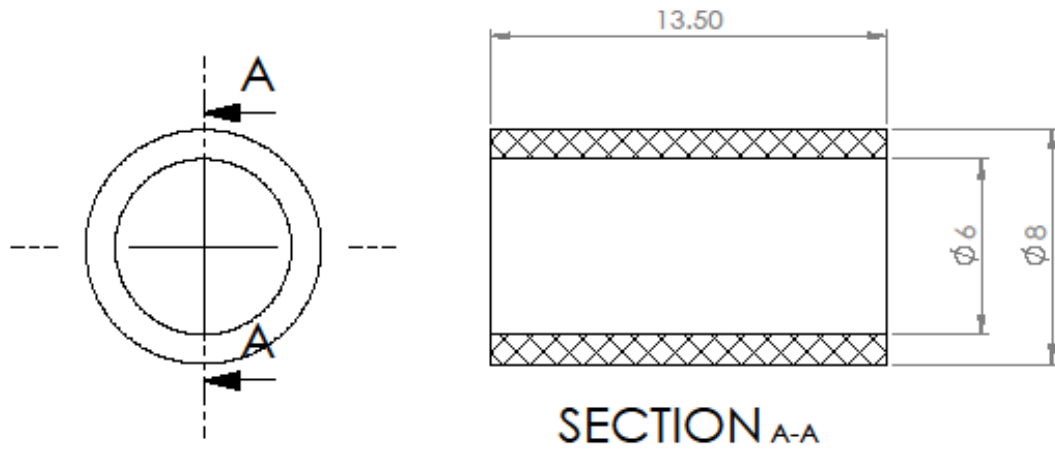
Table 3 List of parts in the aortic root assembly (A.O.P.)

5- Drawings (Compliance chamber and aortic root)

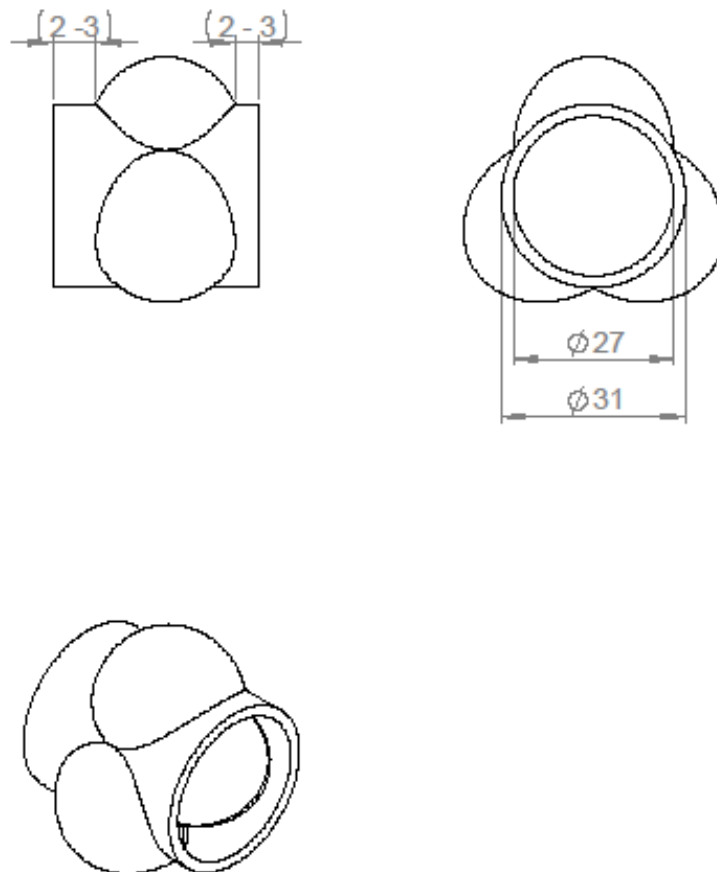
List of drawings

Aortic Root	Drawing 1.0.	Fitting aortic root – Assembly
	Drawing 1.1.	Fitting aortic root - Flanges
	Drawing 1.2.	Fitting aortic root – Probe
	Drawing 1.3.	Aortic root – Sinus of Valsalva
	Drawing 1.4.	Fitting aortic root – Prop
	Drawing 1.5.	Aortic Root – Threaded bar
	Drawing 1.6.	Connection tube – Aortic root
	Drawing 1.7.	Fittings for Aortic Root – V.2.
Square compliance chamber	Drawing 2.0.	Compliance chamber – Assembly
	Drawing 2.1.	Compliance chamber – Aortic root plate
	Drawing 2.2.	Compliance chamber – Back plate
	Drawing 2.3.	Compliance chamber – Side plate to A.C.
	Drawing 2.4.	Compliance chamber – Side with Millar Cth.
	Drawing 2.5.	Compliance chamber – Bottom plate
	Drawing 2.6.	Compliance chamber – Top plate
	Drawing 2.7.	Compliance chamber – Metal bottom plate
	Drawing 2.8.	Compliance chamber – Metal top plate
	Drawing 2.9.	Compliance chamber – Routing studs
	Drawing 2.10.	Compliance chamber – Threaded bar M6
	Drawing 2.11.	Compliance chamber – Threaded bar M8
	Drawing 2.12.	Compliance chamber – Probe
	Drawing 2.13.	Compliance chamber – Prop
Mould	Drawing 3.0.	Silicone valve mold - Assembly
	Drawing 3.1.	Female – Silicone valve mold
	Drawing 3.2.	Male – Silicone valve mold
Trapezoidal compliance chamber	Drawing 4.1.	Compliance chamber – Aortic root plate
	Drawing 4.2.	Compliance chamber – Back plate
	Drawing 4.3.	Compliance chamber – Side plate to A.C.
	Drawing 4.4.	Compliance chamber – Side with Millar Cth.
	Drawing 4.5.	Compliance chamber – Bottom plate
	Drawing 4.6.	Compliance chamber – Top plate
	Drawing 4.7.	Compliance chamber – Metal bottom plate
	Drawing 4.8.	Compliance chamber – Metal top plate
	Drawing 4.9.	Threaded bar M6

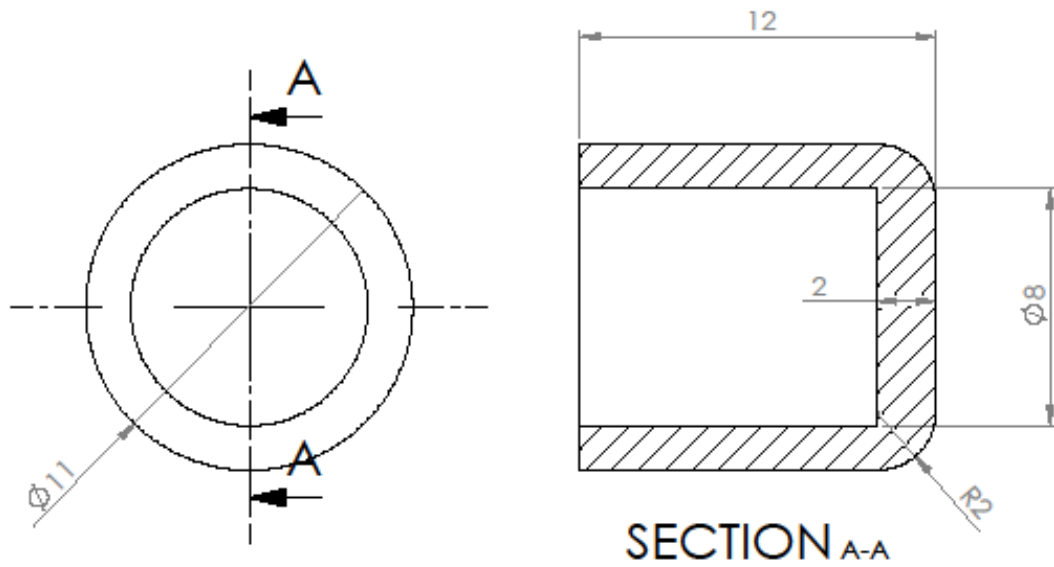




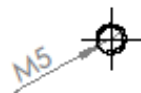
2				ACRYLIC	
Qty.	Item	Item no.	Drawing no.	Material / Model no.	
Ingeniørhøjskolen i Århus Department of Mechanical Engineering Engineering College of Aarhus SolidWorks Student Edition.			Scale:	Group ID: MIBAC4	Date: 02/04/2014
			5:1	Student ID: 201301955	Initial: A.O.P.
Description:			Drawing no.:		
For Academic Use Only. FITTING AORTIC ROOT - PROBE			1.2		



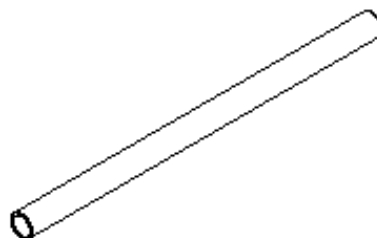
1				ACRYLIC	
Qty.	Item	Item no.	Drawing no.	Material / Model no.	
Ingeniørhøjskolen i Århus Department of Mechanical Engineering Engineering College of Aarhus SolidWorks Student Edition. For Academic Use Only. AORTIC ROOT - SINUS OF VALSALVA			Scale:	Group ID: MIBAC4	Date: 02/04/2014
			1:1	Student ID: 201301955	Initial: A.O.P.
Description:			Drawing no.: 1.3		



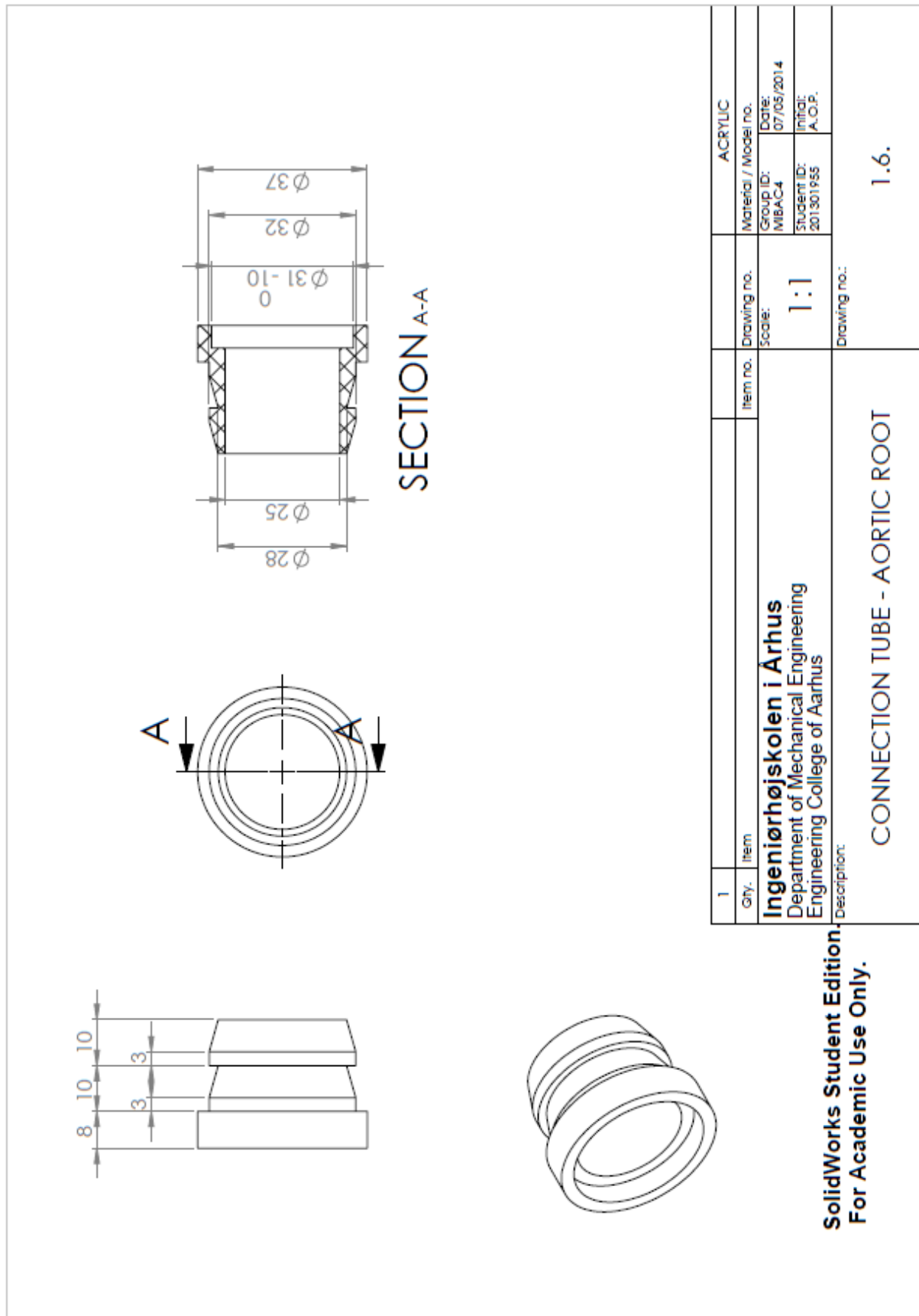
2				RUBBER	
Qty.	Item	Item no.	Drawing no.	Material / Model no.	
Ingeniørhøjskolen i Århus Department of Mechanical Engineering Engineering College of Aarhus Description: SolidWorks Student Edition. For Academic Use Only. FITTING AORTIC ROOT - PROP			Scale:	Group ID: MIBAC4	Date: 02/04/2014
			5:1	Student ID: 201301955	Initial: A.O.P.
			Drawing no.:	1.4	



ALL THREADED WITH M5



4				STEEL	
Qty.	Item	Item no.	Drawing no.	Material / Model no.	
Ingeniørhøjskolen i Århus Department of Mechanical Engineering Engineering College of Aarhus SolidWorks Student Edition. For Academic Use Only.			Scale:	Group ID: MIBAC4	Date: 03/04/2014
			1:1	Student ID: 201301955	Initial: A.O.P.
Description:			Drawing no.:		
AORTIC ROOT - THREADED BAR M5			1.5		

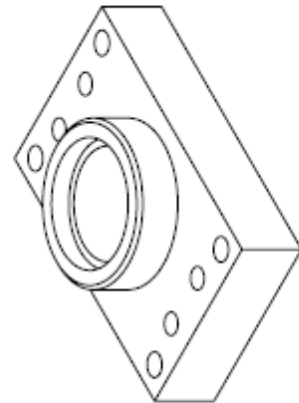
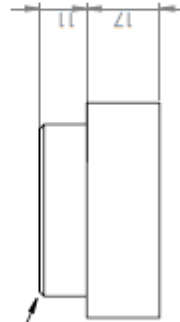


SolidWorks Student Edition.
For Academic Use Only.



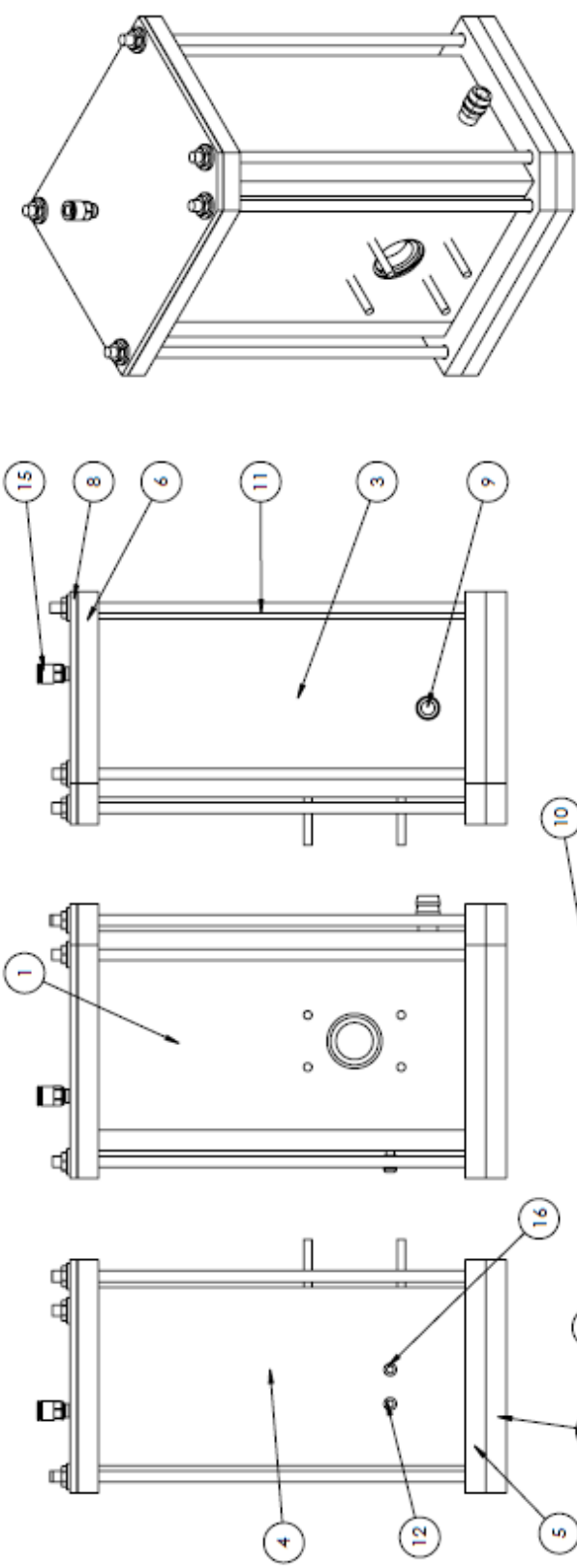
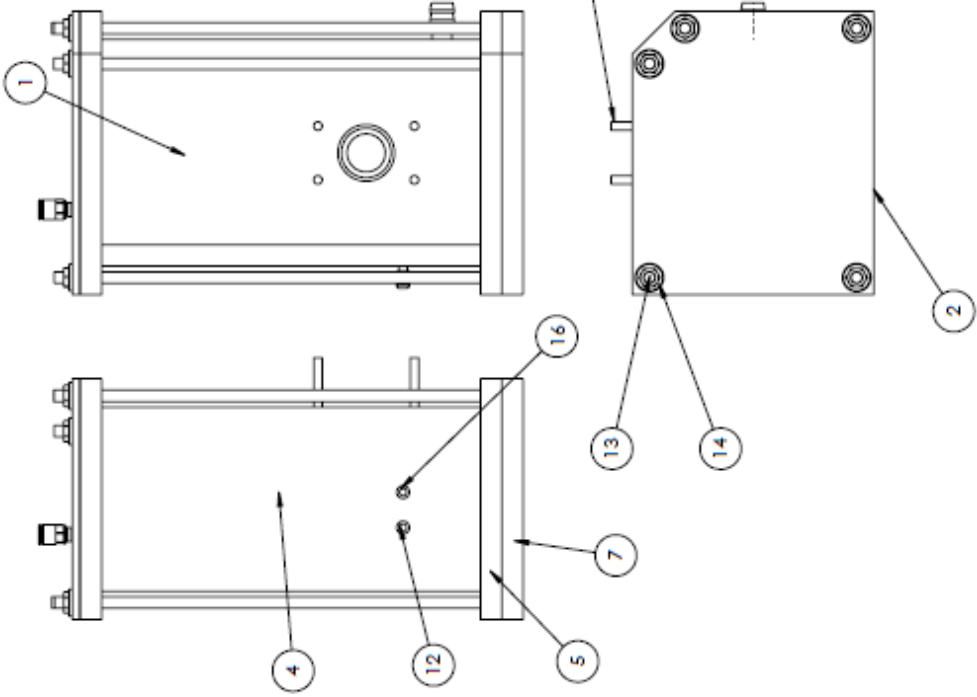
SECTION B-B

CHAMFER 1x45°



**SolidWorks Student Edition.
For Academic Use Only.**

2	Qty.	Item	Item no.	Drawing no.	Material / Model no.	POM
Ingeniørhøjskolen i Århus Department of Mechanical Engineering Engineering College of Aarhus						
			Scale:	1:1	Group ID: MBSAC4 Student ID: 201301955 A.O.P.	Date: 07/05/2014 File:
Description:			Drawing no.:		1.7.	
FITTINGS FOR AROTIC ROOT - V.2.						

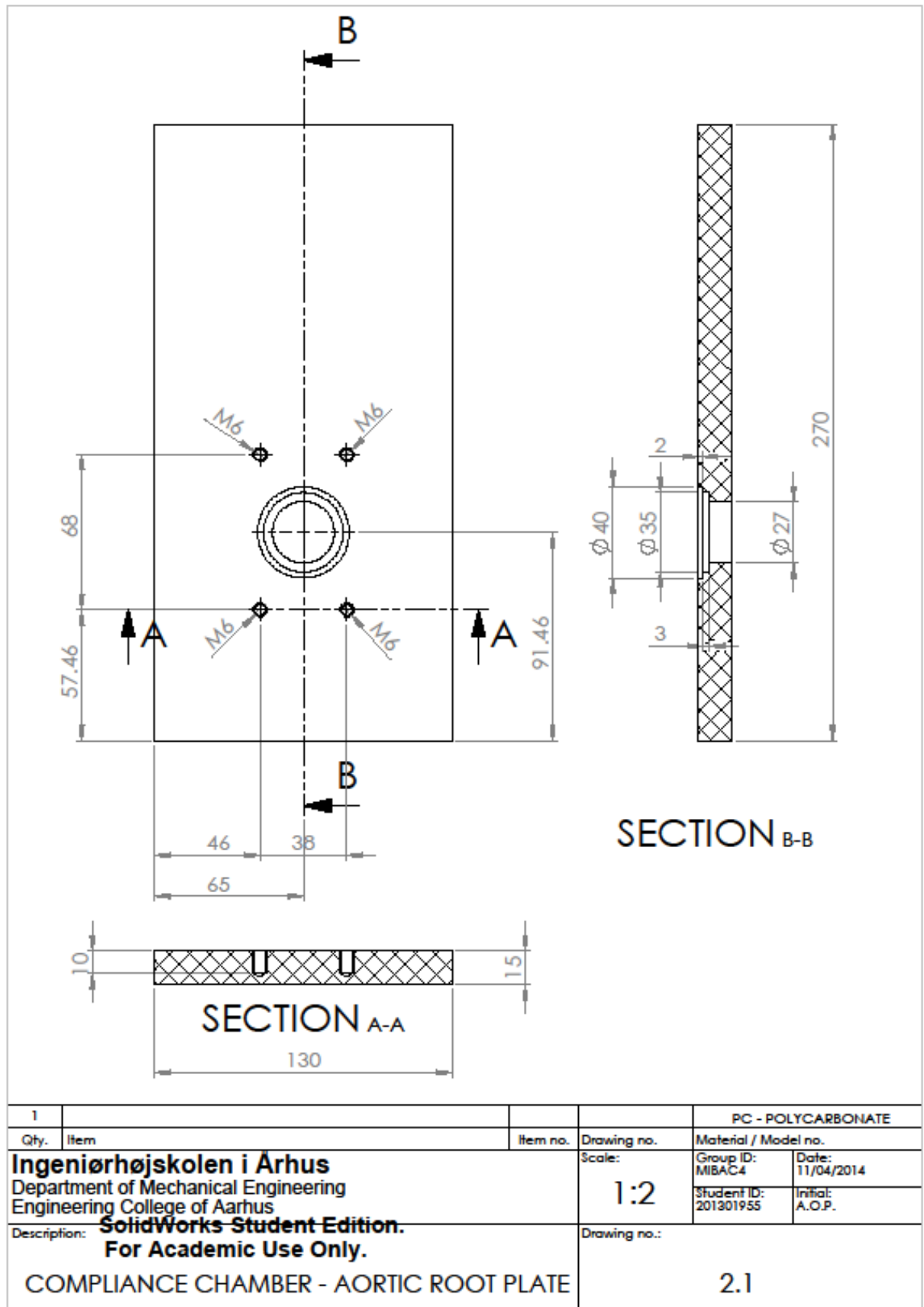



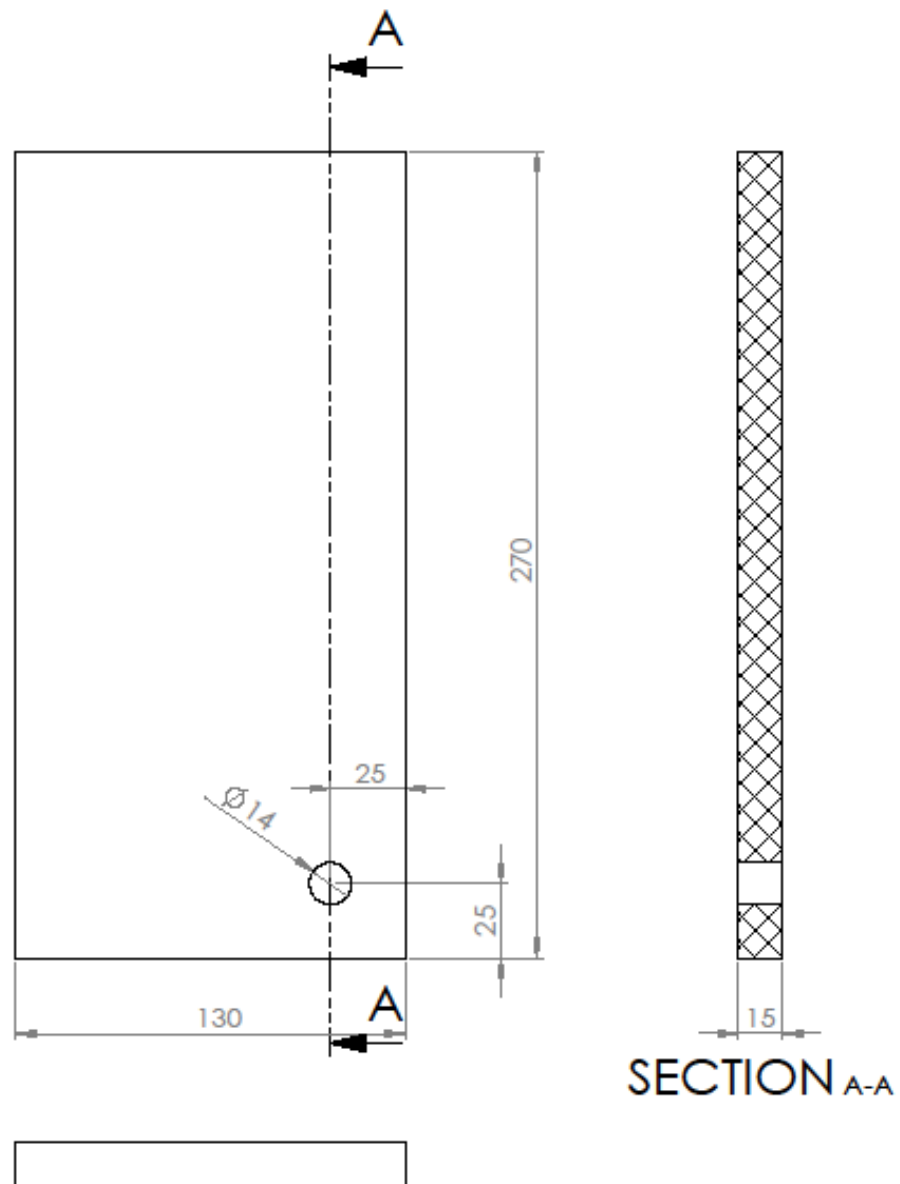
Item no.	Item	Item no.	Item	Item no.	Item	Item no.	Item
2	PROP	16	2.13	RUBBER			
1	558643 NPQM-D-G18-Q8-P10	15	-	-			
10	PLAIN WASHER 8 [mm] b18.22M	14	-	-			
10	HEX NUT JAM M8x1.25	13	-	-			
2	PROBE	12	2.12	-			
5	THREADED BAR M8	11	2.11	STEEL			
4	THREADED BAR M6	10	2.10	STEEL			
1	ROUTING STUDS	9	2.9	STEEL			
1	METAL TOP PLATE	8	2.8	STEEL			
1	METAL BOTTOM PLATE	7	2.7	PC - POLYCARBONATE			
1	TOP PLATE	6	2.6	PC - POLYCARBONATE			
1	BOTTOM PLATE	5	2.5	PC - POLYCARBONATE			
1	SIDE WITH MILLAR CTHL	4	2.4	PC - POLYCARBONATE			
1	SIDE PLATE TO A.C	3	2.3	PC - POLYCARBONATE			
1	BACK PLATE	2	2.2	PC - POLYCARBONATE			
1	ACRIFIC ROOT PLATE	1	2.1	PC - POLYCARBONATE			

Ingeniørhøjskolen i Århus
Department of Mechanical Engineering
Engineering College of Aarhus

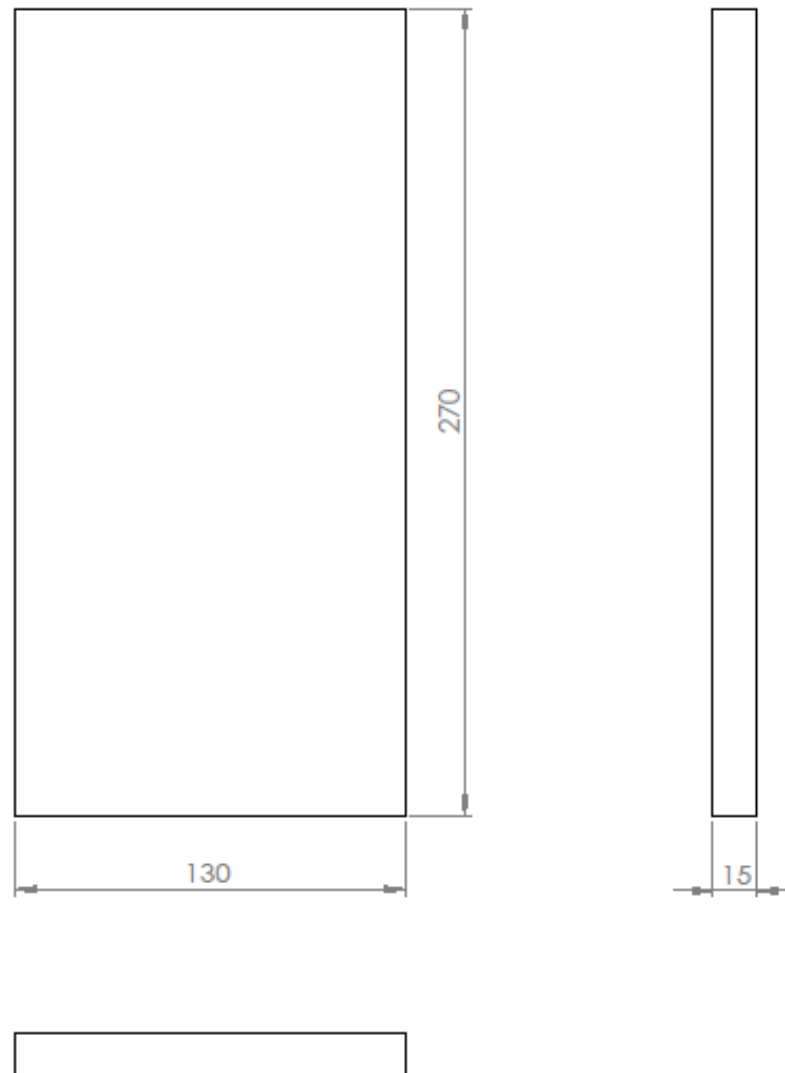
Drawing no.: **2.0**

**SolidWorks Student Edition.
For Academic Use Only.**

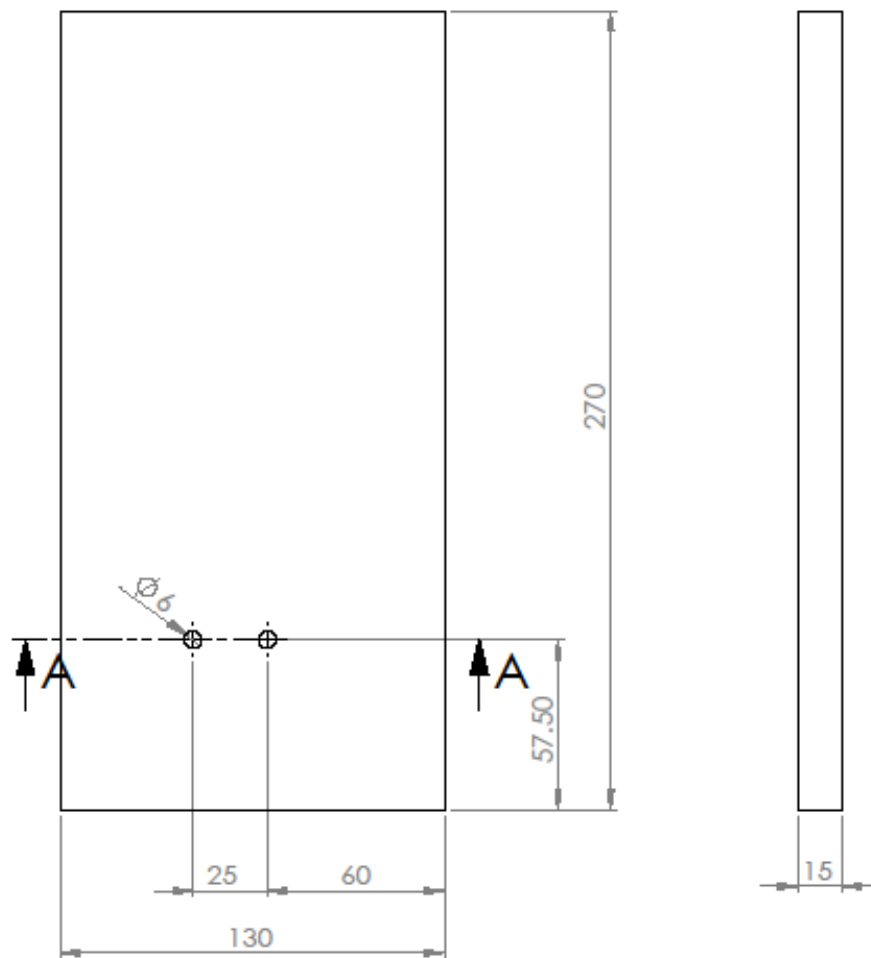




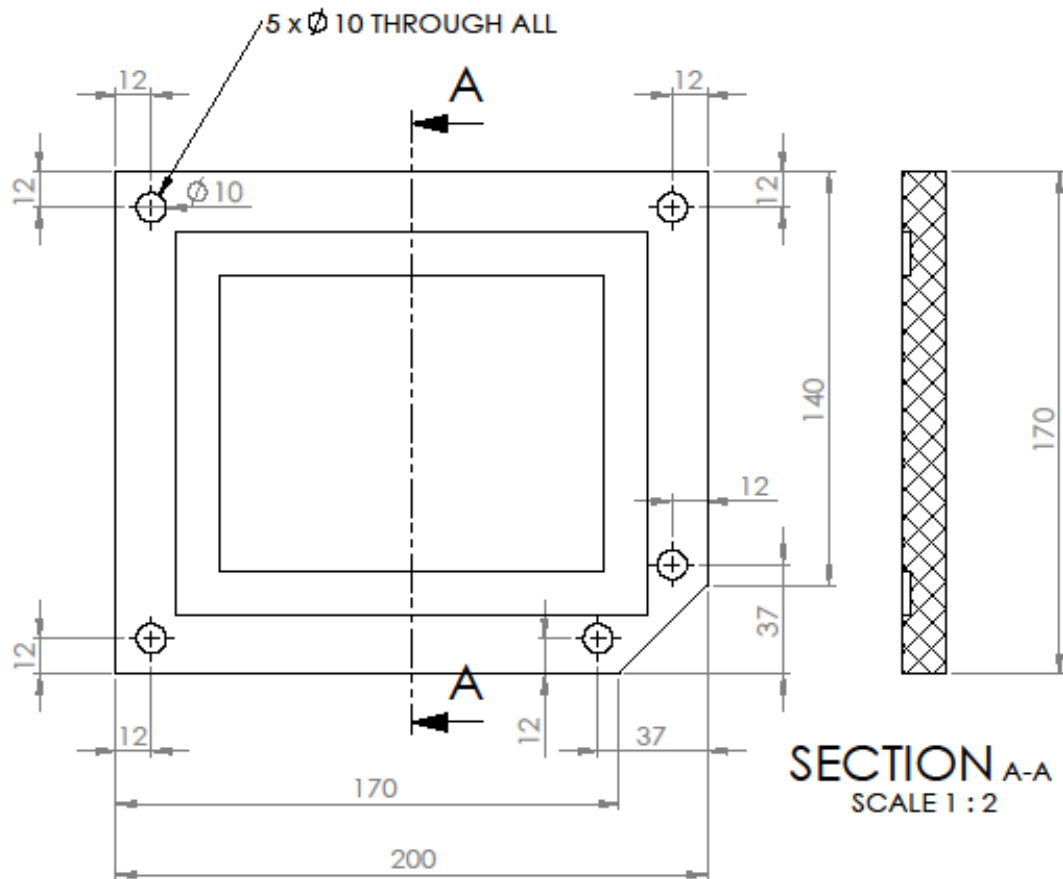
1				PC - POLYCARBONATE	
Qty.	Item	Item no.	Drawing no.	Material / Model no.	
Ingeniørhøjskolen i Århus Department of Mechanical Engineering Engineering College of Aarhus SolidWorks Student Edition. For Academic Use Only.			Scale:	Group ID: MIBAC4	Date: 11/04/2014
			1:2	Student ID: 201301955	Initial: A.O.P.
Description:			Drawing no.:		
COMPLIANCE CHAMBER - BACK PLATE			2.2		



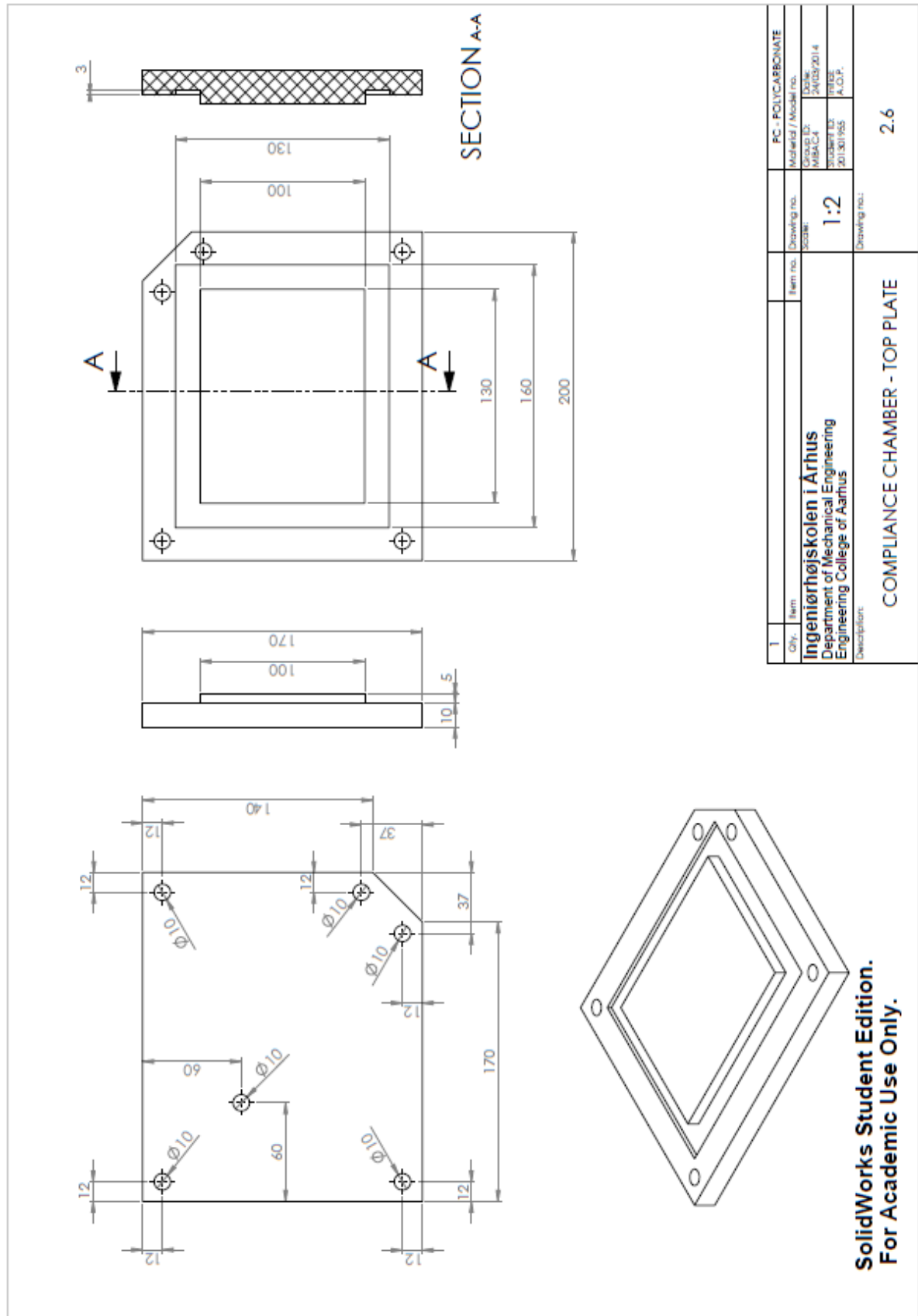
1				PC - POLYCARBONATE	
Qty.	Item	Item no.	Drawing no.	Material / Model no.	
Ingeniørhøjskolen i Århus Department of Mechanical Engineering Engineering College of Aarhus SolidWorks Student Edition. For Academic Use Only.			Scale:	Group ID: MIBAC4	Date: 11/04/2014
			1:2	Student ID: 201301955	Initial: A.O.P.
Description:			Drawing no.:		
COMPLIANCE CHAMBER - SIDE PLATE TO A.C.			2.3		

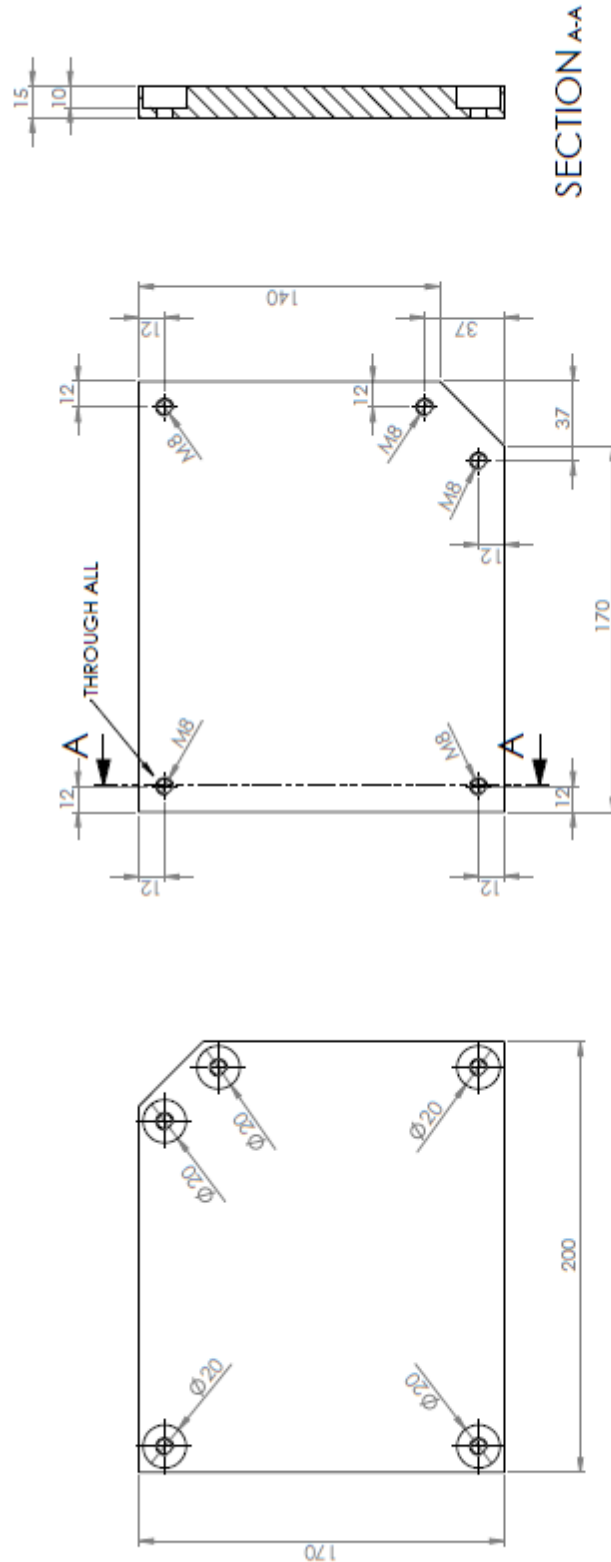


1				PC - POLYCARBONATE	
Qty.	Item	Item no.	Drawing no.	Material / Model no.	
Ingeniørhøjskolen i Århus Department of Mechanical Engineering Engineering College of Aarhus SolidWorks Student Edition. For Academic Use Only.			Scale:	Group ID: MIBAC4	Date: 24/03/2014
			1:2	Student ID: 201301955	Initial: A.O.P.
Description:			Drawing no.:		
COMPLIANCE CHAMBER - SIDE WITH MILLAR CTH.			2.4		

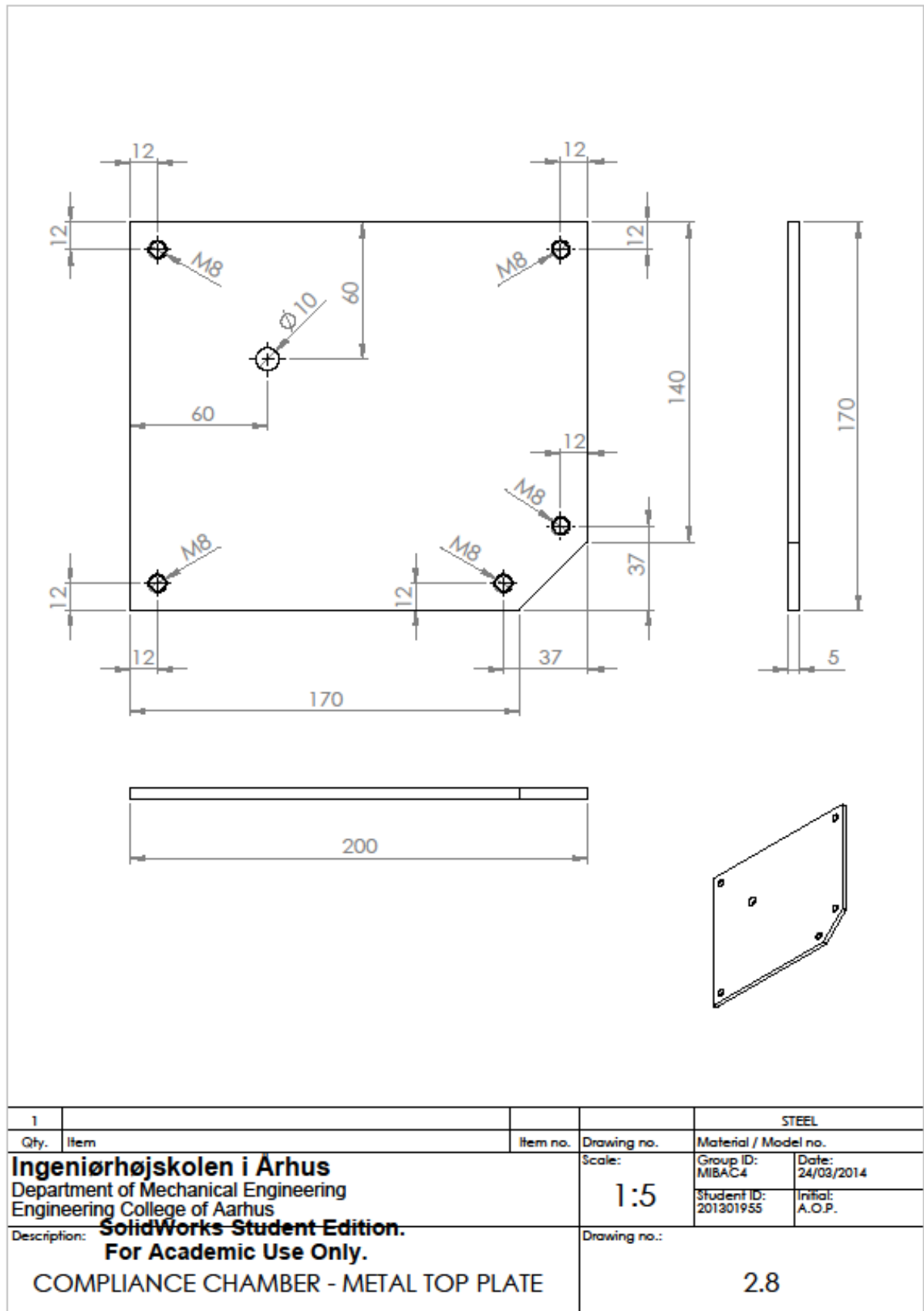


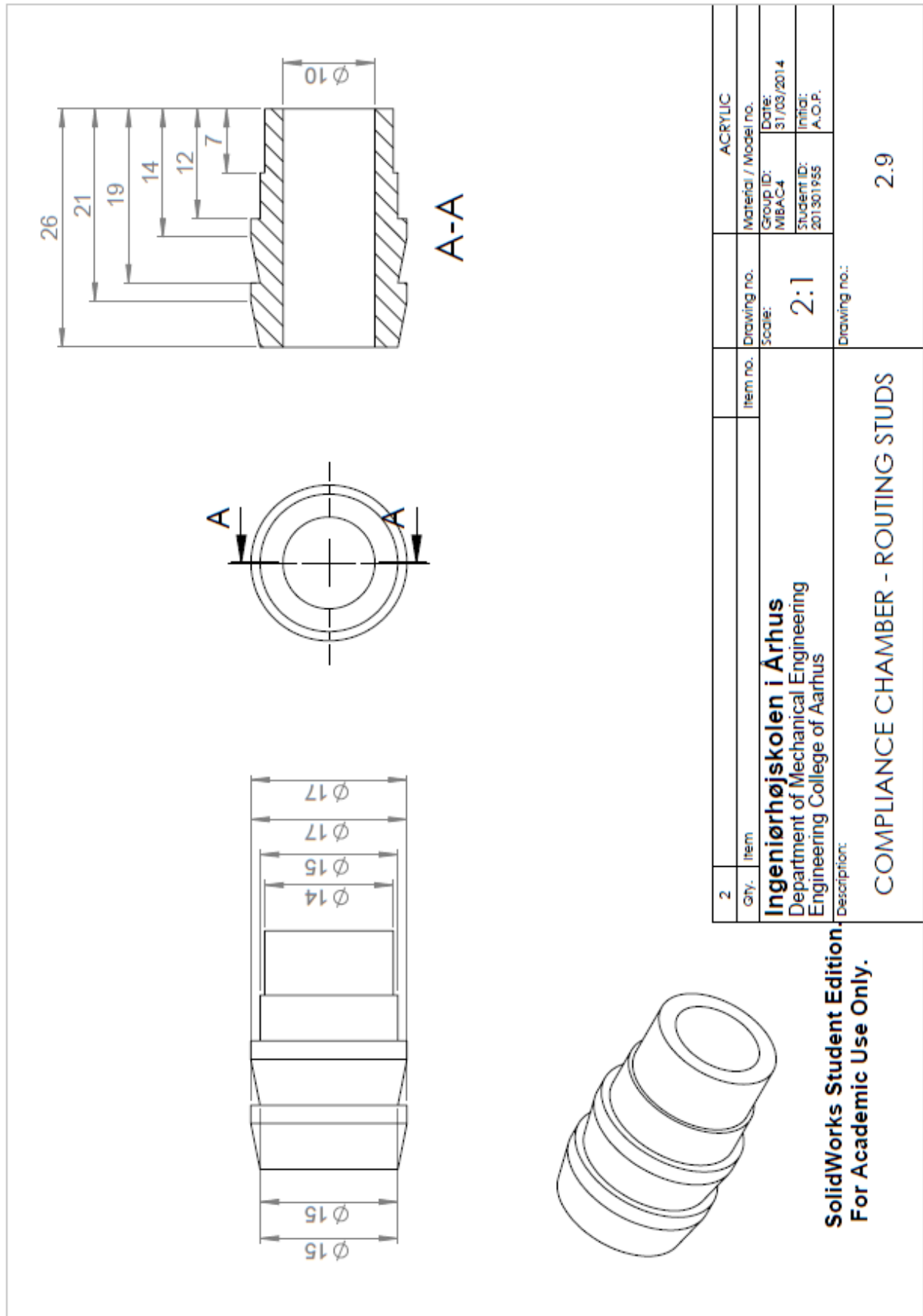
1				PC - POLYCARBONATE
Qty.	Item	Item no.	Drawing no.	Material / Model no.
Ingeniørhøjskolen i Århus Department of Mechanical Engineering Engineering College of Aarhus SolidWorks Student Edition. For Academic Use Only.			Scale:	Group ID: MIBAC4 Date: 24/03/2014
			1:5	Student ID: 201301955 Initial: A.O.P.
Description: COMPLIANCE CHAMBER - BOTTOM PLATE			Drawing no.:	2.5

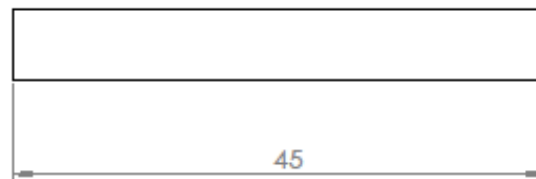
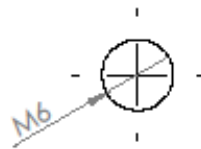




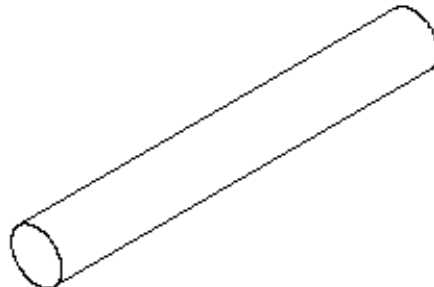
1	Item	Item no.	Drawing no.	Material / Model no.	STEEL
	Ingeniørhøjskolen i Århus Department of Mechanical Engineering Engineering College of Aarhus		Drawing no. Scale:	Material / Model no. Group ID:	Date:
			1:2	Student ID:	Date:
			Drawing no.:		
	COMPLIANCE CHAMBER - METAL BOTTOM PLATE				2.7



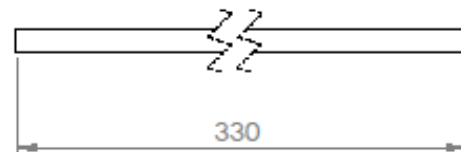
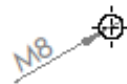




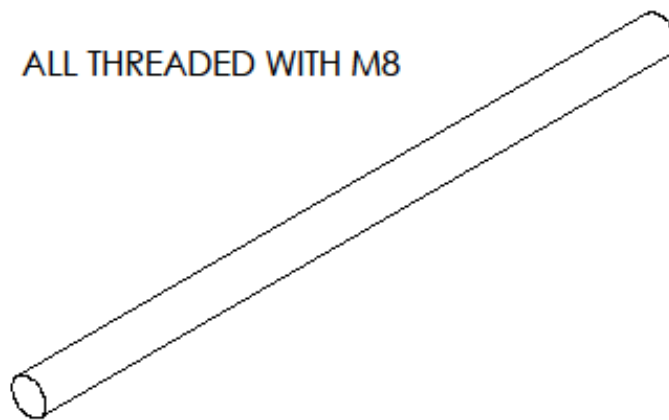
ALL THREADED WITH M6



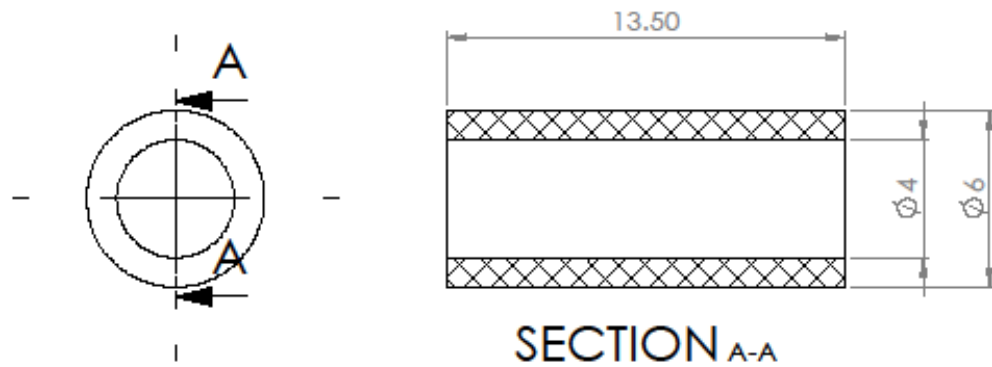
8				STEEL	
Qty.	Item	Item no.	Drawing no.	Material / Model no.	
Ingeniørhøjskolen i Århus Department of Mechanical Engineering Engineering College of Aarhus SolidWorks Student Edition. For Academic Use Only. THREADED BAR M6			Scale:	Group ID: MIBAC4	Date: 01/04/2014
			2:1	Student ID: 201301955	Initial: A.O.P.
Description:			Drawing no.: 2.10		



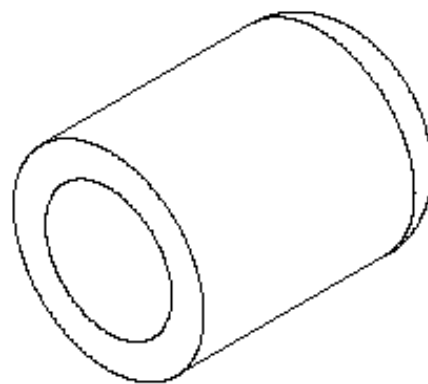
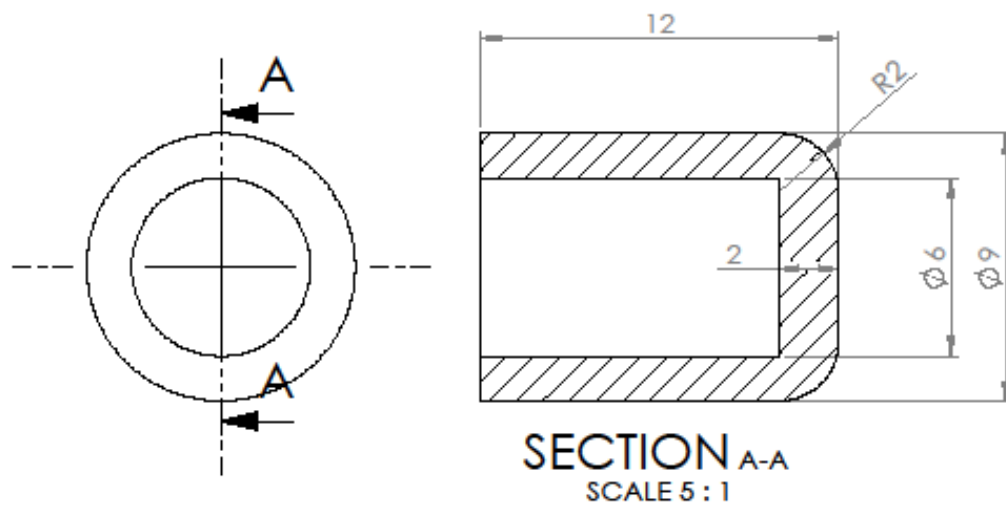
ALL THREADED WITH M8



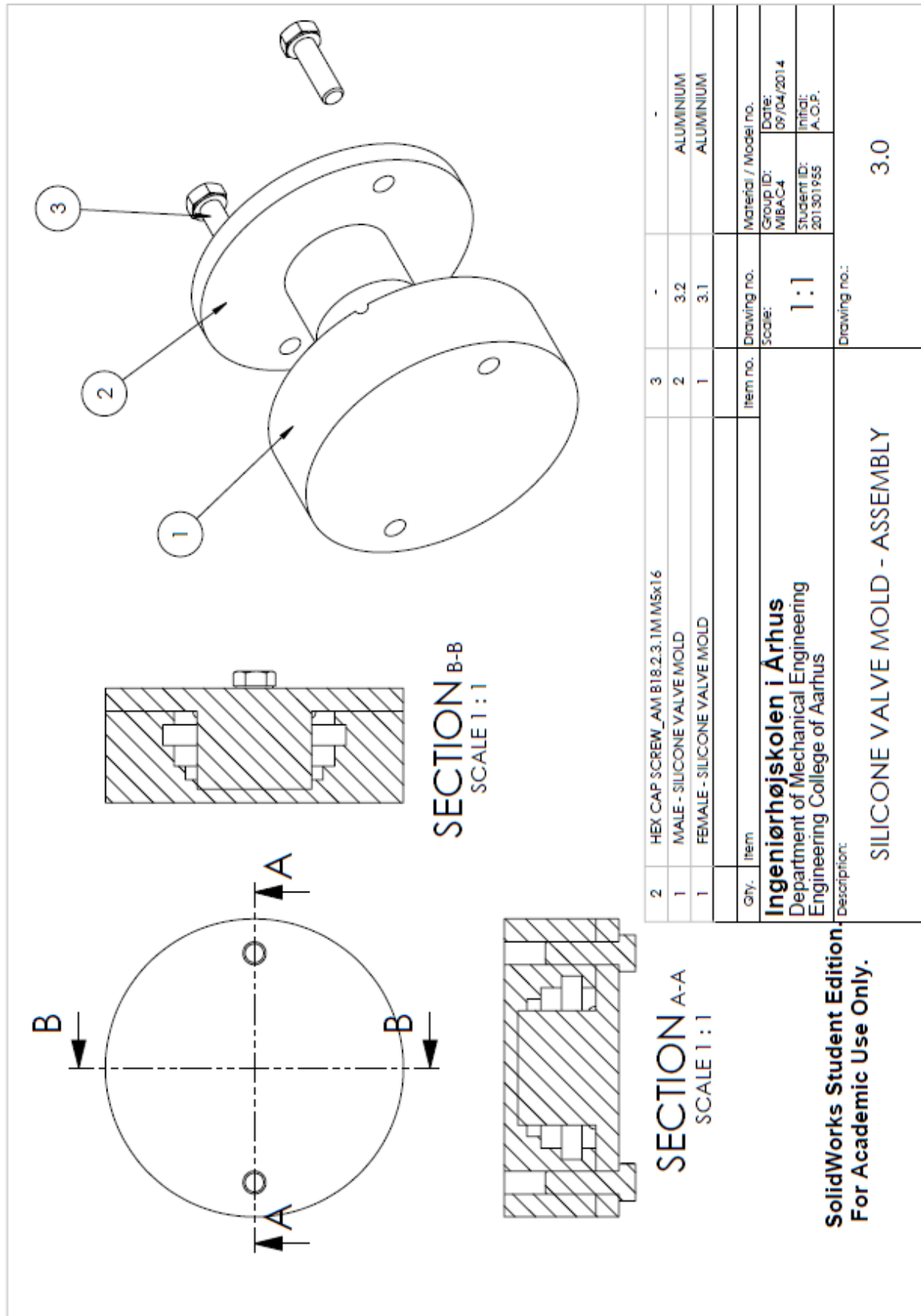
5				STEEL	
Qty.	Item	Item no.	Drawing no.	Material / Model no.	
Ingeniørhøjskolen i Århus Department of Mechanical Engineering Engineering College of Aarhus SolidWorks Student Edition. For Academic Use Only. THREADED BAR M8			Scale:	Group ID: MIBAC4	Date: 01/04/2014
			1:2	Student ID: 201301955	Initial: A.O.P.
Description:			Drawing no.: 2.11		

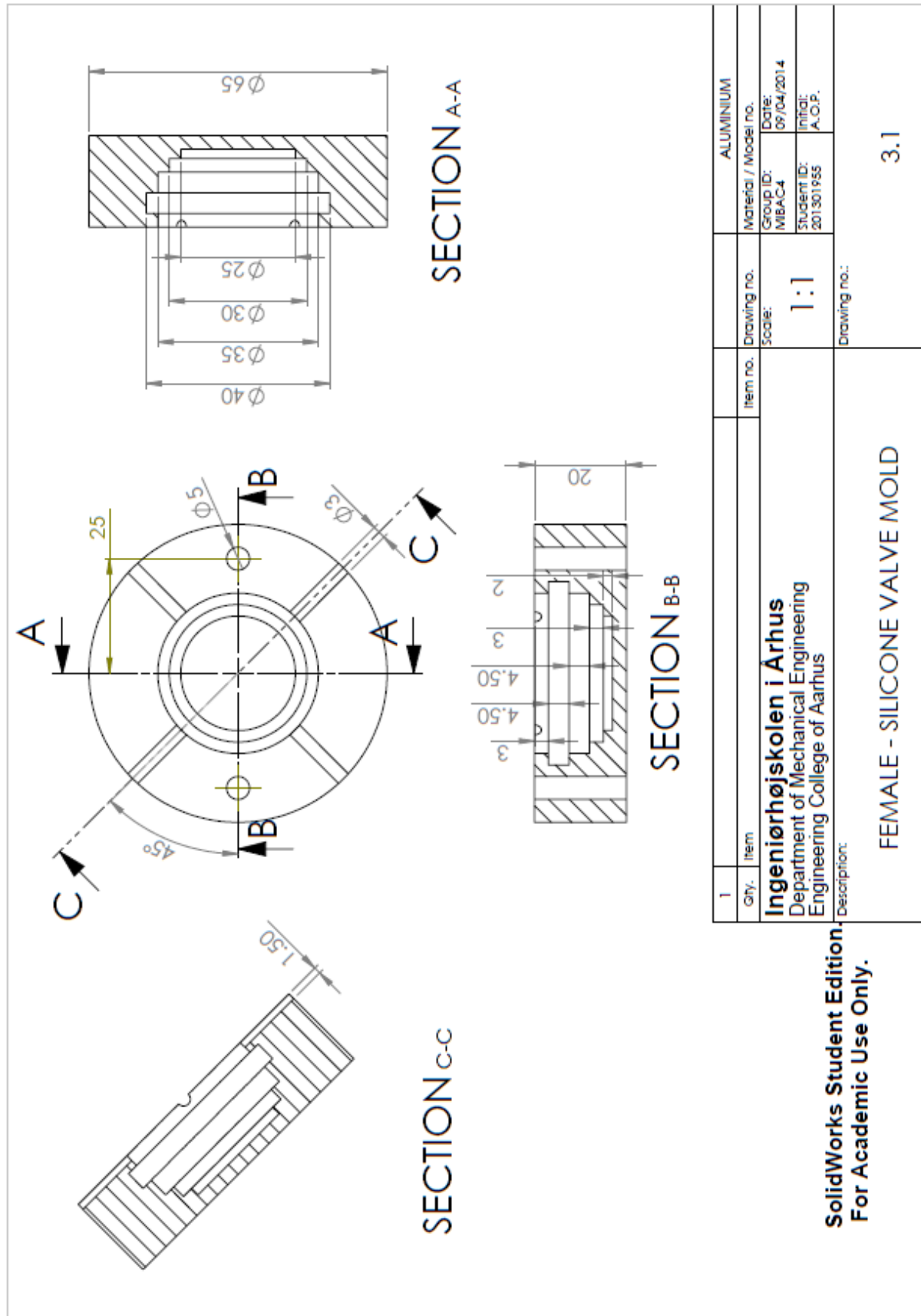


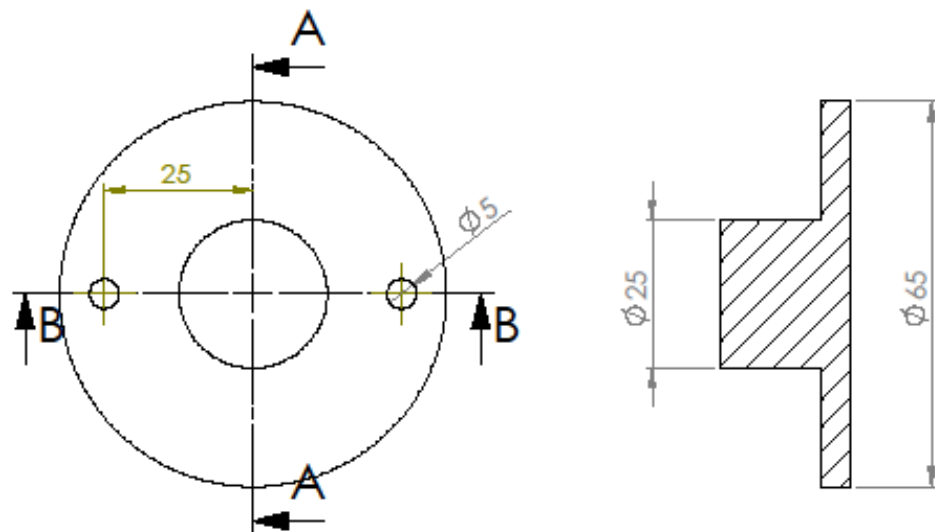
2				ACRYLIC	
Qty.	Item	Item no.	Drawing no.	Material / Model no.	
Ingeniørhøjskolen i Århus Department of Mechanical Engineering Engineering College of Aarhus SolidWorks Student Edition. For Academic Use Only.			Scale:	Group ID: MIBAC4	Date: 01/04/2014
			5:1	Student ID: 201301955	Initial: A.O.P.
Description: PROBE			Drawing no.: 2.12		



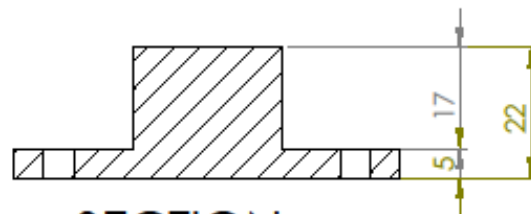
2				RUBBER	
Qty.	Item	Item no.	Drawing no.	Material / Model no.	
Ingeniørhøjskolen i Århus Department of Mechanical Engineering Engineering College of Aarhus SolidWorks Student Edition. For Academic Use Only.			Scale:	Group ID: MIBAC4	Date: 02/04/2014
			2:1	Student ID: 201301955	Initial: A.O.P.
Description: COMPLIANCE CHAMBER - PROP			Drawing no.: 2.13		



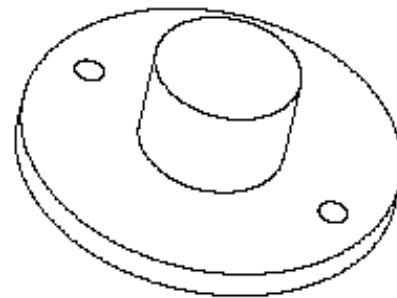




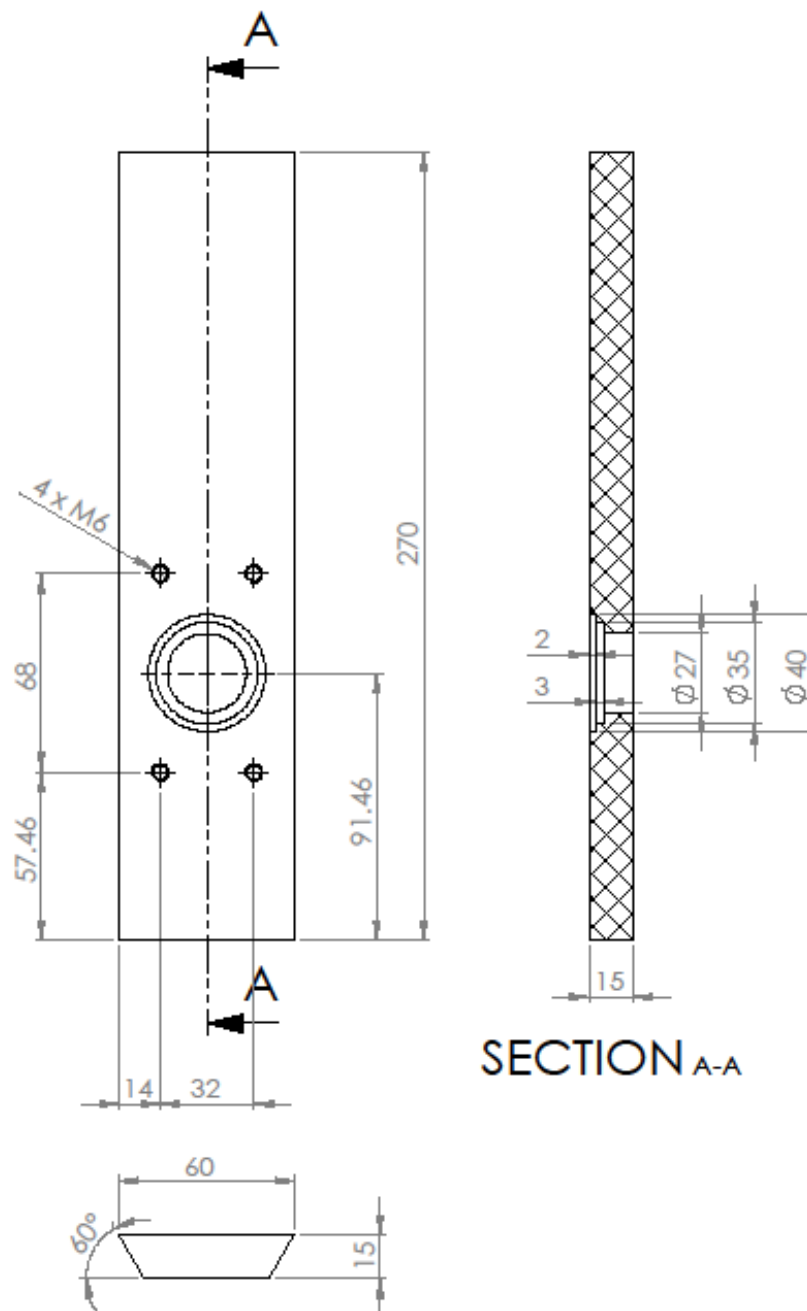
SECTION A-A
SCALE 1 : 1



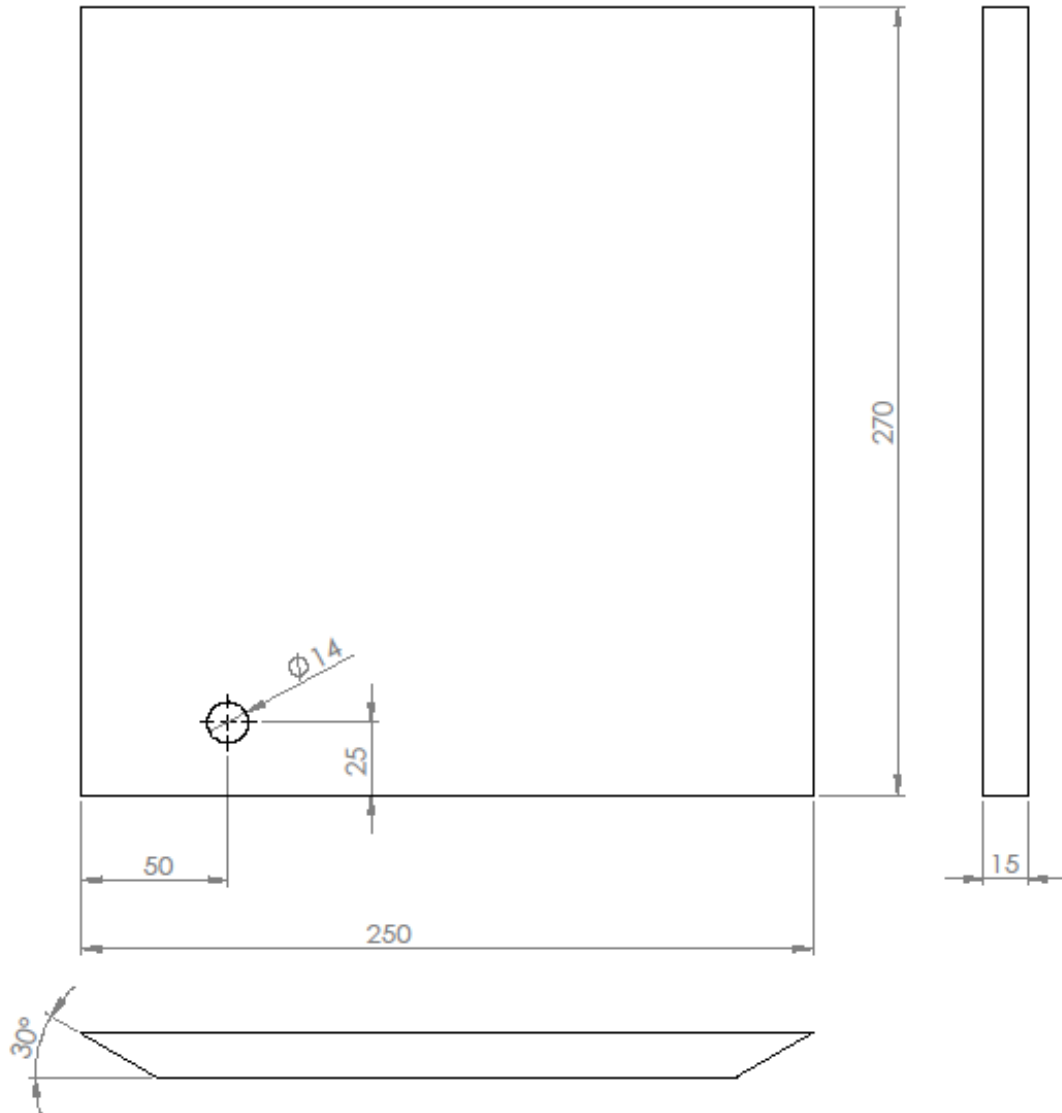
SECTION B-B
SCALE 1 : 1



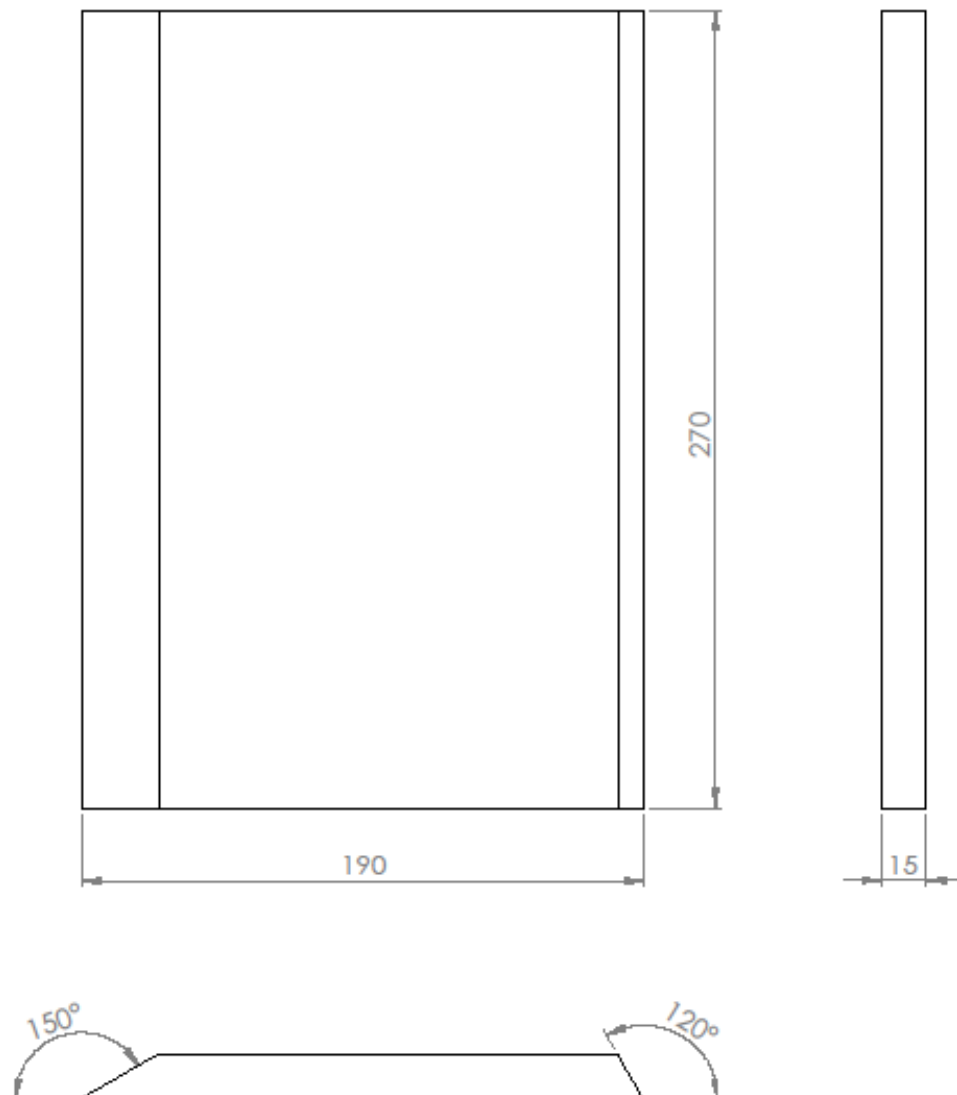
1				ALUMINIUM	
Qty.	Item	Item no.	Drawing no.	Material / Model no.	
Ingeniørhøjskolen i Århus Department of Mechanical Engineering Engineering College of Aarhus SolidWorks Student Edition. For Academic Use Only.			Scale:	Group ID: MIBAC4	Date: 09/04/2014
			1:1	Student ID: 201301955	Initial: A.O.P.
Description: MALE - SILICONE VALVE MOLD			Drawing no.: 3.2		



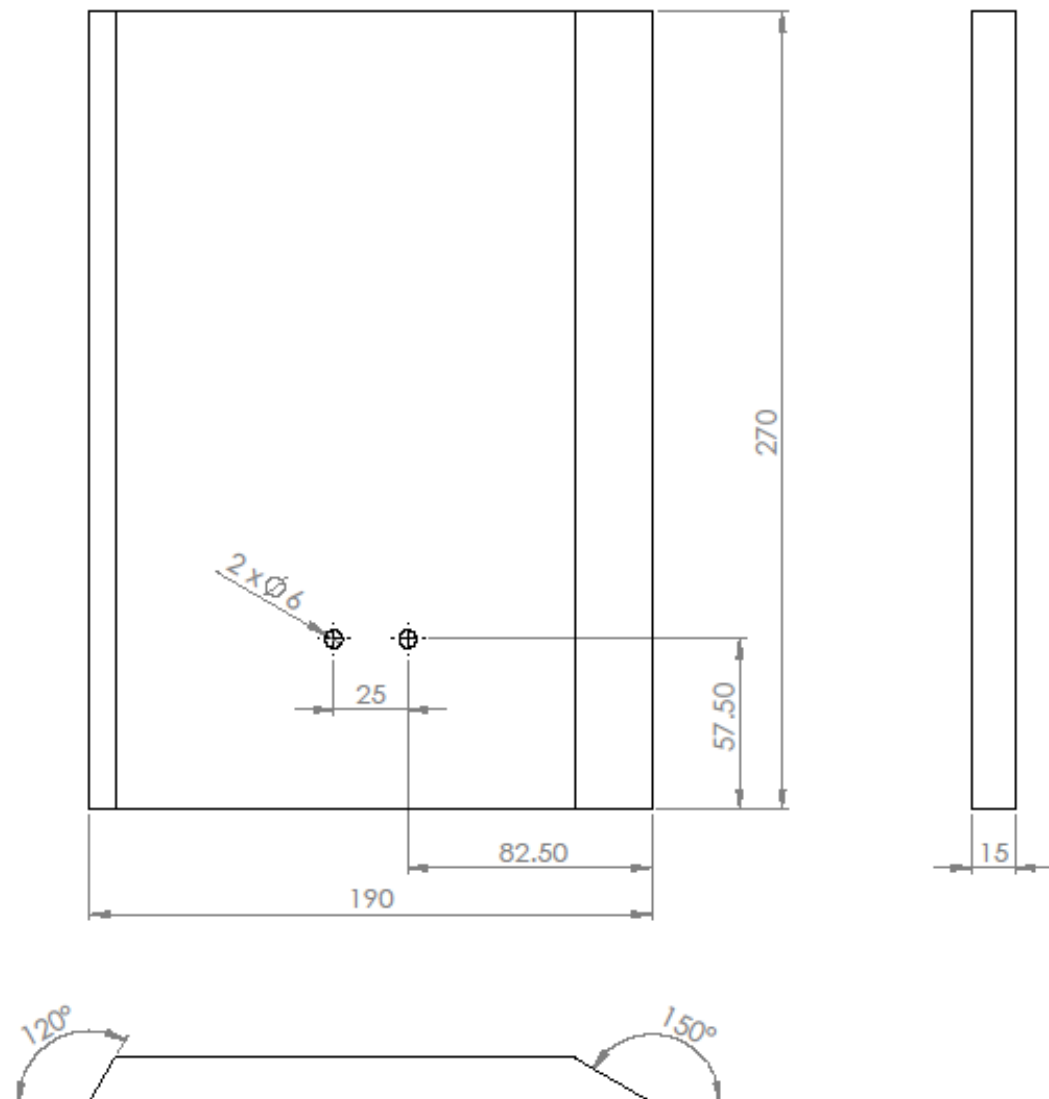
1				PC - POLYCARBONATE
Qty.	Item	Item no.	Drawing no.	Material / Model no.
Ingeniørhøjskolen i Århus Department of Mechanical Engineering Engineering College of Aarhus SolidWorks Student Edition. For Academic Use Only.			Scale:	Group ID: MIBAC4
			1:2	Date: 11/04/2014
Description: ANA phone number: 50120084			Drawing no.:	Initial: A.O.P.
COMPLIANCE CHAMBER - AORTIC ROOT PLATE			4.1	



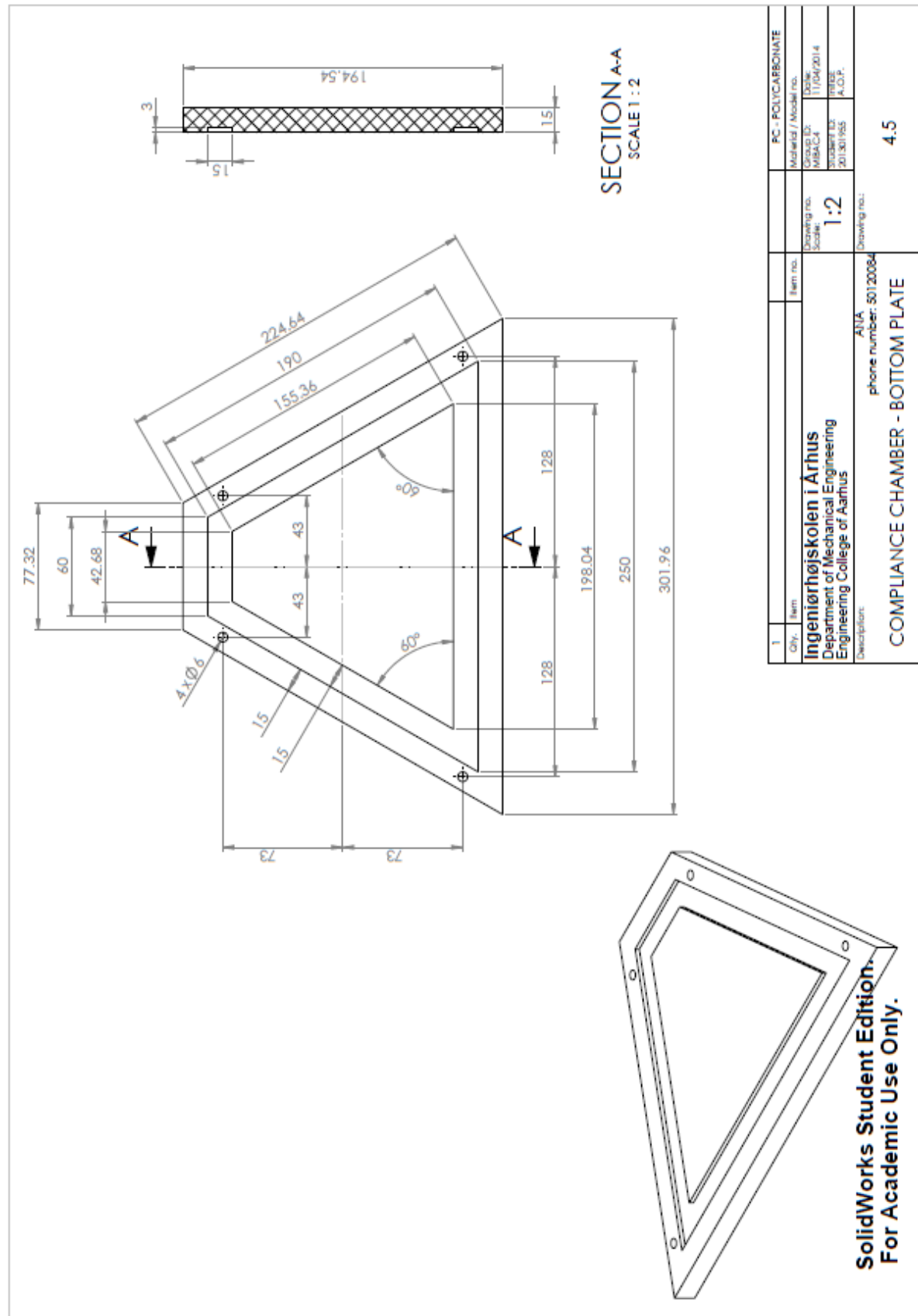
1				PC - POLYCARBONATE	
Qty.	Item	Item no.	Drawing no.	Material / Model no.	
Ingeniørhøjskolen i Århus Department of Mechanical Engineering Engineering College of Aarhus SolidWorks Student Edition. For Academic Use Only. ANA phone number: 50120084			Scale:	Group ID:	Date:
			1:2	MIBAC4	11/04/2014
Description:			Drawing no.:	Student ID:	Initial:
COMPLIANCE CHAMBER - BACK PLATE				201301955	A.O.P.
				4.2	

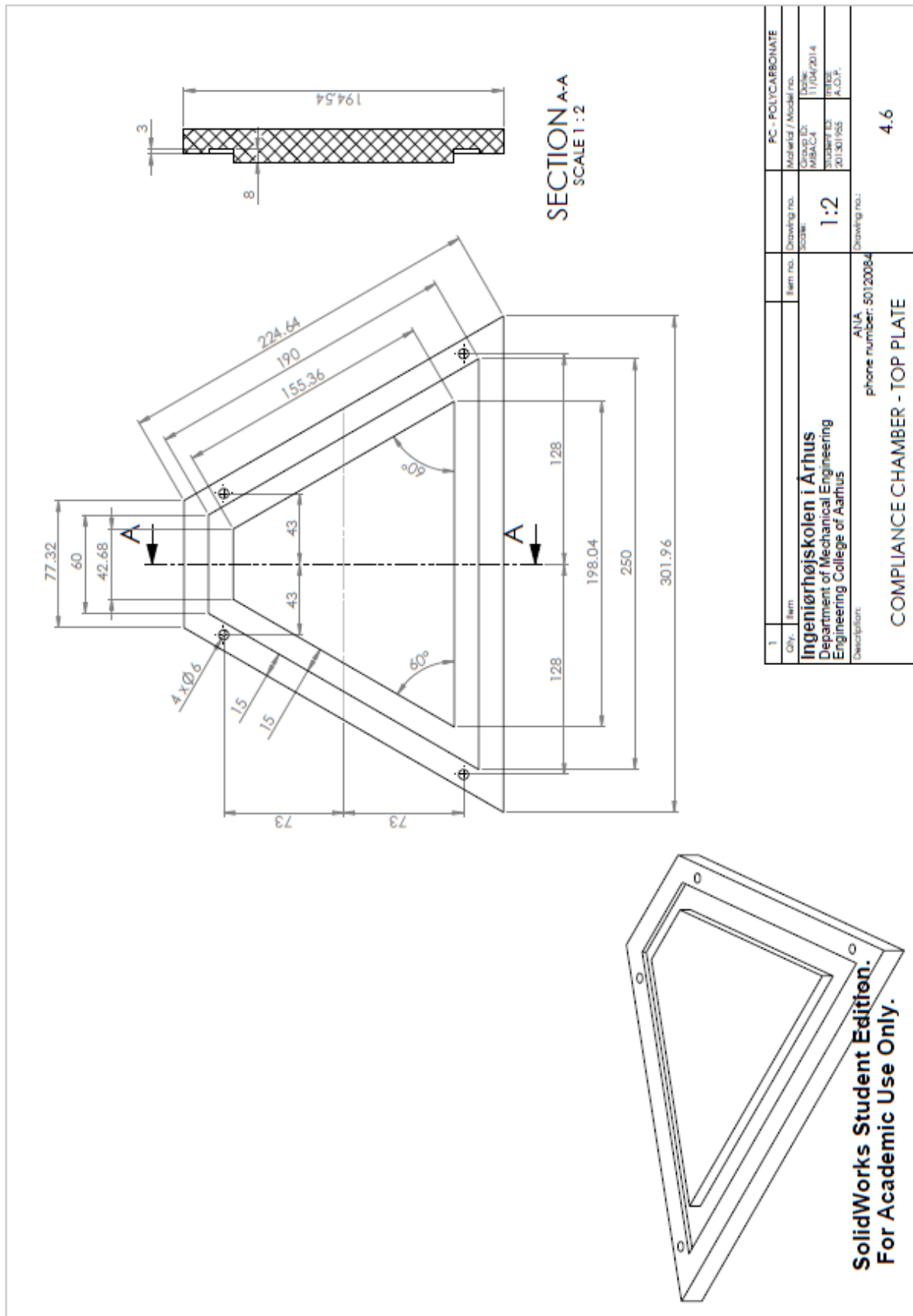


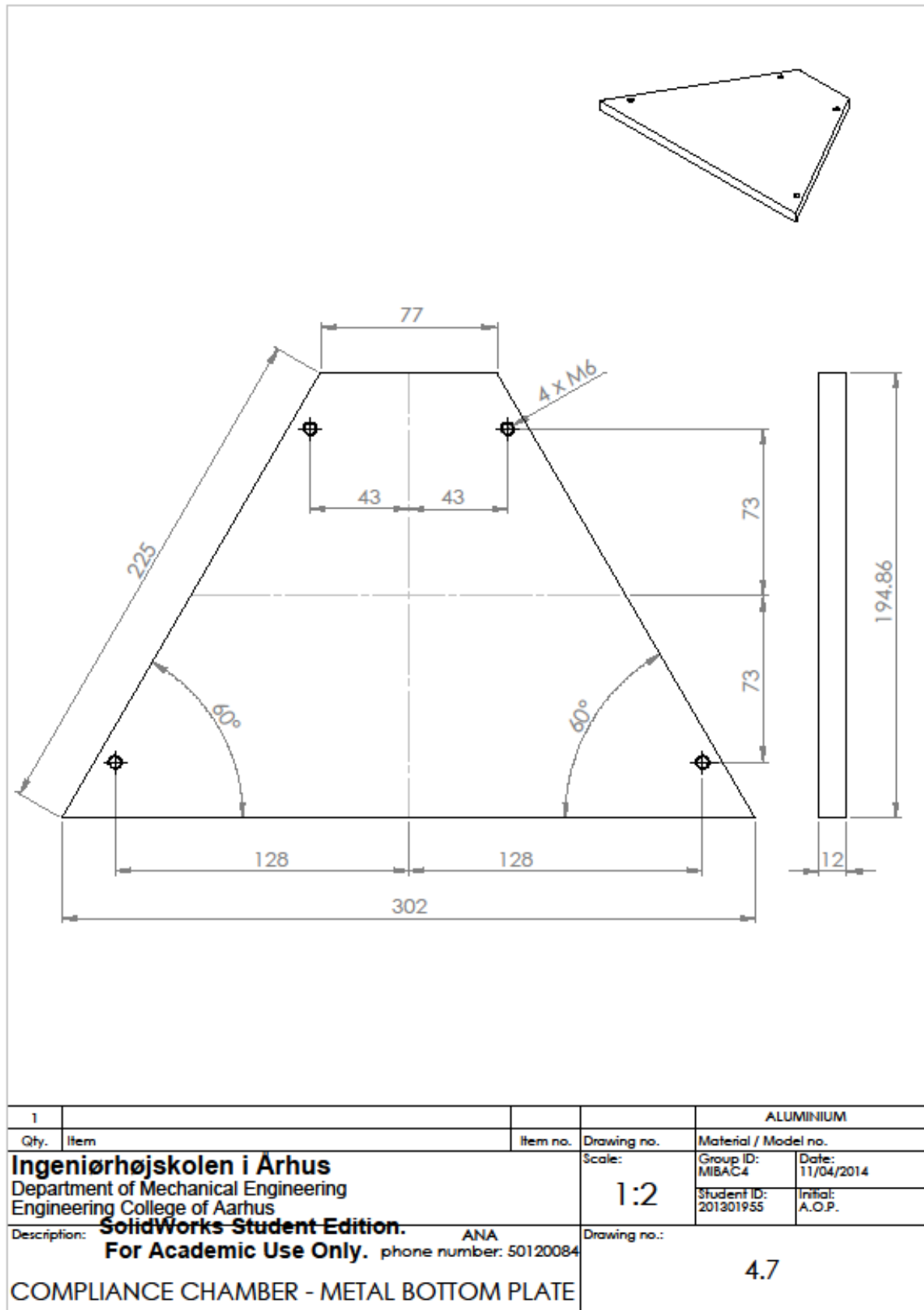
1				PC - POLYCARBONATE	
Qty.	Item	Item no.	Drawing no.	Material / Model no.	
Ingeniørhøjskolen i Århus Department of Mechanical Engineering Engineering College of Aarhus SolidWorks Student Edition. For Academic Use Only. ANA phone number: 50120084			Scale:	Group ID: MIBAC4	Date: 11/04/2014
			1:2	Student ID: 201301955	Initial: A.O.P.
Description:			Drawing no.:	4.3	
COMPLIANCE CHAMBER - SIDE PLATE TO A.C.					

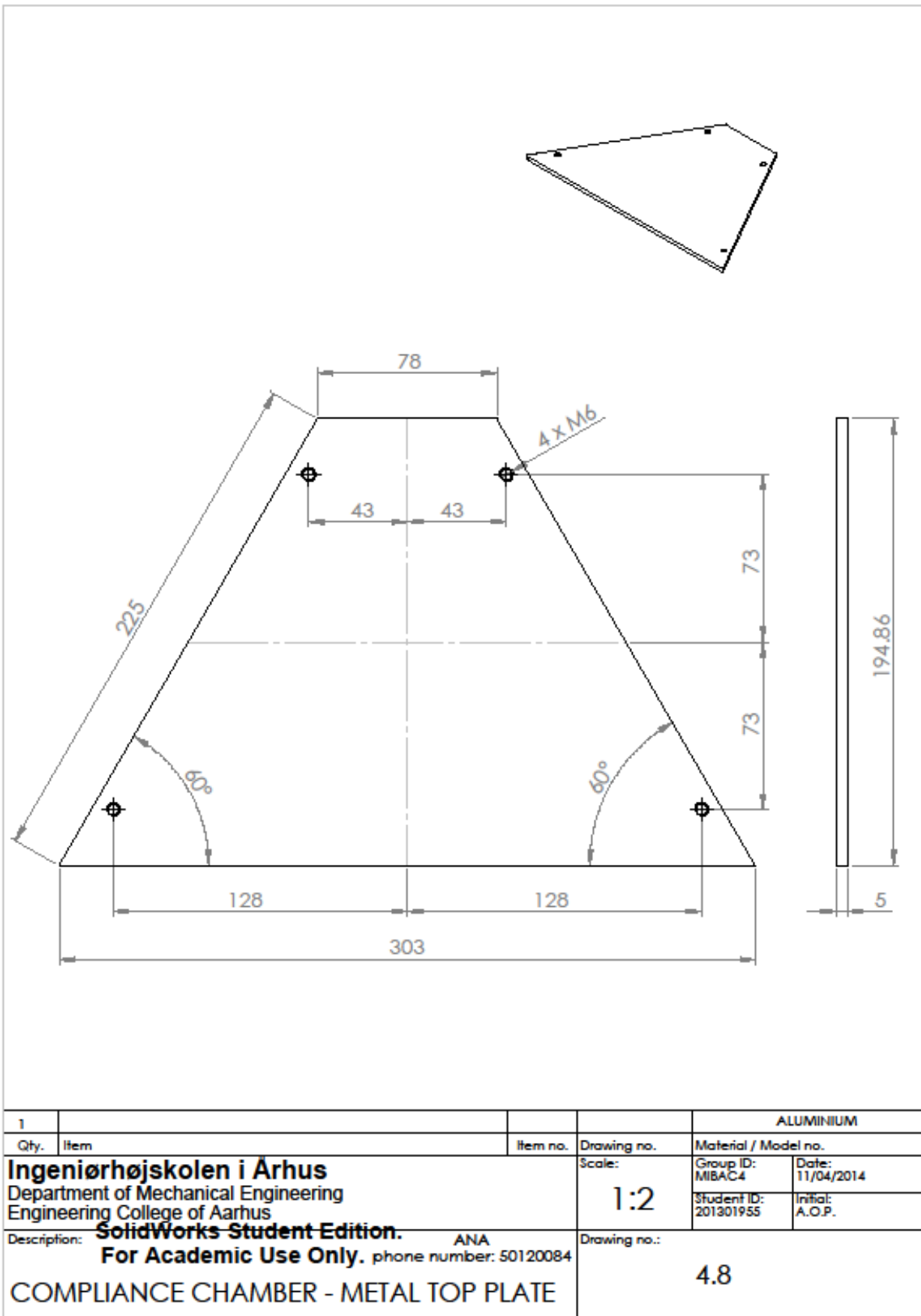


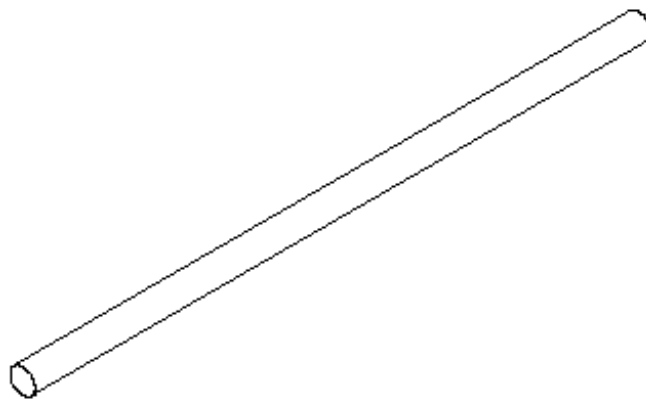
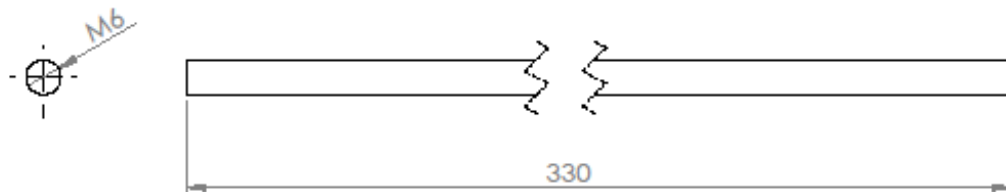
1				PC - POLYCARBONATE	
Qty.	Item	Item no.	Drawing no.	Material / Model no.	
Ingeniørhøjskolen i Århus Department of Mechanical Engineering Engineering College of Aarhus SolidWorks Student Edition. For Academic Use Only. ANA phone number: 50120084			Scale:	Group ID: MIBAC4	Date: 11/04/2014
			1:2	Student ID: 201301955	Initial: A.O.P.
Description: COMPLIANCE CHAMBER - SIDE TO MILLAR CTH.			Drawing no.:	4.4	











4				STEEL	
Qty.	Item	Item no.	Drawing no.	Material / Model no.	
Ingeniørhøjskolen i Århus Department of Mechanical Engineering Engineering College of Aarhus SolidWorks Student Edition. For Academic Use Only. ANA Phone number: 50120084			Scale:	Group ID:	Date:
			1:1	MIBAC4	11/04/2014
Description:			Drawing no.:	Student ID:	Initial:
THREADED BAR M6				201301955	A.O.P.
				4.9	

6- Images and drawings of the mould for the silicone rings

In order to improve the connections between the aortic root and the chambers, minimizing the leakage or trying to avoid it totally, a silicone ring was decided to be used instead of the O-ring used in previous models.

To achieve this silicone ring, a mould in aluminium was designed. Below is possible to see a solid works image of the final silicone ring.



Figure 31 - Silicone ring (A.O.P.)

The mould was designed in aluminium because it was an easy material to achieve in the workshop and due to chemical properties explained in other sections. Below are the images for the mould assembly, the male part and the female part. There are also attached two bolts in order to be possible to have the male and female part centred.

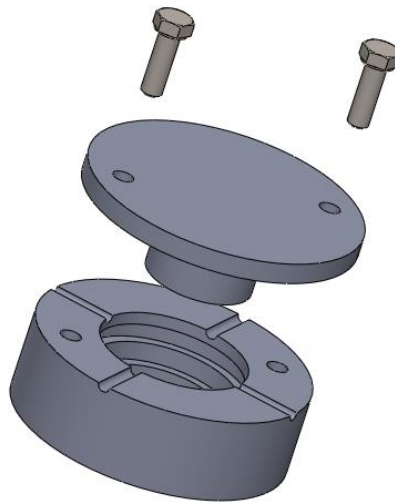


Figure 32 - Mould assembly for the silicone ring (A.O.P.)

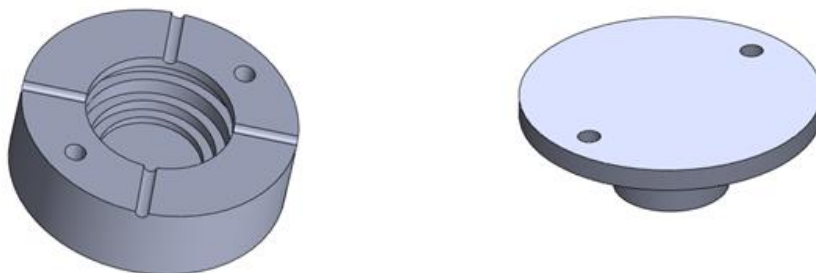


Figure 33 - Female part (right) and male part (left) (A.O.P.)

7- Equipment

Following it described the equipment used to do the connection tests analysis.

- *Torque wrench*: it is a tool which is used to apply the precisely torque to a fastener, such a bolt or a nut.



Figure 34 - Torque wrench (A.O.P.)

- *Bench vice*: is a mechanical device used to secure an object to allow work to be performed on it. It has two parallel jaws, one fixed and the other mobile, threaded in and out by a screw and lever.



Figure 35 - Bench Vice (A.O.P.)

- *Milling machine*: it is a machine which works using rotary cutters to remove material from a work piece, advancing in a direction at an angle with the axis of the tool.
- *Manual thread milling machine*: it is a tool which works using rotary cutters. By using this tool, it is possible to thread a hole manually.
- *Fastener elements*: bolts, nuts, washers are elements used to do the analysis.
- *Specimens*: acrylic specimens were built in the workshop in order to connect and do the experiments with them.



Figure 36 - Specimens (A.O.P.)

Below is shown the final assembly to carry out with the connection tests.



Figure 37 - General assembly (A.O.P.)

8- Fluid mechanics theory to achieve Bernoulli equation

² In order to calculate the pressure inside the compliance chamber, it is necessary to explain briefly the theory that supports the calculations.

To calculate the pressure, it is going to be assumed fluid statics. Therefore, the fluid is going to be considered at rest owing to be evaluated. If a fluid is in rest, it does not experience any net force anywhere. If a small part of fluid, all forces, external and internal must be balanced. By force balance calculations in 'x', 'y' and 'z' direction it is inferred that the fluid cannot depend on the 'y' direction and neither on the 'x' direction. However, it is dependent on the 'z' direction due to the gravity force.

$$0 = p\left(x, y - \frac{\Delta y}{2}, z\right) \Delta x \Delta z - p\left(x, y + \frac{\Delta y}{2}, z\right) \Delta x \Delta z$$

$$p\left(x, y - \frac{\Delta y}{2}, z\right) = p\left(x, y + \frac{\Delta y}{2}, z\right)$$

Equation 1 - Force balance in 'y' direction

$$0 = p\left(x - \frac{\Delta x}{2}, y, z\right) \Delta y \Delta z - p\left(x + \frac{\Delta x}{2}, y, z\right) \Delta y \Delta z$$

$$p\left(x - \frac{\Delta x}{2}, y, z\right) = p\left(x + \frac{\Delta x}{2}, y, z\right)$$

Equation 2 - Force balance in 'x' direction

$$0 = p\left(x, y, z - \frac{\Delta z}{2}\right) \Delta x \Delta y - p\left(x, y, z + \frac{\Delta z}{2}\right) \Delta x \Delta y - g\rho(x, y, z) \Delta x \Delta y \Delta z$$

$$0 = p\left(z - \frac{\Delta z}{2}\right) - p\left(z + \frac{\Delta z}{2}\right) - g\rho(x, y, z) \Delta z$$

$$\frac{p\left(z - \frac{\Delta z}{2}\right) - p\left(z + \frac{\Delta z}{2}\right)}{\Delta z} = -g\rho(x, y, z)$$

$$\frac{dp}{dz} = -g\rho$$

Equation 3 - Force balance in 'z' direction

Consequently, it can be inferred hydrostatic equilibrium for a fluid at rest. Hence, fluid at rest experiences that the pressure is constant in any horizontal plane and a decreasing pressure with height at the ratio of $g\rho$.

² Basics of fluid mechanics, Notes from Uffe Vestergaard Poulsen (Assistant professor – Department of Engineering – Sustainable Energy Systems)

Fluids obey energy conservation; to explain the mechanical energy conservation in particles it is used the mechanical energy equation as the starting point and then do derivative time. Finally it is achieved that the mechanical energy equation derivate is equal to zero, which means that mechanical energy is preserved between two situations.

$$E_{mech}(x, v) = \frac{1}{2}mv^2 + U(x)$$

Equation 4 - Mechanical energy equation

$$\frac{dE_{mech}(x, v)}{dt} = 0$$

Equation 5 - Derivate of the mechanical energy equation

The same procedure is used to fluid particles, achieving Bernoulli equation. There is need to take into account the hydrostatic equilibrium, suppose steady flow and constant density. Therefore, the Bernoulli equation for inviscid, steady and incompressible flow is the one bellow.

$$\frac{1}{2}\rho v^2 + p(r) + g\rho z = cte$$

Equation 6 - Bernoulli equation

9- Compliance chamber pressure calculation

The maximum pressure in the chamber will be in the bottom plate surface, according to the properties explained in the theoretical part – section 8. In order to calculate pressure, the limit water height used (z) is the minimum possible one, just above the aortic root inlet.

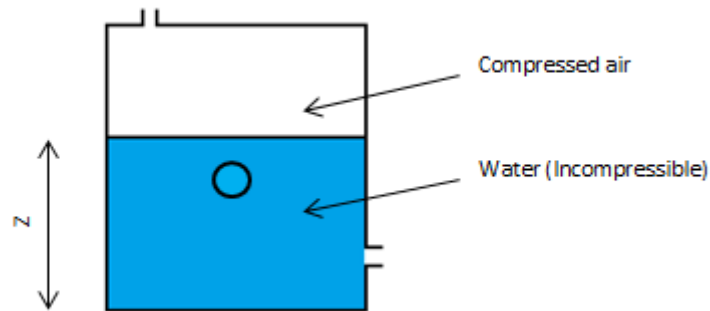


Figure 38 - Simplified compliance chamber (A.O.P.)

The height value, z , for the new compliance chamber designed is 101.96 mm \approx 102 mm

$$\frac{1}{2}\rho v_A^2 + P_A + \rho g z_A = \frac{1}{2}\rho v_W^2 + P_W + \rho g z_W$$

$$P_A - \rho g z_W = P_W$$

Equation 7 - Bernoulli equation applied in this problem ³

$$P_W = 120 \cdot 10^3 [Pa] - 1000 \left[\frac{kg}{m^3} \right] \cdot 9.81 \left[\frac{m}{s^2} \right] \cdot (-0.102[m]) = 121000.62 Pa$$

$$121000.62 [Pa] = 121 [KPa] = 907.14 [mm Hg]$$

Equation 8 - Solution to the Bernoulli equation applied in this problem (A.O.P.)

So the pressure at the bottom plate is 121 [KPa]. This value is significantly close to the compressed air pressure, 120 [KPa] therefore its contribution can be ignored. The water contribution in the new model is consequently possible to be neglected. Same hypothesis has been used for the old model. For screws forces' calculation a value of pressure inside the chamber of 120 [KPa] has therefore been used.

³ Basics of fluid mechanics, Notes from Uffe Vestergaard Poulsen (Assistant professor – Department of Engineering – Sustainable Energy Systems)

10- Compliance chamber's wall force calculations

In this section is the explanation of force calculation in the compliance chamber. For this calculation is going to be supposed the air is since the beginning with a value of 1.2 [bar] constant, as there is no pressure gauge to ensure more accurate pressure values. It is going to be calculated the force due to the water and due to the air in the back plate, isolating the deposit in order to simplify the problem. Moreover, this chamber is the only desired to be calculated. However, in the reality there are more agents that must be taken into account, such as the pump forcing the water direct to the chamber according the value of the cardiac output and the peripheral resistance (clamp).

In order to calculate the force due to the air, below are going to be explained the steps needed to be followed. Pressure can be calculated by using the following equation;

$$P [MPa] = \frac{F [N]}{A [mm^2]}$$

Equation 9 - Pressure

The pressure is supposed constant and the area is a known value, therefore the force value is known too.

To calculate the force in the water section is needed to know the pressure due to the water column by Bernoulli equation as explained in previous sections – appendix section 8.

$$P [Pa] = \rho \left[\frac{kg}{m^3} \right] g \left[\frac{m}{s^2} \right] h[m]$$

Equation 10 – Bernoulli equation

In the following table are shown the values of force owing to the water column and due to the air. It has been calculated since the chamber is completely filled of water without air until it is filled only with air. And below is the graph that represents these forces. It is seen that the force created by the air is much higher than the water column influence.

air [%]	water [%]	Area air [mm ²]	Area water [mm ²]	Height water [mm]	Force air [N]	Pressure water [Pa]	Force water [N]	Sum of forces [N]
0	100	0	34060	262	0	2570.22	43.77	43.77
10	90	3406	30654	235.8	408.72	2313.20	35.45	444.17
20	80	6812	27248	209.6	817.44	2056.18	28.01	845.45
30	70	10218	23842	183.4	1226.16	1799.15	21.45	1247.61
40	60	13624	20436	157.2	1634.88	1542.13	15.76	1650.64
50	50	17030	17030	131	2043.6	1285.11	10.94	2054.54
60	40	20436	13624	104.8	2452.32	1028.09	7.00	2459.32
70	30	23842	10218	78.6	2861.04	771.07	3.94	2864.98
80	20	27248	6812	52.4	3269.76	514.04	1.75	3271.51
90	10	30654	3406	26.2	3678.48	257.02	0.44	3678.92
100	0	34060	0	0	4087.2	0.00	0.00	4087.20

Table 4 - Forces calculation Graph in the compliance chamber's back wall because of air and water (A.O.P.)

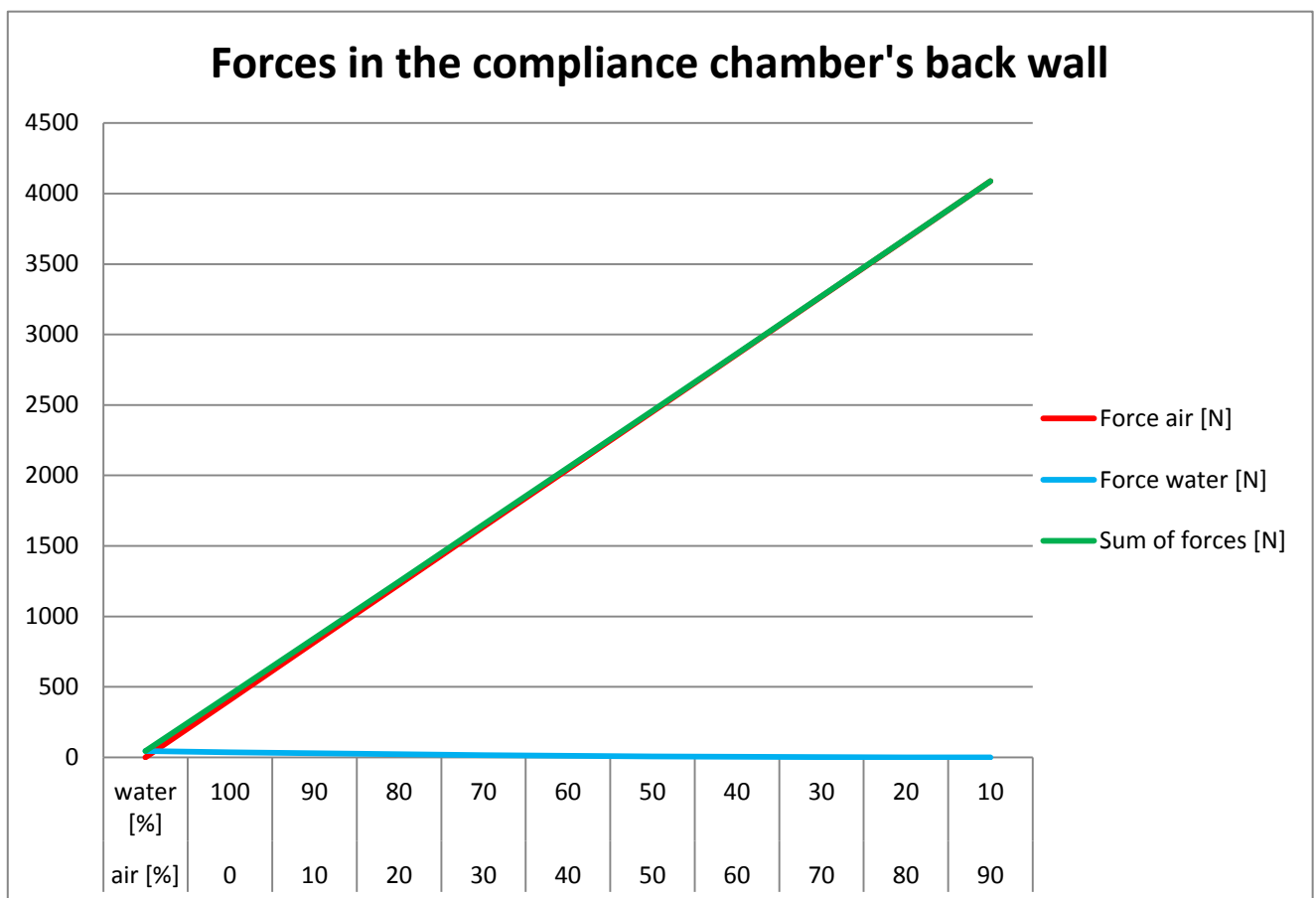


Figure 39 - Graph of forces in the compliance chamber's back wall (A.O.P.)

When the sum of forces produces a shear stress higher than the one that the connection can support, then the connection breaks. The connections in the walls are suffering a shear stress which can be calculated by the following equation^{4 5}; the shear stress in glue connections depend on the material and its thickness, the glue and the glued area.

$$\tau_{max} = \tau_{mean} \sqrt{\frac{G l_o^2}{2 E s d}} \coth \sqrt{\frac{G l_o^2}{2 E s d}}$$

Equation 11 - Volkersen's Equation

$$\tau_{mean} = \frac{F}{A} = \frac{F}{b l_o}$$

Equation 12 - Middle shear stress value

Note that τ_{max} is the maximum stress the connection can support, **G** is the shear modulus, **E** is the Young Modulus, **F** is the force, **A** is the shear area (with **b** the width and **l_o** the overlapping length), **s** is the plate thickness and **d** is the glue layer thickness.

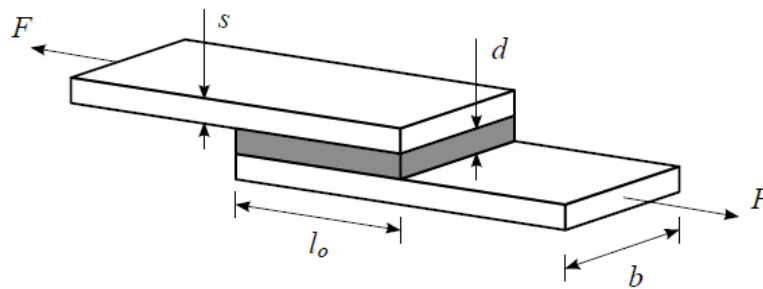


Figure 40 - Glue connection of two plates with dimensions⁶

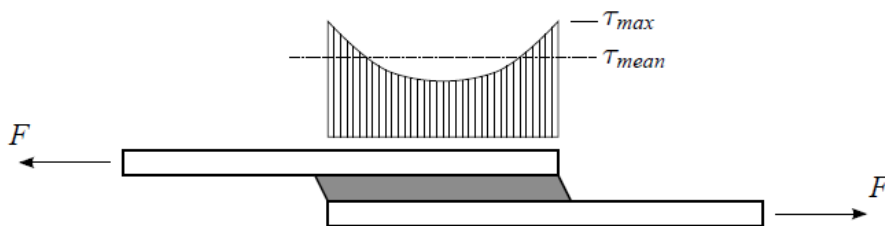


Figure 41 - Shear stress distribution in a glue connection of two plates⁷

⁴ Notes from Thomas Greve (Aarhus University school of Engineering – Materials)

⁵ <http://biblioises.com.ar/Contenido/500/550/Tecnologia%20Adhesivos.pdf> (pages 83 – 86)

⁶ Notes from Thomas Greve (Aarhus University school of Engineering – Materials)

⁷ Notes from Thomas Greve (Aarhus University school of Engineering – Materials)

11- Compliance chamber screws force and stress theoretical calculations

In order to calculate the forces in the screws it is going to be used the following equation which relates force and pressure.

$$P [Pa] = \frac{F[N]}{A[m^2]}$$

Equation 13 - Relation between force and pressure

As it was explained in the previous section, the pressure that is going to be used is 120 [kPa], supposed uniform in the whole chamber. The pressure is always normal to the surface in which is applied.

The volume chamber that is going to be taken into account is the internal one, neglecting the thickness of the walls. The walls are going to be analysed alike very thin layers, i.e. simplifying them to a 2D problem since one of the dimensions (the thickness of the wall) is much smaller than the other two dimensions (height and width of the walls).

Furthermore; it is not going to take into consideration the glue between the walls neither the force caused by the other kind of connections, such as the recess in between some walls (top plate and bottom plate with the side plates). Therefore, the only force analysis which is going to be analysed is the screw connection.

The chamber assembly is symmetrical and that simplifies the problem. However, there are only screws in the top plate. The bottom plate as is in direct contact with the table thus there was no need for those screws. Focusing in the side walls and in the back and front plate, in order to make them symmetrical for the force calculation, the glue part in the bottom area is going to be approximated to the same number of screws as there is the upper part.

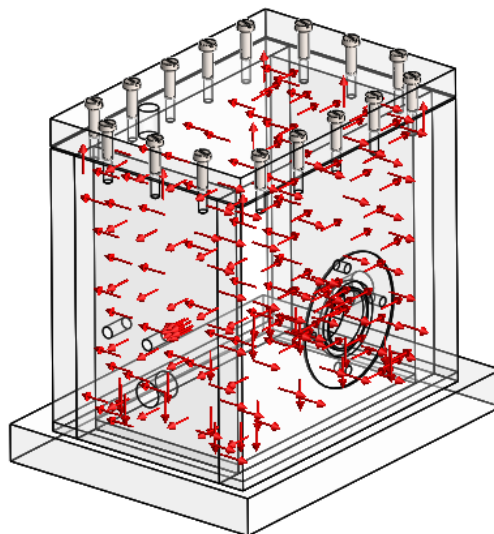


Figure 42 - Pressure distribution in the compliance chamber (A.O.P.)

- 1- Firstly, it is going to be calculated those forces in the old compliance chamber. The first wall to be analysed is the top plate.

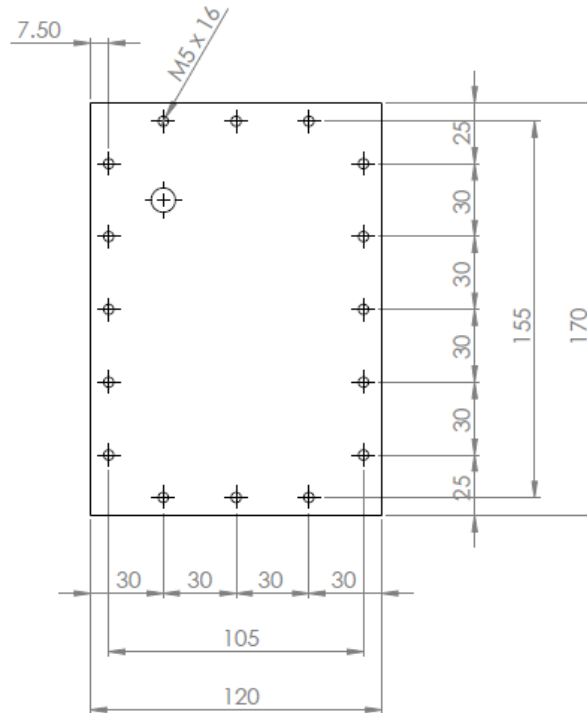


Figure 43 - Top plate dimensions (A.O.P.)

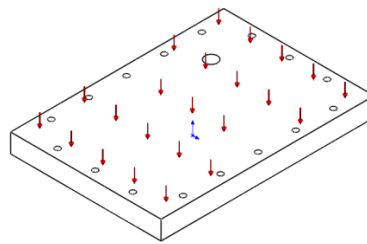


Figure 44 - Pressure distribution in the top plate (A.O.P.)

The surface area;

$$A = 120 \times 170 = 20400 \text{ [mm}^2\text{]}$$

To calculate de force in each screw;

$$\text{Total force in the plate, } F[\text{N}] = 0.12 \left[\frac{\text{N}}{\text{mm}^2} \right] \times 20400 \text{ [mm}^2\text{]} = 2448 \text{ [N]}$$

$$\text{Force in each screw, } F_s[\text{N}] = \frac{F}{\text{number of screws}} = \frac{2448}{16} = 153 \text{ [N]}$$

To calculate the stress in the screw, first is calculated the cross section area perpendicular to the force;

$$A_{screw} = \pi r^2 = \pi 2.5^2 = \frac{25}{4} \pi [mm^2]$$

$$Stress, \sigma = \frac{F_{screw}}{A_{screw}} = \frac{153}{\frac{25}{4} \pi} = 7.7922 [MPa]$$

- 2- The second wall to be analysed is the side one, as the chamber is symmetric, the analysis is only going to be done in one of the sides; being equal for the other one.

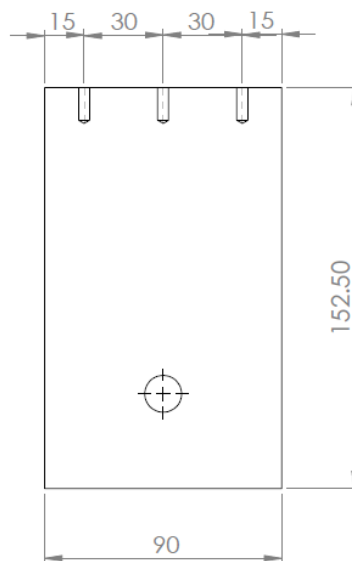


Figure 45 - Side plate dimensions (A.O.P.)

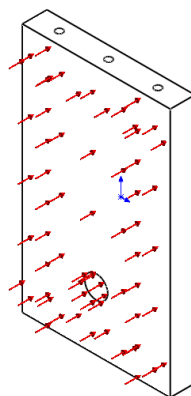


Figure 46 - Pressure distribution in the side plate (A.O.P.)

The surface area;

$$A = 90 \times 152,50 = 13725 \text{ [mm}^2\text{]}$$

To calculate the force in each screw;

$$\text{Total force in the plate, } F[\text{N}] = 0.12 \left[\frac{\text{N}}{\text{mm}^2} \right] \times 13725 \text{ [mm}^2\text{]} = 1647 \text{ [N]}$$

$$\text{Force in each screw, } F_s[\text{N}] = \frac{F}{\text{number of screws}} = \frac{1647}{6} = 274,5 \text{ [N]}$$

Note: the number of screws in real is only 3, but the glue area has been approximated into the same number of screws as in the upper part, making the wall symmetrical and clearer to be calculated, as the approximation is not relevant for the results.

To calculate the stress in the screw, first is calculated the cross section area perpendicular to the force;

$$A_{\text{screw}} = 16 \times 5 = 80 \text{ [mm}^2\text{]}$$

$$\text{Stress, } \sigma = \frac{F_{\text{screw}}}{A_{\text{screw}}} = \frac{274,5}{80} = 3.4312 \text{ [MPa]}$$

- 3- The third wall to be analysed is the front plate, as the chamber is symmetric, the analysis for the back plate is equal to it.

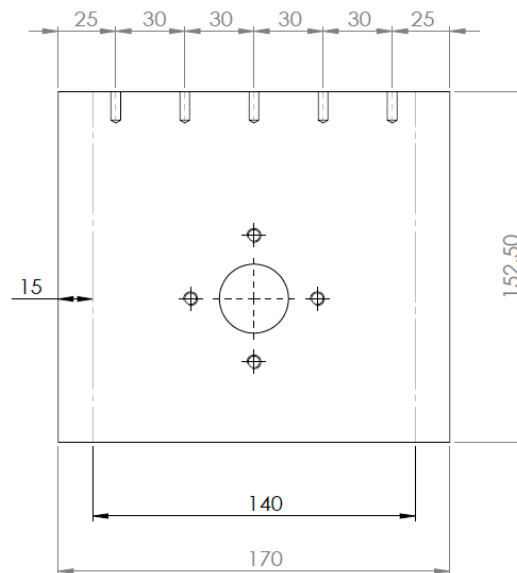


Figure 47 - Side plate dimensions (A.O.P.)

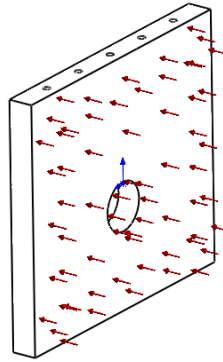


Figure 48 - Pressure distribution in the side plate (A.O.P.)

The surface area; the one chosen is because I neglect the thickness of the walls, to simplify the calculations.

$$A = 170 \times 152.5 = 25925 \text{ [mm}^2\text{]}$$

To calculate de force in each screw;

$$\text{Total force in the plate, } F[\text{N}] = 0.12 \left[\frac{\text{N}}{\text{mm}^2} \right] \times 25925 \text{ [mm}^2\text{]} = 3111 \text{ [N]}$$

$$\text{Force in each screw, } F_s[\text{N}] = \frac{F}{\text{number of screws}} = \frac{3111}{10} = 311.1 \text{ [N]}$$

Note: the number of screws in real is only 5, but as it was explained before the glue area is going to be approximated to the same number of screws as in the upper part, making the wall symmetrical and clearer to be calculated, as the approximation is not relevant for the results.

To calculate de stress in the screw, first is calculated the cross section area perpendicular to the force;

$$A_{\text{screw}} = 16 \times 5 = 80 \text{ [mm}^2\text{]}$$

$$\text{Stress, } \sigma = \frac{F_{\text{screw}}}{A_{\text{screw}}} = \frac{311.1}{80} = 3.8887 \text{ [MPa]}$$

To sum up, in the following graphs are going to be resume the forces and the stresses in the screws in each side with its direction.

Forces:

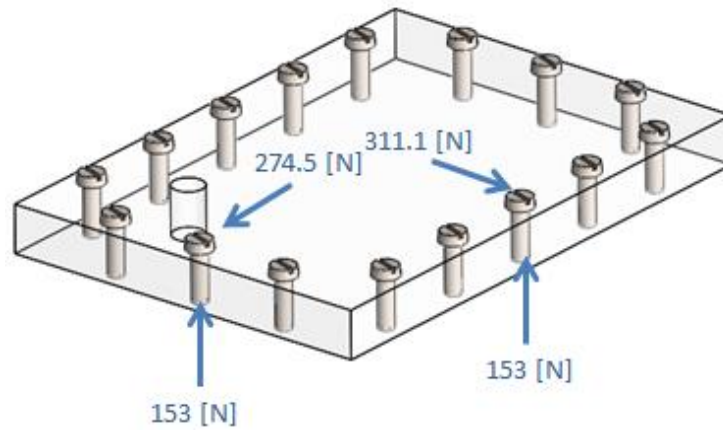


Figure 49 - Forces in the screws/Old chamber (A.O.P.)

Stresses:

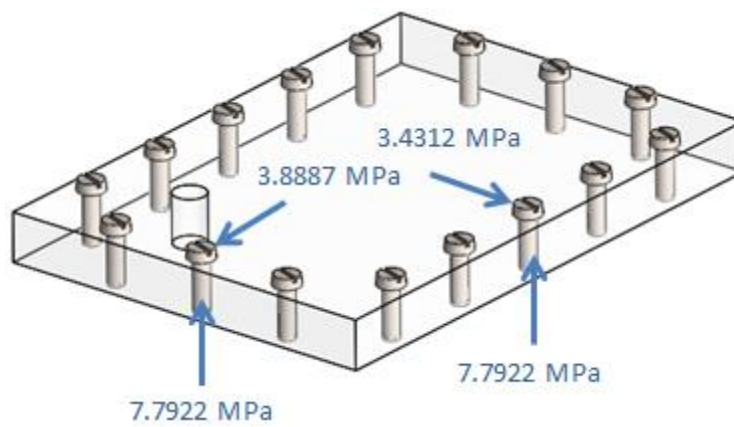


Figure 50 - Stresses in the screws/Old chamber (A.O.P.)

- 4- Analysing the new model is only required to calculate the top plate, due to the connections are outside the pressure area so it only would affect the top plate screw's connections.

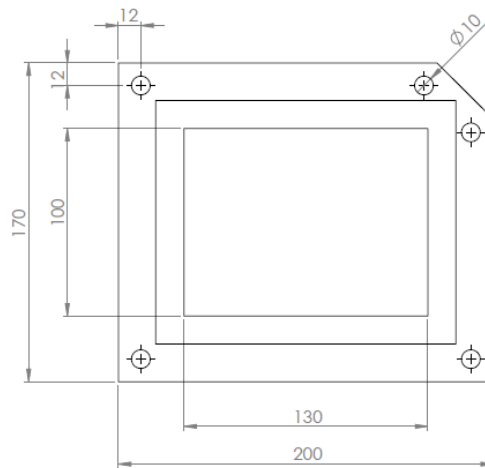


Figure 51 - Top plate dimensions (A.O.P.)

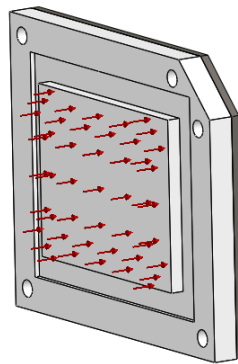


Figure 52 - Pressure distribution in the top plate (A.O.P.)

The surface area;

$$A = 176 \times 146 = 25696 \text{ [mm}^2\text{]}$$

To calculate de force in each screw;

$$\text{Total force in the plate, } F[\text{N}] = 0.12 \left[\frac{\text{N}}{\text{mm}^2} \right] \times 25696 \text{ [mm}^2\text{]} = 3083.52 \text{ [N]}$$

$$\text{Force in each screw, } F_s[\text{N}] = \frac{F}{\text{number of screws}} = \frac{3083.52}{4} = 770.88 \text{ [N]}$$

Note: the number of screws in real is 5. This calculation has been done with 4 screws in order to do the system symmetrical to be able to use the formula above, as if it was a rectangle wall with a hole in each corner.

To calculate the stress in the screw, first is calculated the cross section area perpendicular to the force;

$$A_{screw} = \pi r^2 = \pi 4^2 = 16\pi \text{ [mm}^2\text{]}$$

$$\text{Stress, } \sigma = \frac{F_{screw}}{A_{screw}} = \frac{770.88}{16\pi} = 15.3361 \text{ [MPa]}$$

To sum up, in the following graphs are going to be resumed the forces and the stresses in the screws.

Forces:

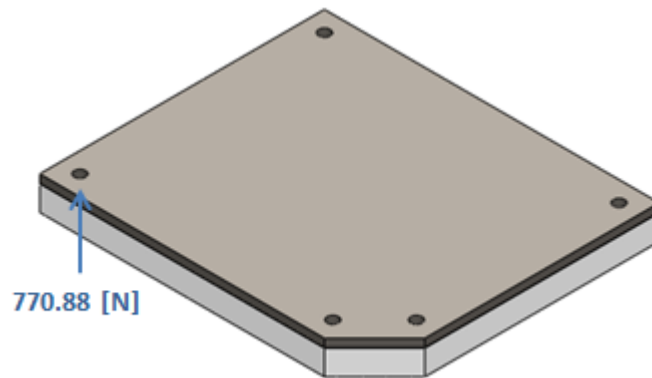


Figure 53 - Forces in the screws (A.O.P.)

Stresses:

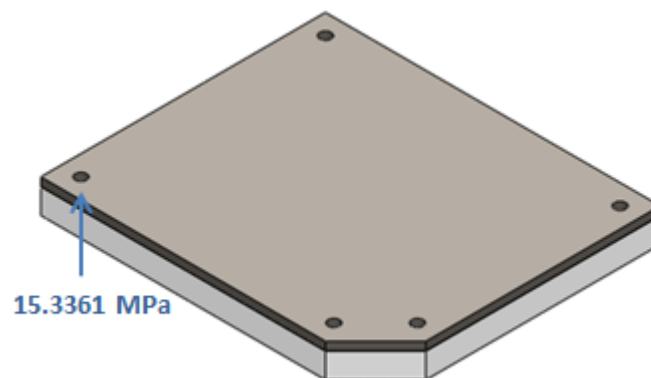


Figure 54 - Stresses in the screws (A.O.P.)

12- Compliance chamber screw's stress simulations

⁸ All the theoretical calculations done in the previous section were also done with Solid-Works simulations, achieving enough closed values to be compared. It was simulated not only the old model but also the new one, showing the new one will present less cracking problems due to the change of material and the new configuration. Note that, even though the results are fairly closed to the theoretical calculations, many assumptions were done. In this section are going to be explained the simulations and the assumptions done. Also it is detailed a comparison between the theoretical and Solid Works calculations.

First, it is explained the old model and the three walls analysed: top, side and front plate.

1- Top plate:

Two simulations were done, the first one with threaded holes and the second one without them. Once the first simulation was done, the threaded results achieved were not good enough and it was recommended to analyse it with clearance holes. Therefore, the first assumption is using clearance holes, that would not provide the exactly stress that the screws are suffering but it would be able to compare the old model connection with the new model ones. This assumption will be used for all the walls.

For simulate the behaviour of the top plate, there was supposed roller fixture in the sides of the plate and fixed geometry in the 16 holes. The pressure is distributed along the whole plate.

Below are seen the results of the simulations with threaded holes:

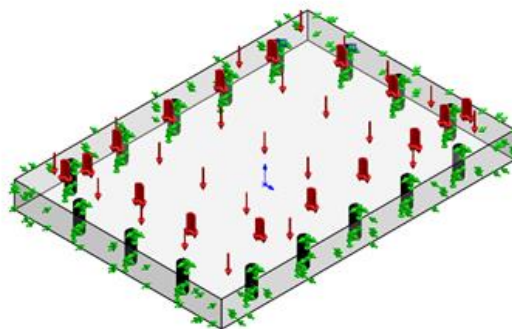


Figure 55 - Pressure distribution and fixtures (A.O.P.)

⁸ More accurate simulations were done by M7BACH, they can be found in "Otimizing af In Vitro model til fremtidige hjerteklap studier", 2014 [report – section X](#)

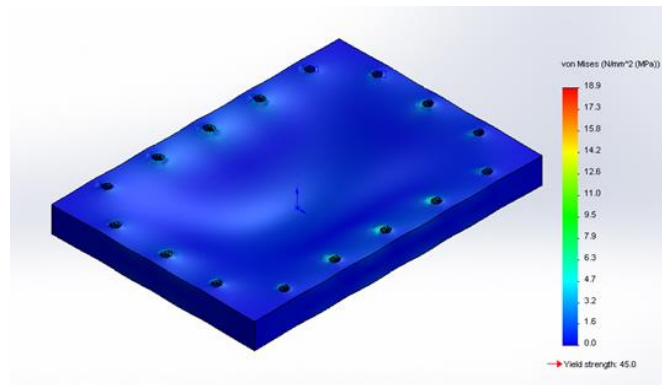


Figure 56 – Stress/Top plate old model (A.O.P.)

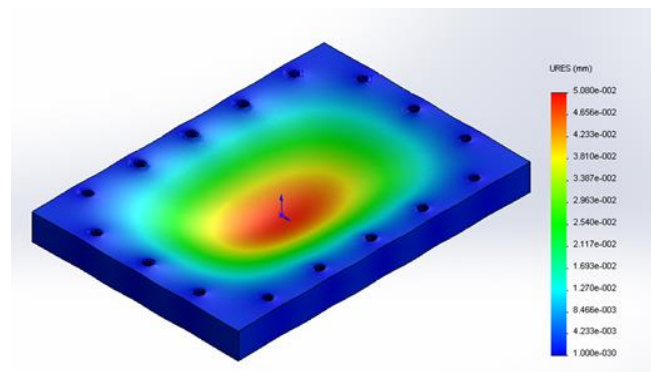


Figure 57 - Displacements/Top plate old model (A.O.P.)

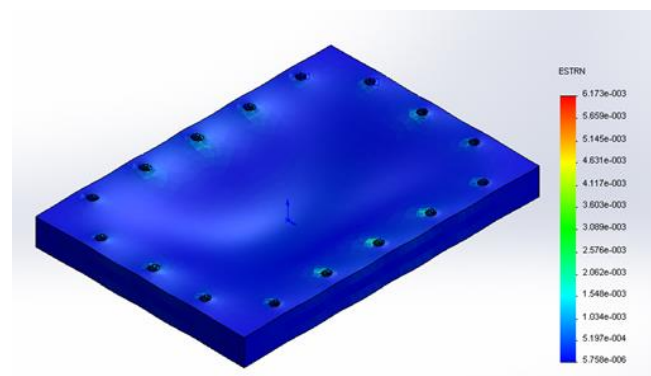


Figure 58 - Strain/Top plate old model (A.O.P.)

Below are seen the results of the simulations with clearance holes:

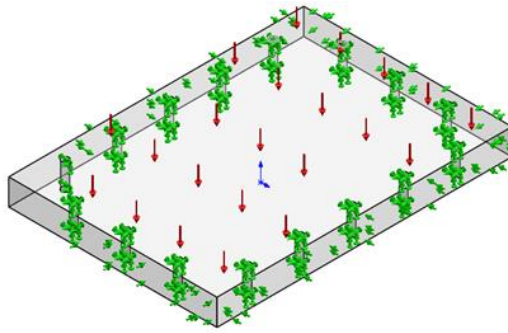


Figure 59 - Pressure distribution and fixtures/Top plate old model (A.O.P.)

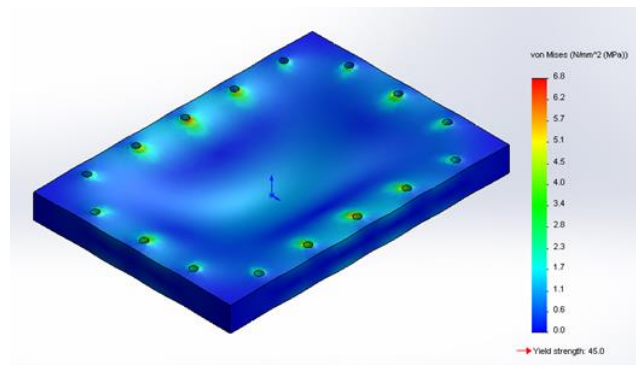


Figure 60 - Stress/Top plate old model (A.O.P.)

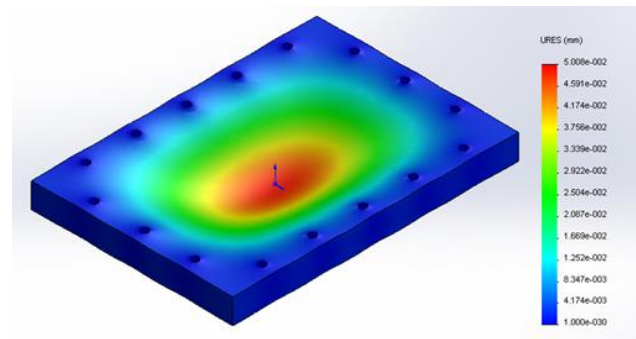


Figure 61 - Displacements/Top plate old model (A.O.P.)

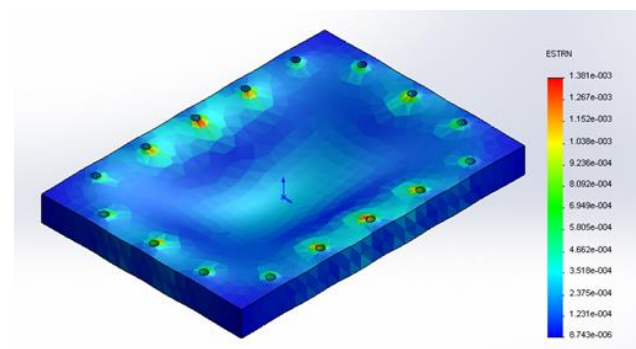


Figure 62 - Strain/Top plate old model (A.O.P.)

Below is a table that sums up all the results and compares them with the theoretical calculations.

	Maximum Stress [MPa]	Maximum Displacement [mm]	Maximum strain
Threaded hole	18.9110	0.05008	0.006173
Clearance hole	6.7945	0.05008	0.001381
Theoretical calculations	7.7922	-	-

Table 5 - Simulation's results/Top plate old model (A.O.P.)

Simulating the threaded holes does not drive into good results, which was also a recommendation before. The displacement achieved is very small and it may not produce any problem in the model. Also the maximum stress does not reach the yield point of the material which is 45 [MPa] due to it is PMMA. But, the stress caused by the pressure is therefore an agent to increase the probabilities of breakage in the screws, adding other agents such as moisture absorption and the stress problems due to a bolt connection.

2- Side plate:

As the previous results with the threaded hole were not successful, this simulation was avoided in the side plate. The assumption of using clearance holes is therefore applied.

For simulate the behaviour of the side plate, there was supposed fixed geometry in the three holes, in the sides and also in the bottom of the plate. The pressure is distributed along the whole plate.

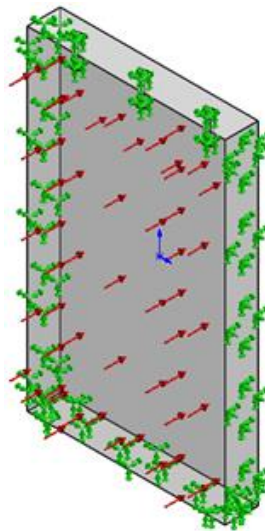


Figure 63 - Pressure distribution and fixtures/Side plate old model (A.O.P.)

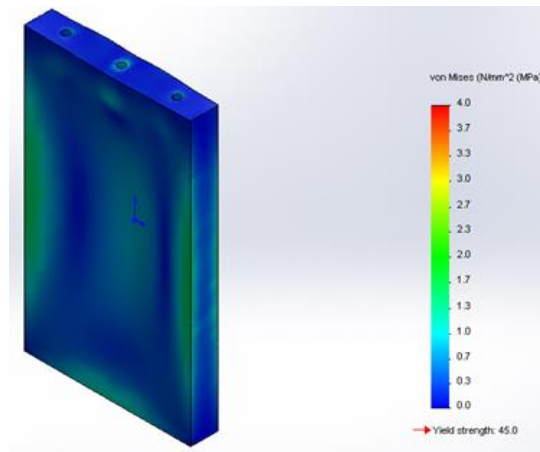


Figure 64 - Stress/Side plate old model (A.O.P.)

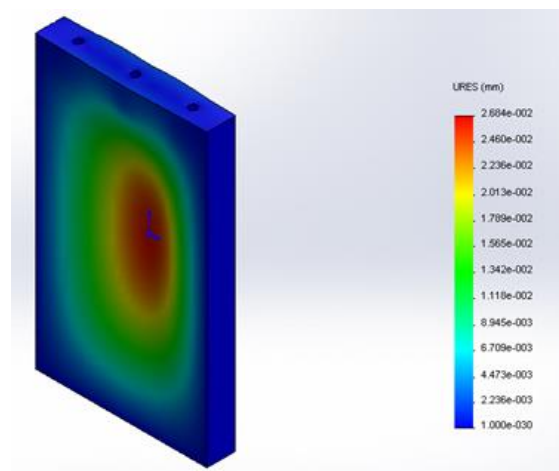


Figure 65 - Displacements/Side plate old model (A.O.P.)

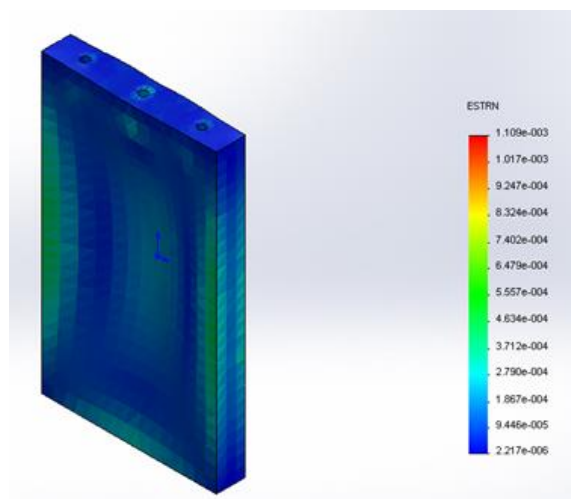


Figure 66 - Strain/Side plate old model (A.O.P.)

Below is a table that summarises all the results and compares them with the theoretical calculations.

	Maximum Stress [MPa]	Maximum Displacement [mm]	Maximum strain
Clearance hole	3.9864	0.02684	0.001109
Theoretical calculations	3.4312	-	

Table 6 - Simulation's results/Side plate old model (A.O.P.)

The displacement achieved is again negligible and it might not produce any deformation in the model. On the other hand, maximum stress does not reach the yield point of the PMMA material, which is 45 [MPa]. This value is small, but may be one of the reasons for the cracking problem.

3- Front plate:

The assumption of using clearance holes is used. For simulate the behaviour of the front plate, there was supposed fixed geometry in the five holes, in the sides and also in the bottom of the plate. The pressure is distributed along the whole plate.

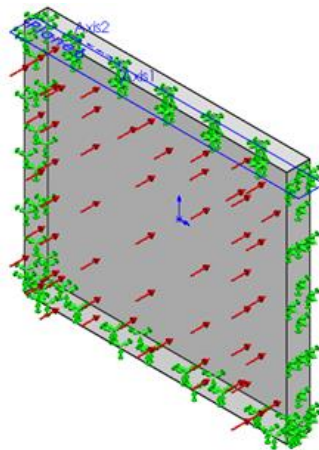


Figure 67 - Pressure distribution and fixtures/Top plate old model (A.O.P.)

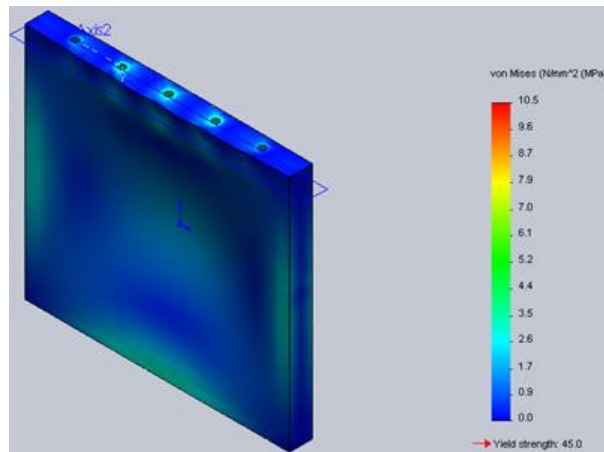


Figure 68 - Stress/Front plate old model (A.O.P.)

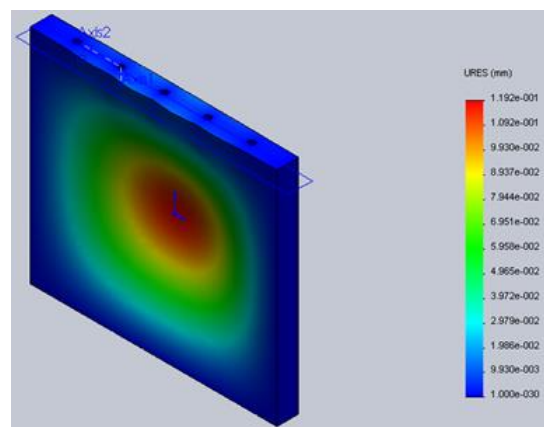


Figure 69 - Displacements/Front plate old model (A.O.P.)

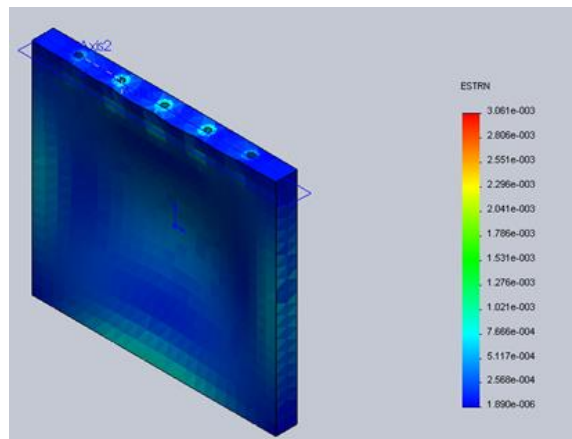


Figure 70 - Strain/Front plate old model (A.O.P.)

Below is a table that summarises all the results and compares them with the theoretical calculations.

	Maximum Stress [MPa]	Maximum Displacement [mm]	Maximum strain
Clearance hole	10.481	0.1192	0.003061
Theoretical calculations	3.888	-	

Table 7 Simulation's results/Front plate old model (A.O.P.)

Equally to the side wall and top wall, the displacement value achieved negligible. There is a notable difference between the stress value reached by theoretical calculations and SolidWorks simulation. Even though the maximum stress is bigger than the previous ones, it does not reach the yield point of the PMMA material, 45 [MPa]. This value is still small compared to the tensile strength of the material, when the material starts cracking, this value is 76 [MPa] but may be one of the reasons for the cracking problem.

⁹ More accurate simulations for this wall using advanced fixtures in Solid Works have been done, taking into account the glue connection between the walls. However, threaded holes were substituted by clearance holes for the simulation since not possible realistic results can be achieved in Solid Works. Even though it is known that in each thread of a bolted joint there is a stress concentration. This study has been done for the back plate of the old model. Achieving the maximum stress value in the middle hole with a value of 17.2 [MPa] and 0.158 [mm] with 1.6 [bar] as pressure value.

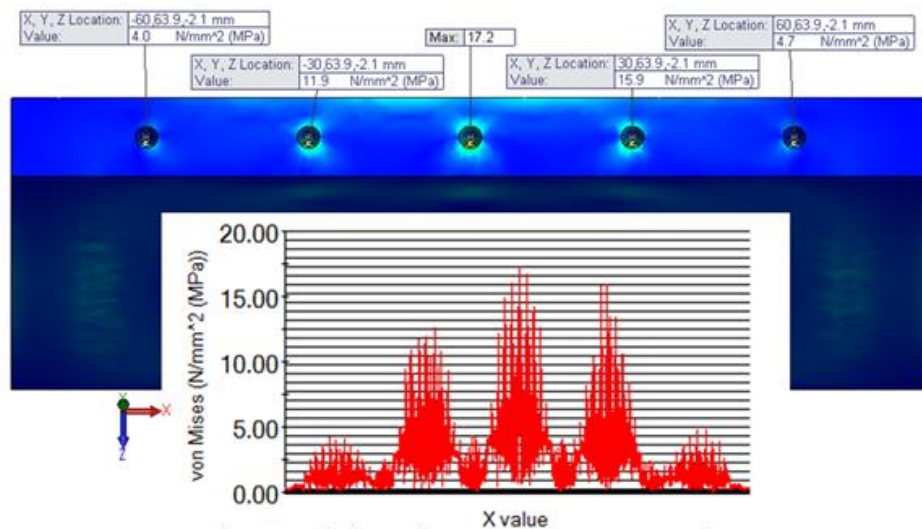


Figure 71 - Stress distribution in the holes of the old model's back plate ¹⁰

⁹ Done by Tobias (M7BACH) – appendix section number X of M7BACH group's report

¹⁰ Photo from M7BACH group's report

Besides, the calculations of the new model to compare it with the old one are expressed below. Note that there was only needed to simulate the top plate since the connections are outside the pressure area, so it only would affect the top plate screw's connections.

4- Top plate:

The assumption of using clearance holes is again used. For simulate the behaviour of the front plate, there was supposed fixed geometry in the five holes of the steel plate, not the PC ones since the holes are some millimetres bigger than the threaded bars. Furthermore, the sides of the plate are also supposed as fixed geometry due to the new configuration designed for it. The pressure is distributed along the whole plate.

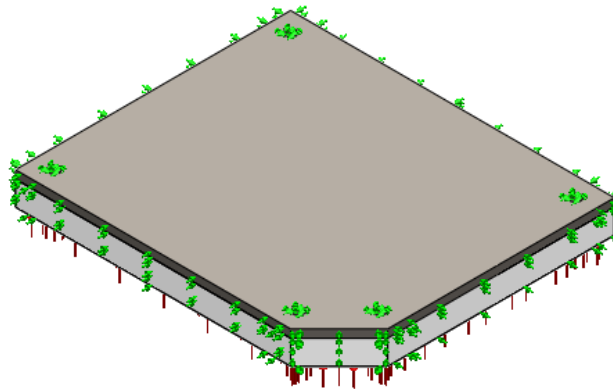


Figure 72 - Pressure distribution and fixtures/Top plate new model (A.O.P.)

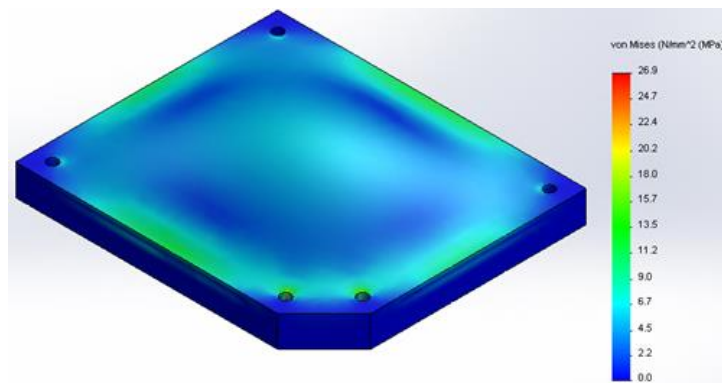


Figure 73 - Stress/Top plate new model (A.O.P.)

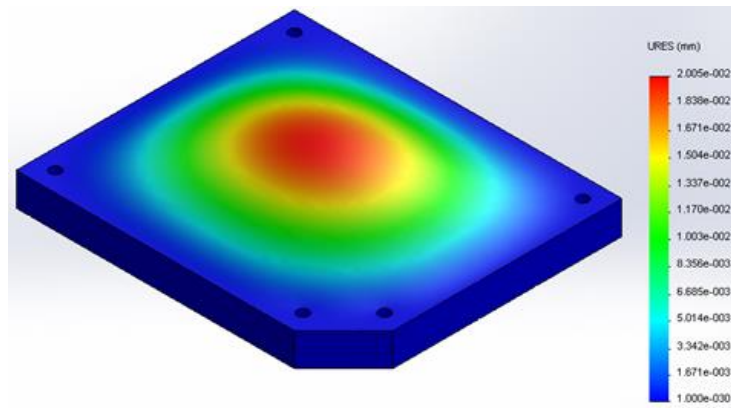


Figure 74 - Displacements (A.O.P.)

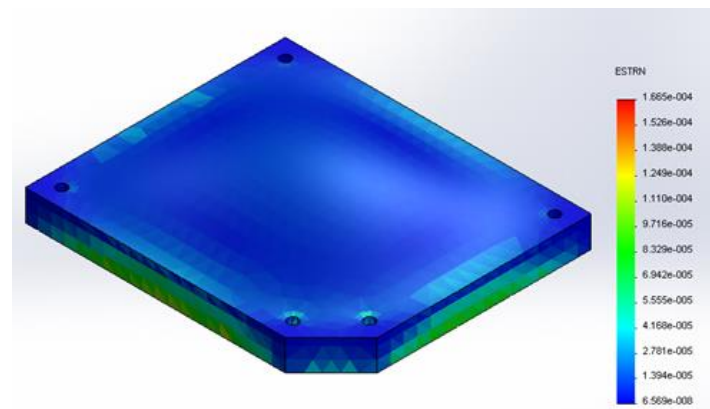


Figure 75 - Strain/Top plate new model (A.O.P.)

Below is a table that summarises all the results and compares them with the theoretical calculations.

	Maximum Stress [MPa]	Maximum Displacement [mm]	Maximum strain
Clearance hole	26.932	0.02005	0.0001665
Theoretical calculations	15.336	-	

Table 8 Simulation's results/Top plate new model (A.O.P.)

The results for this new model are bigger compared with the top plate of the old model since the number of screws has been decreased and surface area increased, however due to material improvements the probability to achieve breakage in the model is lower. The new material that is suffering the pressure in its holes is steel S235 which has a yield point around 235 [MPa], value distant enough from the 27 [MPa], value achieved in the holes according to SolidWorks calculations. Once again, the displacement value achieved is negligible.

Summarizing, the new model will reach more stress value in the threaded holes but, as the material has been improved the results for the cracking mode due to pressure will be better. On the other hand, as the holes in the polycarbonate are clear there is no viable way to crack them due to pressure, moisture absorption or other agents that have been studied.

13- Pressure drops in the entire model

^{11 12} Pressure drops in pipes are caused by friction, kinetic energy changes, friction in circular pipes and vertical differences. All these factors are going to be taken into account in order to calculate the pressure drop in the entire model.

By using Bernoulli equation is possible to calculate the pressure drop between two points in the model. Following is shown the equation.

$$\Delta P = \frac{1}{2} \rho (c_2^2 - c_1^2) + \rho g (z_2 - z_1) + \rho W_{dist\ 1-2}$$

Equation 14 - Bernoulli equation for Pressure drops

The first term is the pressure drop due to cross section changes, the second one for difference in height and the last one due to friction.

In order to characterize the flow, the non-dimensional Reynolds number is used. Thanks that number is possible to know if the flow is laminar turbulent. Its equation is seen below.

$$Re = \frac{c\ d}{\nu} = \frac{c\ d\ \rho}{\mu}$$

Equation 15 - Reynolds' number equation

Note that 'c' means velocity [m/s], 'd' is diameter of the tube [mm], 'ρ' is density [kg/m³], 'ν' kinematic viscosity [m²/s] and 'μ' dynamic viscosity [Pa·s]

When the Reynolds number is less than 2000 the flow is considered laminar. From 2000 to 4000 is called transition period, when is not clear if the flow has a laminar or turbulent behaviour. Turbulent flow is considered when the Re number is more than 4000. The Reynolds number values for both aortic roots with the two CO are the following ones, reaching turbulent flow for all the configurations.

<i>Reynolds Number [-]</i>		<i>Cardiac Output</i>	
		<i>5 [L/min]</i>	<i>11 [L/min]</i>
Aortic Root	<i>Short</i>	3916	8616
	<i>Long</i>	4230	9305

Table 9 - Reynolds number in the aortic root (A.O.P.)

¹¹ Termodynamik. Teoretisk grundlag – Praktisk anvendelse. 3. Udgave. Nyt Teknisk Forlag

¹² Haemodynamik og hjerte-kar systemet (Peter Johansen 2009)

The cardiac output, which is the volume of blood ejected from the left ventricle chamber into the aorta each minute, is a known value which basically is flow. This value for an average person in normal conditions is around 5 [L/min] and the maximum which is going to be used in the analysis is 11 [L/min]. The model is a closed one; therefore, principle of continuity can be applied as seen below achieving that the flow is constant which means that there is the same amount of water at the beginning and at the end.

$$m_1 = m_2 \rightarrow v_1 \Delta t A_1 \rho = v_2 \Delta t A_2 \rho \rightarrow v_1 A_1 = v_2 A_2 \rightarrow Q_{in} = Q_{out}$$

Equation 16 - Continuity principle

By this principle is possible to calculate the velocity of the flow in each point of the model, the velocity values for both aortic roots' configurations and CO are seen the table below.

$$Q = v A$$

Equation 17 - Flow

<u>Velocity [m/s]</u>		Cardiac Output	
		5 [L/min]	11 [L/min]
Aortic Root	Short	0.15	0.32
	Long	0.17	0.37

Table 10 - Velocity in the aortic root (A.O.P.)

Four kinds of pressure drops calculations have been done: the first one is to compare the pressure drop due to length in the aortic root. This study is to analyse if there would be any relevant pressure drops when the long aortic root (the one with the silicone tube attached) is used. The second one is a calculation of pressure drops due to cross section changes between the different chambers and its connections. The third one is a pressure drop due to bending in the tube that connects the compliance chamber and the atrium chamber. And finally, the fourth is the calculation for the pressure drop in the ventricle chamber. All the calculations have been done for a Cardiac Output of 5 [L/min] which is the regular one and 11 [L/min] which is the maximum achieved.

¹³ First has been calculated the pressure drops due to length in the aortic root which is caused due to turbulence and friction in the walls. Note that has been used aortic root with blocked sinuses for this calculation, the sinus of Valsalva in the aortic root will generate less pressure drop as it was probed in previous analysis due to the sinus of Valsalva let the valve do a greater open. The model has been designed to be able to put different aortic roots' lengths. Mainly, there are two possible lengths, one short for pressure calculations and one long for flow calculations if a clamp flow meter is desired to be used. The length would also be changed when biological valves are used.

¹³ Note that these calculations have been done by the web-page <http://pressure-drop.com/>

Flow medium:	Water 20 °C / liquid
Volume flow::	5 l/min
Weight density:	998.206 kg/m ³
Dynamic Viscosity:	1001.61 10 ⁻⁶ kg/ms
Element of pipe:	circular
Dimensions of element:	Diameter of pipe D: 27 mm Length of pipe L: 0.085 m
Velocity of flow:	0.15 m/s
Reynolds number:	3916
Velocity of flow 2:	-
Reynolds number 2:	-
Flow:	turbulent
Absolute roughness:	0.0013 mm
Pipe friction number:	0.04
Resistance coefficient:	0.13
Resist.coeff.branching pipe:	-
Press.drop branch.pipe:	-
Pressure drop:	0.01 mbar 0 bar

Figure 78 - Table result for the short aortic root with CO of 5 [L/min] ¹⁴

Flow medium:	Water 20 °C / liquid
Volume flow::	11 l/min
Weight density:	998.206 kg/m ³
Dynamic Viscosity:	1001.61 10 ⁻⁶ kg/ms
Element of pipe:	circular
Dimensions of element:	Diameter of pipe D: 27 mm Length of pipe L: 0.085 m
Velocity of flow:	0.32 m/s
Reynolds number:	8616
Velocity of flow 2:	-
Reynolds number 2:	-
Flow:	turbulent
Absolute roughness:	0.0013 mm
Pipe friction number:	0.03
Resistance coefficient:	0.1
Resist.coeff.branching pipe:	-
Press.drop branch.pipe:	-
Pressure drop:	0.05 mbar 0 bar

Figure 79 - Table result for the short aortic root with CO of 11 [L/min] ¹⁵

¹⁴ <http://pressure-drop.com/>

¹⁵ <http://pressure-drop.com/>

Flow medium:	Water 20 °C / liquid
Volume flow::	5 l/min
Weight density:	998.206 kg/m³
Dynamic Viscosity:	1001.61 10-6 kg/ms
Element of pipe:	circular
Dimensions of element:	Diameter of pipe D: 25 mm Length of pipe L: 0.150 m
Velocity of flow:	0.17 m/s
Reynolds number:	4230
Velocity of flow 2:	-
Reynolds number 2:	-
Flow:	turbulent
Absolute roughness:	0.0016 mm
Pipe friction number:	0.04
Resistance coefficient:	0.24
Resist.coeff.branching pipe:	-
Press.drop branch.pipe:	-
Pressure drop:	0.03 mbar 0 bar

Figure 80 - Table result for the long aortic root with CO of 5 [L/min] ¹⁶

Flow medium:	Water 20 °C / liquid
Volume flow::	11 l/min
Weight density:	998.206 kg/m³
Dynamic Viscosity:	1001.61 10-6 kg/ms
Element of pipe:	circular
Dimensions of element:	Diameter of pipe D: 25 mm Length of pipe L: 0.150 m
Velocity of flow:	0.37 m/s
Reynolds number:	9305
Velocity of flow 2:	-
Reynolds number 2:	-
Flow:	turbulent
Absolute roughness:	0.0016 mm
Pipe friction number:	0.03
Resistance coefficient:	0.19
Resist.coeff.branching pipe:	-
Press.drop branch.pipe:	-
Pressure drop:	0.13 mbar 0 bar

Figure 81 - Table result for the long aortic root with CO of 11 [L/min] ¹⁷

¹⁶ <http://pressure-drop.com/>
¹⁷ <http://pressure-drop.com/>

Pressure drop [mbar]		Cardiac Output	
		5 [L/min]	11 [L/min]
Aortic Root	Short	0.01	0.05
	Long	0.03	0.13

Table 11 - Summary of the pressure drops in the aortic root due to length (A.O.P.)

Can be concluded that there is an increasing pressure drop with length but its value is not larger enough to change significantly the results. However, as a recommendation to optimize the model is the use of the shorter aortic root for pressure calculations and to use the longer aortic root for flow measurements when the flow meter is needed to be inserted in the system.

The second calculation is the analysis of pressure drops due to cross section changes in all the connections of the model for a CO of 5 [L/min] and 11 [L/min]. This calculation has been done by Bernoulli equation and neglecting the friction factor because it is not relevant. The height factor will be also neglected because it is the same. So, the equation use is the one seen below.

$$\Delta P = \frac{1}{2} \rho (c_2^2 - c_1^2)$$

Equation 18 - Bernoulli equation (velocity)

This calculation has been done for all the connections seen in the model, achieving the following pressure drops for a CO of 5 [L/min]:

- Aorta to compliance chamber: achieving a pressure drop of about -10.47 [Pa]
- Compliance chamber to the tube that connects it to the atrium chamber: achieving a pressure drop of about 271.08 [Pa]
- Tube connected from the compliance chamber to the atrium: achieving a pressure drop of -271.09 [Pa]
- Atrium chamber to the mitral valve: achieving a pressure drop of 14.25 [Pa]
- Mitral valve to ventricle chamber: achieving a pressure drop of -14.07 [Pa]
- Ventricle chamber to aorta: achieving a pressure drop of 10.31 [Pa]
- Aorta to aorta: achieving a pressure drop of 0 [Pa]

CO = 5 [L/min]	Connections						
	Aorta	Compliance	Tube	Atrium	Mitral	Ventricle	Aorta
S [mm ²]	$\pi r^2 =$ $\pi(27/2)^2$ = 572.55	130x111.32 = 14471.6	$\pi r^2 =$ $\pi(12/2)^2$ = 36 π	220x271.81 = 59798.2	$\pi r^2 =$ $\pi(25/2)^2$ = 490.87	$\pi r^2 =$ $\pi(74/2)^2$ = 4300.84	$\pi r^2 =$ $\pi(27/2)^2$ = 572.55
V [m/s]	0.145	5.75e-3	0.737	1.393e-3	0.169	0.019	0.145
ΔP [Pa]	-10.47	-271.09	-14.07				
ΔP [Pa]	0	271.08	14.25	10.31			

Table 12 - Pressure drops due to cross section changes for CO = 5L/min (A.O.P.)

For a CO of 11 [L/min] was achieved the following pressure drops:

- Aorta to compliance chamber: achieving a pressure drop of about -51.03 [Pa]
- Compliance chamber to the tube that connects it to the atrium chamber: achieving a pressure drop of about 1309.76 [Pa]
- Tube connected from the compliance chamber to the atrium: achieving a pressure drop of -1309.84 [Pa]
- Atrium chamber to the mitral valve: achieving a pressure drop of 69.43 [Pa]
- Mitral valve to ventricle chamber: achieving a pressure drop of -68.56 [Pa]
- Ventricle chamber to aorta: achieving a pressure drop of 50.23 [Pa]
- Aorta to aorta: achieving a pressure drop of 0 [Pa]

CO = 11 [L/min]	Connections						
	Aorta	Compliance	Tube	Atrium	Mitral	Ventricle	Aorta
S [mm ²]	$\pi r^2 = \pi(27/2)^2 = 572.55$	$130 \times 111.32 = 14471.6$	$\pi r^2 = \pi(12/2)^2 = 36\pi$	$220 \times 271.81 = 59798.2$	$\pi r^2 = \pi(25/2)^2 = 490.87$	$\pi r^2 = \pi(74/2)^2 = 4300.84$	$\pi r^2 = \pi(27/2)^2 = 572.55$
V [m/s]	0.320	0.0126	1.62	3.06e-3	0.373	0.042	0.320
ΔP [Pa]	-51.03	-1309.84	-68.56				
ΔP [Pa]	0	1309.76	69.43	50.23			

Table 13 - Pressure drops due to cross section changes for CO = 11L/min (A.O.P.)

Note: S = surface, v = velocity, ΔP = pressure drop

The bigger pressure drops are seen in the tube that connects the compliance chamber and the compliance chamber. Then the ones that connects the chambers and the valves (aorta and mitral).

The third calculation of pressure drop is done in the bent of the tube that connects the compliance chamber and the atrium chamber. This one has been done by using the following equation and graph.

$$\Delta P = \frac{1}{2} f_s \rho u^2 \frac{\pi R_b}{D} \frac{\theta}{180} + \frac{1}{2} k_b \rho u^2$$

Equation 19 - Bend loose equation ¹⁸

Note: f_s = Moody's fiction factor, ρ = density, u = mean flow velocity, R_b = bend radius, D = diameter of the tube, θ = bend angle and k_b = bend loss coefficient.

¹⁸ <http://thermopedia.com/content/577/?tid=104&sn=1422>

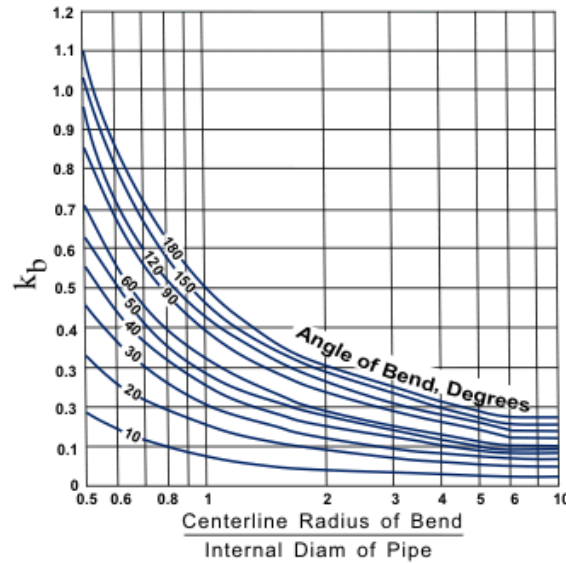


Figure 82 - Bend loss coefficient calculation graph ¹⁹

The calculations and the explanation for 5 [L/min] are seen below:

The friction factor has been calculated by Moody's diagram. First is needed to be known the Reynolds number for the tube and the velocity. With this number and the factor $\frac{k_s}{d}$ where k_s is the roughness and d is the diameter is possible to enter in the diagram to obtain the friction factor.

$$Q = v A \rightarrow v = \frac{Q}{A} = \frac{5}{\frac{1000 \cdot 60}{\pi \left(\frac{12}{2}\right)^2}} e^{-5} = 0.7368 \text{ [m/s]}$$

Equation 20 - Velocity calculation with a CO = 5 [L/min] in the tube (A.O.P.)

$$Re = \frac{c d}{\nu} = \frac{0.7368 \cdot 12 e^{-3}}{1.004 e^{-6}} = 8806.71$$

Equation 21 - Reynolds number for the tube with a CO = 5 [L/min] (A.O.P.)

$$\frac{k_s}{d} = \frac{0.0016}{12} = 1.3 e^{-4}$$

Equation 22 - Relation between the roughness and the diameter of the pipe with a CO = 5 [L/min] (A.O.P.)

$$f_s = 0.034$$

Equation 23 - Friction factor for the tube with a CO = 5 [L/min] (A.O.P.)

¹⁹ <http://thermopedia.com/content/577/?tid=104&sn=1422>

In order to calculate the bend loss coefficient is needed to use the graph seen in the figure 68, achieving a value of:

$$k_b = 0.25$$

Equation 24 - Bend loss coefficient with a CO = 5 [L/min] (A.O.P.)

Putting all these values together is achieved the pressure drop:

$$\Delta P = \frac{1}{2} 0.034 \cdot 998.206 \cdot 0.7368^2 \frac{\pi 200 e^{-3} 180}{12 e^{-3} 180} + \frac{1}{2} 0.25 \cdot 998.206 \cdot 0.7368^2 = 550.09 [Pa]$$

$$= 5.5 [mbar]$$

Equation 25 - Pressure drop calculation with a CO = 5 [L/min] due to bend (A.O.P.)

This value was also done by the same web-page used before, achieving a value of 4.97 [mbar].

The same calculations are followed to achieve the pressure drop due to bend in the tube with a CO of 11 [L/min]:

$$\Delta P = \frac{1}{2} 0.028 \cdot 998.206 \cdot 1.621^2 \frac{\pi 200 e^{-3} 180}{12 e^{-3} 180} + \frac{1}{2} 0.25 \cdot 998.206 \cdot 1.621^2 = 2923.66 [Pa]$$

$$= 29.23 [mbar]$$

Equation 26 - Pressure drop calculation with a CO = 11 [L/min] due to bend (A.O.P.)

This value was also calculated by the same web-page used before, achieving a value of 19.43 [mbar].

Finally, the fourth calculation is to analyse the pressure drop in the ventricle chamber due to bends. The flow does not go straight inside the ventricle, as it is seen in the photo below; therefore two bents have been assumed to simplify the calculations. These calculations have been done in the same way as the third one by using the Bend loose equation and then the results have been compared with the same web-page.

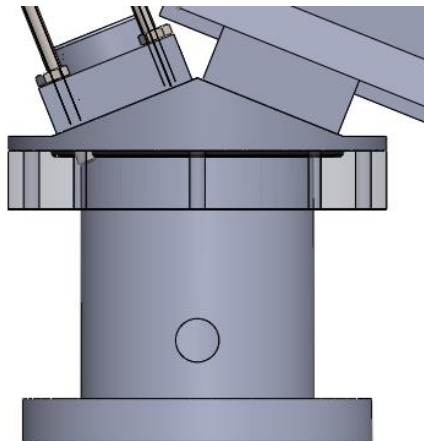


Figure 83 - Ventricle chamber with the two valves' connection (A.O.P.)

The first bent hypothesis is between the mitral valve and the aortic root. The flow will go from the mitral to the aorta once is closed. The angle is supposed around 136.33° and the radius of the bent is 26.934 [mm].

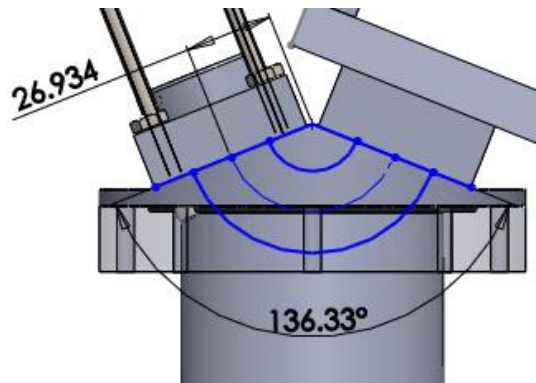


Figure 84 - Ventricle chamber bent one (A.O.P.)

The second bent hypothesis is between the pump valve and the aortic root. The flow will be drove by the pump into the aorta. The imaginary bent tube's angle is supposed around 37.22° and the radius is 111.681 [mm].

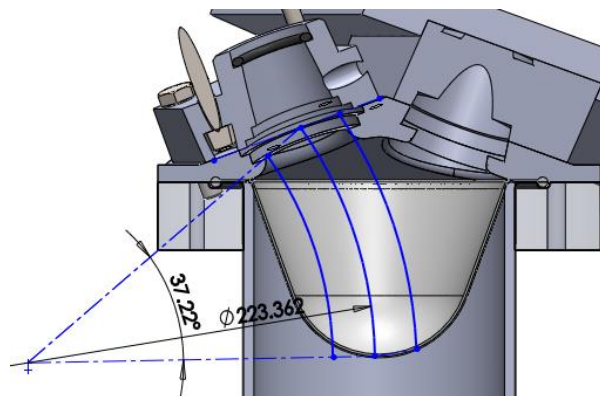


Figure 85 - Ventricle chamber bent two (A.O.P.)

In the table below are going to be summarized the results in the bents supposed in the ventricle achieved by the web page and hand calculations (same procedure as explained in the third one).

	Pressure drop			
	Bent Mitral to Aorta		Bent Pump to Aorta	
	Web-page calculations	Hand-calculations	Web-page calculations	Hand-calculations
5 [L/min]	0.12 [mbar]	0.084 [mbar]	0.03 [mbar]	0.017 [mbar]
11 [L/min]	0.45 [mbar]	0.36 [mbar]	0.13 [mbar]	0.072 [mbar]

Table 14 - Pressure drops due to bend in the ventricle chamber (A.O.P.)

14- Fluid passing through the new model

In order to know if the new model achieved has a more laminar flow, one of the changes done is increasing the size of the atrium chamber. The way to calculate the time that the volume of water needs to complete the entire cycle is the calculation done below.

$$\text{Exchange of water} = \frac{\text{Cardiac Output}}{\text{Total Volume}}$$

$$V_{Total} = V_{Compliance} + V_{Atrium} + V_{Ventricle}$$

$$V_{Compliance} = 130 \times 100 \times 111.32 = 1.44 \text{ [L]}$$

$$V_{Atrium} = 220 \times 220 \times 135.92 = 6.56 \text{ [L]}$$

$$V_{Ventricle} = \pi \times 74^2 \times 100 = 0.43 \text{ [L]}$$

$$V_{Total} = 1.44 + 6.56 + 0.43 = 8.43 \text{ [L]}$$

$$CO = 8 \text{ [L/min]}$$

$$\text{Exchange of water} = \frac{8 \left[\frac{\text{L}}{\text{min}} \right]}{8.43 \text{ [L]}} = 0.95 \left[\frac{1}{\text{min}} \right]$$

Equation 27 - Fluid passing through the new model calculations

²⁰ Comparing this value with the previous model, which has an exchange of water of $1.6 \left[\frac{1}{\text{min}} \right]$, it is possible to say that the volume of water going through the new model per minute has a lower value, meaning that the system goes slower than the previous one, so the flow may behave more laminar.

²⁰ Comparison with the “The effect of sinus of Valsalva on TAVI valves” results

15- Silicone

²¹ ²² Some chemical reactions happened between the mould and the silicone, and that is why some troubles were seen along the design mould period. In this section it is going to be explained that chemical reaction mainly.

The silicones provided by the supplier are RTV-ZA12 A+B. The final silicone used was a half – half in weight proportion mixture in order to improve its properties, such as hardness. Furthermore it was provided some SH 350 oil. In order to avoid some of the bubbles that appear during the mixture procedure was also thought about using just one kind of silicone.

The mould was done in several materials, in order to try which one was the better option. Firstly it was built using a 3D printer in ABS material. However, as some problems associated with this plastic material were seen, it was decided to make it in aluminium.

To make the silicone elements was initially tried only by using the ABS mould and filled it with the silicone. Nevertheless, the solution was not accurate since the silicone element was sticky and soft, not achieving the desired properties. Later on, some of the oil provided and wood polish was used in order to cover the surface expecting better results.

Finally the mould was decided to be made in aluminium, and it was covered with some solutions in order to avoid the chemical reaction that happens between it and the silicone, due to the OH groups formed.

The reason for the inaccurate properties achieved in the silicone was because of the OH groups that the silicone and the aluminium have. So they react creating the HO₂ bubbles. The reaction of the silicone and the aluminium can be seen below.

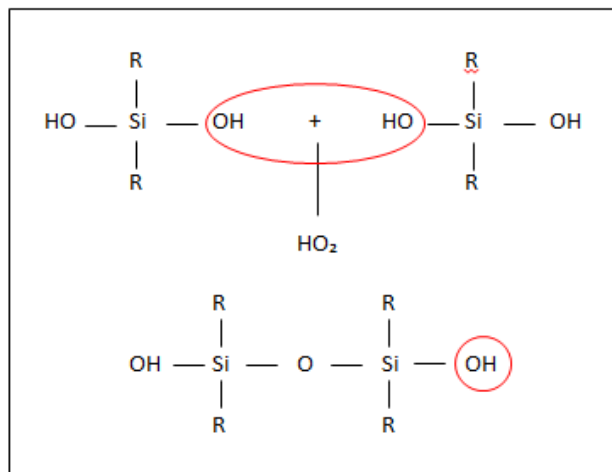


Figure 86 - Chemical reaction of the silicone (A.O.P.)

²¹ Finn Monrad Rasmussen (Associate professor – Engineering College of Aarhus – Materials)

²² Stevens, Malcolm P. Polymer chemistry: an introduction. 3rd ed. New York: Oxford University Press, 1999. Print.

The aluminium has covalent bonds and its formula is the following one: $\text{Al}_2\text{O}_3 \longrightarrow \text{Al}_2\text{O}_2\text{H}$

Thereby there are also OH groups that react with the OH groups of the silicone, creating those bubbles. The material will react adversely with the silicone.

For that reason some additional materials, to cover the mould's surface, are needed in order to avoid that reaction between hydroxides. There were some ideas suggested such as polish like nail polish, hairspray, a mixture made of Styrofoam and acetone and a mixture made of Styrofoam and toluene. The Styrene has no OH groups; hence it cannot react with the silicone so it does create a coat between the aluminium and the silicone.

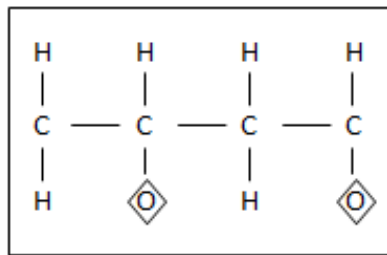


Figure 87 - Chemical reaction of the Styrene (A.O.P.)

16- List of materials

²³ Following are the data sheet for the materials used given by the supplier company, Vink.

www.vink.dk

Teknisk datablad - PMMA

Egenskaber	Test metode DIN (ASTM)	Test metode ISO	Enhed	PMMA Altuglas® CN støbt	PMMA Altuglas® EX extr.	PMMA Altuglas® EI 50
Densitet	53479	1183	g/cm ³	1,19	1,19	1,16
Fugtoptagelse:						
- 24 timer / 8 dage i vand ved 23°C	53495	62	%	0,3 / 0,5	0,3 / 0,5	0,36 / -
- mættet i vand 23°C			%	1,75	1,75	
Termiske egenskaber						
Smeltepunkt			°C			
Varmeledningsevne ved 23°C	52612		W/(°C x m)	0,17	0,19	
Lineær termisk udvidelseskoefficient	52328	EN 2155-1	mV/(m x °C)	65 x 10 ⁻⁶	65 x 10 ⁻⁶	82 x 10 ⁻⁶
HDT temp. metode A: 1,8 N/mm ²	53461	75 / A	°C	109	102	
Tilladelig anvendelsestemperatur i luft:						
- max. kortvarigt			°C	110	105	
- max. vedvarende			°C	85	80	73
- minimum			°C	-40	-40	
Brandbarhed:						
- fl index	(2863/77)		%	18	18	
- i henhold til UL 94				HB	HB	
- i henhold til tysk norm	4102			B2	B2	B2
K-værdi:						
- 3 mm tykkelse			W / m ² / °C	5,4	5,4	
- 5 mm tykkelse			W / m ² / °C	5,1	5,1	
- 10 mm tykkelse			W / m ² / °C	4,5	4,5	
Mekaniske egenskaber v. 23 °C						
Trækforsøg						
- trækstyrke ved flydning / brud	53455	527	N/mm ²	* / 76	* / 74	* 50
- forlængelse ved brud	53455	527	%	6	5	45
- E-modul	53455	527	N/mm ²	3300	3300	2100
Slagstyrke:						
- Charpy uden kær	53453	179 / 2D	kJ/m ²	12	10	85
- Izod med kær	(D 256 A)	180 / 1A	kJ/m ²	1,4	1,3	5 ¹⁾
Rockwell hårdhed	(D785)	2039-1		M 100	M 95	
Elektriske egenskaber						
Dielektrisk styrke	53481		kV/mm	20 til 25	20 til 25	
Specifik modstand	53481		Ω x cm	> 10 ¹⁵	> 10 ¹⁵	
Dielektrisk konstant - ved 50 Hz	53483			3,7	3,7	
- ved 1 MHz	53483			2,6	2,6	
Optiske egenskaber						
Lustransmission:						
- ved 3 mm tykkelse	5036	T 51068	%	92	92	91,5
- ved 5 mm tykkelse	5036	T 51068	%	92	92	
- ved 8 mm tykkelse	5036	T 51068	%		92	
- ved 10 mm tykkelse	5036	T 51068	%	92		

Note: 1 g/cm³ = 1,000 kg/m³; 1 N/mm² = 1 MPa; 1 kV/mm = 1 MV/m

* Ingen flydepunkt

¹⁾ Udført efter Charpy med kær i.h.t. ISO 179/1

Alle informationer er givet ud fra vor bedste viden og uden ansvar for Vink Plast ApS. Tekniske oplysninger bygger på informationer fra forskellige råvarerleverandere. Randers, december 2013.

Vink Plast ApS · Kristrup Engvej 9 · 8960 Randers SØ · Tlf. 89 110 100 · Fax 86 415 890 · www.vink.dk
Information taken from the supplier: <http://www.vink.dk>



Teknisk datablad - PC - blad 1 af 2

Egenskaber	Test metode ISO/(IEC)	Enhed	PC 1000	Lexan 9030 og Exell D	Lexan Margard MR5E	Lexan SG 305
Farve			natur (klar)	transparent	transparent	transparent
Densitet (vægtfylde)	1183	g/cm ³	1,2	1,2	1,2	1,2
Fugtoptagelse:						
- nedsænket 24/96 timer i 23°C i vand	62 62	mg %	13 / 23 0,18 / 0,33		10 / -	10 / -
- mættet i luft ved 23°C/50% RH		%	0,15	0,15		
- mættet i vand ved 23°C		%	0,40	0,35		0,35
Termiske egenskaber						
Glas overgangs temperatur		°C				
Vicat blødgøringspunkt, B/120	306	°C		145	145	145
Varmeledningsvne		W/(°C x m)	0,21	0,2	0,2	0,2
Gennemsnitlig temperaturudvidelseskoefficient:						
- værdi mellem 23°C og 80°C	11359			70 x 10 ⁻⁶	70 x 10 ⁻⁶	70 x 10 ⁻⁶
- værdi mellem 23°C og 100°C		m/(m x °C)	65 x 10 ⁻⁶			
- værdi mellem 23°C og 150°C		m/(m x °C)	65 x 10 ⁻⁶			
HDT Formbestandighed i varme metode A/1,8MPa	75	°C	130	127		138
Tilladelig anvendelsestemperatur i luft:						
- maksimal kortvarigt - 10 timer		°C	135			
- maksimal kontinuert 5000/20000 timer		°C	130 / 120	- / 100	- / 100	- / 100
- minimum (spredningstemperatur)		°C	-50	-40 (-110)	-40 (-110)	-40 (-110)
Brandbarhed:						
- fl index	4589	%	25		25	
- klassifikation i.h.t. UL94 3 / 6 mm tykkelse			HB / HB			
Mekaniske egenskaber						
Trækforsøg:						
- trækstyrke ved svigt / brud	527-1/-2	N/mm ²	74 / -	60 / 70	60 / 70	60 / 70
- forlængelse ved svigt / brud	527-1/-2	%	- / 50	6 / 120	6 / 120	6 / 120
- E-modul	527-1/-2	N/mm ²	2400	2300	2350	2300
Trykforsøg:						
- til 1 / 2 % deformation	604	N/mm ²	18 / 35 / 72			
- svarende til 1% forlængelse efter 1000 timer	899-1	N/mm ²	17			
Slagstyrke:						
- Charpy uden krævs	179-1/1eU	kJ/m ²	ingen brud			
- Charpy med krævs	179-1/1eA	kJ/m ²	9			
- Charpy med krævs	179/1C	kJ/m ²		35		
- Izod med krævs	180/A	kJ/m ²	9			
- Izod uden krævs 23°C / -30°C	180/4U	kJ/m ²		ingen brud		ingen brud
- Izod med krævs 23°C / -30°C	180/4A	kJ/m ²		65 / 10		65 / 10
Kugletrykshårdhed - tørt materiale	2039-1	N/mm ²	120			
Overfladehårdhed - Rockwell - tørt materiale	2039-2		M75			
Overfladehårdhed H358/30 95	2039-1			95		
Formkrymp		%		0,6 - 0,8		
Elektriske egenskaber						
Dielektrisk styrke	(60243-1)	kV/mm	25			
Specifik gennemslagsmodstand	(60093)	Ω x cm	> 10 ¹⁴	10 ¹⁵		
Overflademodstand	(60093)	Ω	> 10 ¹⁰			
Dielektrisk konstant: - ved 50/60 Hz	(60250)			2,7		
- ved 100 Hz	(60250)		3			
- ved 1 MHz	(60250)		3	2,7		
Dielektrisk tabstal tan: - ved 50/60 Hz	(60250)			0,001		
- ved 100 Hz	(60250)		0,001			
- ved 1 MHz	(60250)		0,008	0,01		
Krybestrømsmodstand Index (CTI)	(60112)		350 (225)			
Optiske egenskaber						
Lys transmission 3 mm	ASTM-D1003	%		89	84 - 90%	44

Note: 1 g/cm³ = 1,000 kg/m³; 1 N/mm² = 1 MPa; 1 kV/mm = 1 MV/m

Alle informationer er givet ud fra vor bedste viden og uden ansvar for Vink Plast ApS. Tekniske oplysninger bygger på informationer fra forskellige råvarerleverandere. Randers, december 2013.

Vink Plast ApS · Kristrup Engvej 9 · 8960 Randers SØ · Tlf. 89 110 100 · Fax 86 415 890 · www.vink.dk



Teknisk datablad - POM - blad 1 af 2

Egenskaber	Test metode ISO/IEC	Enhed	Ertacetal® POM-C	Ertacetal® POM-H	Ertacetal® POM H-TF
Farve			natur / sort	natur / sort	brun
Densitet	1183-1	g/cm ³	1,41	1,43	1,50
Fugtoptagelse:					
- 24/96 hi vand ved 23°C	62 62	mg %	20 / 37 0,24 / 0,45	18 / 36 0,21 / 0,43	16 / 32 0,18 / 0,36
- mættet i luft 23°C/50% RH		%	0,20	0,20	0,17
- mættet i vand 23°C		%	0,80	0,80	0,72
Termiske egenskaber					
Smeltepunkt	11357-1/-3	°C	165	180	180
Varmeledningsevne ved 23°C	11357-1/-2	W/(°C x m)	0,31	0,31	0,31
Linear termisk udvidelseskoefficient:					
- middelværd mellem 23°C og 60°C		m/(m x °C)	110 x 10 ⁻⁶	95 x 10 ⁻⁶	105 x 10 ⁻⁶
- middelværd mellem 23°C og 100°C		m/(m x °C)	125 x 10 ⁻⁶	110 x 10 ⁻⁶	120 x 10 ⁻⁶
HDT temp. metode A: 1,8 N/mm ²	75-1/-2	°C	100	110	100
Tilladelig anvendelsestemperatur i luft:					
- max. kortvarigt		°C	140	150	150
- max. vedvarende: 5000/20000 h		°C	115 / 100	105 / 90	105 / 90
- minimum		°C	-50	-50	-20
Brandbarhed:					
- It index	4589-1/-2	%	15	15	-
- ht. UL 94 (6 mm tykkelse)			HB / HB	HB / HB	HB / HB
Mekaniske egenskaber v. 23 °C					
Trækforsøg:					
- trækstyrke ved flydning / brud	527-1/-2	N/mm ²	66 / -	78 / -	- / 55
- forlængelse ved brud	527-1/-2	%	50	50	10
- E-modul	527-1/-2	N/mm ²	2800	3300	3100
Træk- og krybeforsøg:					
- Spænding svarende til en forlængelse på 1% efter 1000 timer	899-1	N/mm ²	13	15	13
Trykforsøg:					
- 1% offset trykstyrke	604	N/mm ²	23	29	26
- 2% offset trykstyrke	604	N/mm ²	40	49	44
- 5% offset trykstyrke	604	N/mm ²	72	85	77
Slagstyrke - Charpy uden kær v	179-1/1eU	kJ/m ²	150	200	30
Slagstyrke - Charpy med kær v	179-1/1eA	kJ/m ²	8	10	3
Slagstyrke - Izod med kær v	180/A	kJ/m ²		10	3
Kugletrykshårdhed H 358 / 30	2039-1	N/mm ²	140	160	140
Rockwell hårdhed	2039-2		M 84	M 88	M 84
Pin on disk ved 23 °C:					
- dynamisk friktionskoefficient			0,3-0,45	0,3-0,45	0,2-0,3
- slidstyrke		µm / km	45	45	8
Bektriske egenskaber					
Dielektrisk styrke	(60243-1)	kV/mm	20	20	20
Specifik modstand	(60093)	Ω x cm	> 10 ⁴	> 10 ⁴	> 10 ⁴
Overflademodstand	(60093)	Ω	> 10 ⁹	> 10 ⁹	> 10 ⁹
Dielektrisk konstant - ved 100 Hz	(60250)		3,8	3,8	3,6
- ved 1 MHz	(60250)		3,8	3,8	3,6
Dielektrisk tabetal tan - ved 100 Hz	(60250)		0,003	0,003	0,003
- ved 1 MHz	(60250)		0,008	0,008	0,008
Krybestrømsmodstand index (CTI)	(60112)		600	600	600

Note: 1 g/cm³ = 1,000 kg/m³; 1 N/mm² = 1 MPa; 1 kV/mm = 1 MV/m

Alle informationer er givet ud fra vor bedste viden og uden ansvar for Vink Plast ApS. Tekniske oplysninger bygger på informationer fra forskellige råvarerleverandere. Randers, december 2013.

Vink Plast ApS · Kristrup Engvej 9 · 8960 Randers SØ · Tlf. 89 110 100 · Fax 86 415 890 · www.vink.dk



17- Transonic flow sensor specifications

²⁴ Following are the specifications for the hose clamp-on flow sensor model and the tubing required.

ME-PXL Series Clamp-on Flowsensors

Transonic® PXL Clamp-on Tubing Flowsensors clip on the outside of flexible laboratory tubing. No physical contact is made with the fluid media. A thin smear of Vaseline® or petroleum jelly should be applied to the section of tubing where the Sensor is applied to provide a good seal between the transducers and the tube for best ultrasonic signal transmission. PXL-Series Flowsensors can be factory calibrated and programmed for up to 4 different fluid, temperature, tubing, and flow rate combinations. Sensor size is determined by the outside diameter of the tubing. Standard PXL Sensors are sized in 1/16" increments. Metric sizes are available for metric tubing.



SENSOR SIZE	PHYSICAL SPECIFICATIONS ¹					
	DIMENSION ALONG TUBE		DEPTH		LENGTH	
	in	mm	in	mm	in	mm
2PXL	0.8	21	0.7	17	1.3	32
3PXL	0.8	21	0.7	17	1.3	32
4PXL	0.9	23	0.8	20	1.4	35
5PXL	0.9	23	0.8	20	1.4	35
6PXL	1.0	24	0.9	23	1.5	39
7PXL	1.0	26	1.0	25	1.7	42
8PXL	1.1	28	1.0	24	1.7	44
9PXL	1.3	33	1.0	25	1.8	47
10PXL	1.2	32	1.1	27	2.0	51
11PXL	1.4	35	1.1	28	2.2	56
12PXL	1.5	38	1.2	31	2.4	61
14PXL	1.6	41	1.4	36	2.6	66
16PXL	1.9	47	1.5	39	3.0	75
20PXL	2.3	58	1.8	46	3.7	93

1. Standard cable length is 2 meters.

APPLICATIONS

- Artificial Heart & VAD Performance
- Medical Device & Pump Engineering
- Manufacturing & Compliance Flow Testing



SENSOR SIZE	BIDIRECTIONAL FLOW OUTPUTS				SYSTEM ACCURACY SPECIFICATIONS ²			
	RESOLUTION ¹	LOW FLOW (% SCALE)	STANDARD FLOW SCALE	MAX FLOW (STD SCALE)	MAX ZERO OFFSET	ABSOLUTE ACCURACY	LINEARITY	ULTRASOUND FREQUENCY
	ml/min	1V output in ml/min	1V output in ml/min	5V output in L/min	ml/min	% of reading	%	MHz
2PXL	0.5	50	200	1	± 4.0	± 10	± 4	3.6
3PXL	1.0	100	400	2	± 8.0	± 10	± 4	3.6
4PXL	1.0	100	400	2	± 8.0	± 10	± 4	2.4
5PXL	1.0	100	400	2	± 8.0	± 10	± 4	2.4
6PXL	2.5	250	1 L	5	± 15	± 10	± 4	2.4
7PXL	5	500	2 L	10	± 30	± 10	± 4	1.8
8PXL	5	500	2 L	10	± 30	± 10	± 4	1.8
9PXL	5	500	2 L	10	± 30	± 10	± 4	1.8
10PXL	10	1 L	4 L	20	± 60	± 10	± 4	1.2
11PXL	10	1 L	4 L	20	± 60	± 10	± 4	1.2
12PXL	10	1 L	4 L	20	± 60	± 10	± 4	1.2
14PXL	25	2.5 L	10 L	50	± 150	± 10	± 4	1.2
16PXL	25	2.5 L	10 L	50	± 150	± 10	± 4	1.2
20PXL	50	5 L	20 L	100	± 300	± 10	± 4	0.9

Calibration is dependent on tubing material, wall thickness, ultrasound velocity of liquid flowing through the tube & temperature.

1. Resolution represents the smallest detectable flow change at 0.1 Hz filter (average flow output).
2. Stated system accuracy specifications apply to PXL Flowsensors with TS410 Flow Modules. (a) Absolute accuracy is comprised of zero stability, resolution and linearity effects. Stated values apply when flow rate is greater than 5% of maximum range and zero offset is nulled. (b) If the Sensor is calibrated on-site with the system Flow Module for the tubing and liquid in use, absolute accuracy may be improved to the Linearity value. (c) On-site calibration is recommended if the Sensor is routinely used to measure flows less than 5% of the maximum range to account for non-linearities associated with flow profile.

²⁴ <http://www.transonic.com/>

CLAMP-ON FLOWSENSOR TUBING SPECIFICATIONS						
SENSOR SIZE	FRACTIONAL (1/16 INCH INCREMENTS)			STOCK TUBING ²	METRIC	
	TUBING ID	WALL THICKNESS	TUBING OD		TUBING OD mm	SENSOR # WITH SUFFIX
2PXL	3/32	1/32 ¹	1/8-5/32	A, B	4	2PXL-M4
3PXL	1/8	1/32 ¹	3/16-7/32	A	5	3PXL-M5
4PXL	1/8	1/16	1/4	A, B	6 7	4PXL-M6 4PXL-M7
5PXL	3/16	1/16	5/16	A	8	5PXL-M8
6PXL	1/4	1/16	3/8	A, B, C	9	6PXL-M9
7PXL	1/4	3/32	7/16	A, B, C	10	7PXL-M10
8PXL	3/8 5/16	1/16 3/32	1/2	A, B N/A	12	8PXL-M12
9PXL	3/8	3/32	9/16	A, B, C	14	9PXL-M14
10PXL	1/2	1/16	5/8	A, B	16	10PXL-M16
11PXL	1/2	3/32	11/16	A, B		
12PXL	1/2	1/8	3/4	A, B	20	12PXL-M20
14PXL	5/8 11/16	1/8 3/32	7/8	A N/A	23	14PXL-M23
16PXL	3/4	1/8	1	A	25	16PXL-M25
20PXL	1	1/8	1 1/4	A		

1. In sizes 2-3PXL ratio of tubing wall thickness to OD must not exceed 1:5 for PVC; 1:3 for silicone
2. A= Tygon R-3603, B= Tygon S-50-HL, C= MEDIFLEX

18- Glue options for the walls' connection

²⁵ ²⁶ Below is shown the list to connect some different materials each other. It has been used to check the available unions to connect the polycarbonate walls each other and polycarbonate and acrylic if required. For both cases the epoxy solution is accurate and that was the solution chosen for all the chambers at the beginning. Due to some troubles seen in the compliance chamber walls since it is supporting the high compressed air pressure and also the direct action from the pump, better glue was desired in order to reinforce it. Acrylate has been tried as a possible solution, leading into non desirable results such as breakage. Ruderer 108 was the glue required in order to glue PC walls if they are going to be submitted to high pressure levels.

Klæbning af plast mod plast

Materialer	ABS	GA+CAB	PA	PC	PMMA	PS	St. PVC	BL PVC	PP	AP	UP
ABS	O 8, 9, 13 K 3, 11, 18	K 7, 4, 18	K 7, 18	K 3, 18, 4	K 4, 7	K 3, 4, 11	K 4, 5, 11	K 7, 11	K 7, 18	K 3, 18	K 3, 18
GA+CAB		O 1, 5, 6 K 6, 1, 7	K 18, 7	K 7	K 1, 4, 3, 10	K 4	K 4, 3, 18, 1, 10	K 4, 7	K 3, 18, 10, 16	K 3, 18, 10, 16	K 3, 18, 17
PA			O 10, 11, 19 K 8, 7, 18, 18, 11-13, 8-13, 8-18	K 18, 8-18	K 18, 7, 10, 18	K 4	K 7, 10, 11, 16	K 7, 11-13	K 7, 13, 11-13, 4, 10, 11	K 3, 13, 11-13, 4, 10, 11, 16, 13	K 7, 17, 18
PC				O 5, 7 K 6, 7, 18, 17	K 4, 18	K 4, 18	K 4, 18		K 7, 18, 8-18	K 3, 18, 8-18	K 3, 17, 18, 8-18
PMMA					O 5, 7, 8, 16, 15 K 4, 1, 6, 7, 18, 17, 10	K 4, 10	K 3, 4, 7, 1-8, 10, 11	K 11	K 3, 18, 11, 8-18	K 7, 18, 8-18	K 7, 17, 11, 18, 8-18
PS						O 2, 5, 7, 14, 13 K 4, 5, 1-8, 11, 12	K 4, 1-8, 1, 11	K 1-8, 11	K 4, 18, 17, 18, 1	K 4, 10, 17, 18, 1	K 4, 17, 18, 10
St. PVC							O 4, 13 K 4, 3, 6, 7, 10, 11	K 7, 11	K 7, 11, 10, 18	K 3, 11, 10, 18	K 7, 11, 17, 18
BL PVC								O 13 K 3, 4, 7, 10, 11, 12, 1-8	K 3, 18, 11-13	K 7, 11, 11-13	K 7, 11, 17
PP									K 13, 14, 18, 18, 7, 10	K 13, 14, 13, 18, 7, 10	K 18, 13-18
AP										K 13, 14, 13, 18, 7, 10	K 18, 13-18
UP											K 17, 18, 8-13, 7, 13

Figure 88 - Different options for gluing materials

²⁵ MTKMA1 Slides – Finn Monrad Rasmussen (Associate professor – Engineering College of Aarhus – Materials)

²⁶ Hansen, Steen. Klæbning af plast. [Nyt oplag] ed. Taastrup: Dansk Teknologisk Institut, Plastteknologi, 1993. Print.

Below is seen the meaning of each number seen in the previous list of materials' glue connections.

Koder til klæbeskemaer	<i>K = Klæbestoffer</i>
<i>O = Opløsningsmidler</i>	1. Polyvinylacetat
1. Acetone	2. Polyvinylchlorid
2. Benzen	3. Efterchloreret PVC
3. Butylacetat	4. Acrylat
4. Cyclohexanon	5. Polystyren
5. Ethylenchlorid	6. Cellulosenitrat
6. Methylcellosolve	7. Polyurethan
7. Methylenchlorid	8. Polyamid
8. Methylethylketon	9. Styrengummi
9. Methylisobutylketon	10. Neoprengummi
10. Myresyre (konc.)	11. Nitrilgummi
11. Phenol	12. Polyvinylether
12. Resorcin	13. Phenol
13. Tetrahydrofuran	14. Melamin
14. Toluën	15. Carbamid
15. Xylen	16. Resorcin
	17. Umættet polyester
	18. Epoxy

Figure 89 Explanation of the number in Figure 72

To sum up, for the connection PC with PC the glue options available are: adhesives (from the best to the worst – acrylate, polyurethane, unsaturated polyester and epoxy) and solvents (from the best to the worst – ethylenchlorid and methylenchlorid). On the other hand, for the connection PMMA with PC: only adhesives (from the best to the worst – acrylate and epoxy).

19- Tests ²⁷

19.1. Signal processing

During data acquisition, noise due to random and uncontrollable variables in the measuring equipment and environmental circumstance will be recorded. In order to determine which part of the noise is the results of random circumstances and which part is the result of constant systematic variables in the model, the random variables have to be eliminated. This can be achieved by taking advantage of the fact that a cardiac cycle is periodic. By comparing each measured data point for every acquired sample, with the correlating sample set a mean cardiac cycle can be obtained that will contain only the constant systemic noise.

The sample range of one cardiac cycle will have to be defined:

$$\text{Heart rate} = 72 \text{ [BPM]}$$

$$\text{Duration of one heart cycle} = f = \frac{72}{60} = 1,2 \text{ [Hz]}$$

$$\text{Samples pr second} = 1000$$

The sample range of one cardiac cycle:

$$\text{Samples pr cardiac cycle} = \frac{1000}{1,2} = 833,33$$

To ensure validity of the mean curve the number of cardiac cycles to be compared is estimated to 15 cardiac cycles. The calculation of the mean cycle will be performed in the signal processing program Labview.

In figure 90 it is shown how the amount of frequency noise has been reduced, which mean that the mean cardiac cycle is only registering constant systemic noise. It is now possible to investigate and analyze which frequencies are trending.

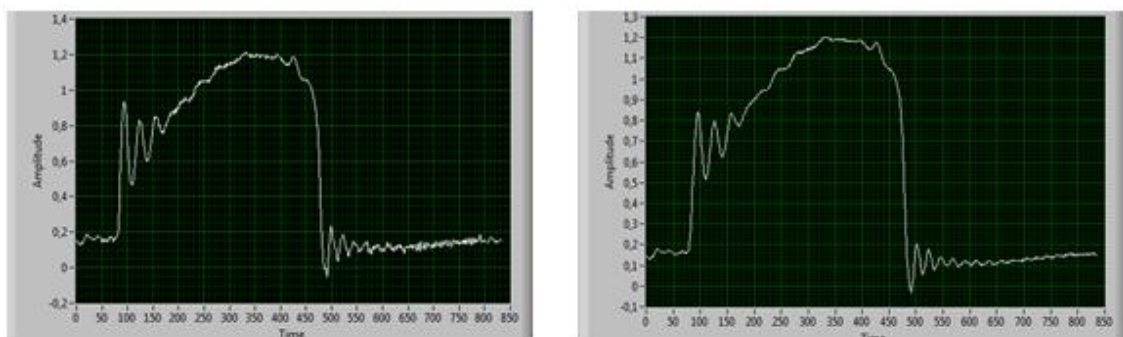


Figure 90 - Noise reducing in the cardiac cycle curve

²⁷ This section has been intire done bwith M7BACH14

19.2. Comparison of results - Analysis methods

The goal and aim of the project is to reduce the amount of recorded noise. In order to determine whether improvements have been made, based on the amount of noise present, it will be necessary to somehow quantify the entity. A method could be simply to calculate the area under cardiac cycle curve, and compare the size of the areas. However, that could create too many uncertainties since the measured pressure sometimes exceeds or subceeds the targeted pressure of 120 [mmHg] when recording. This method is therefore rejected. The character of the fluctuation and the frequency size do however appear to be unaffected by small pressure differences. The solution may therefore be to isolate the fluctuations and calculate the area bounded by peaks and valleys that defines the noise. Figure 91 shows the noise in start systole and start diastole as being the area of interest.

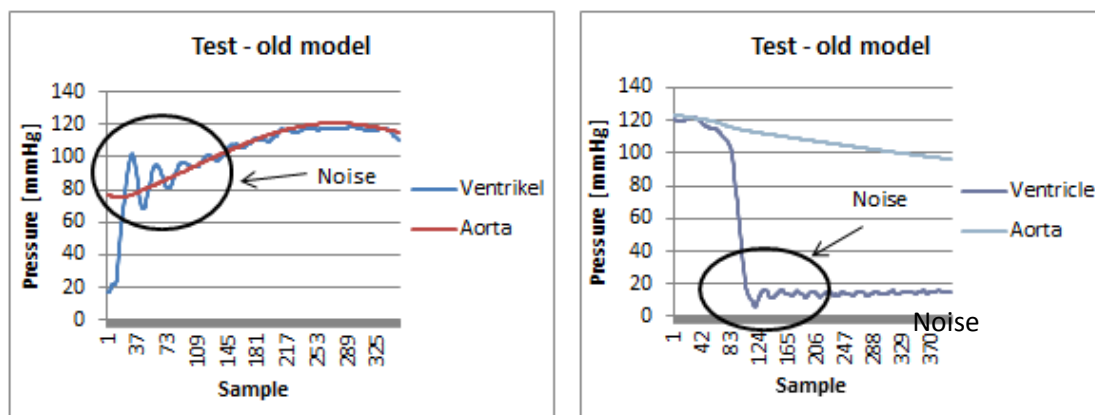


Figure 91 - Noise in the cardiac output to be eliminated

Labview can be programmed to detect peaks and valleys. The amplitude line is the trend line between the amplitudes. To evaluate the amplitude line trend lines are created for the peaks and the valleys. The amplitude line is the difference between these two and defines the zero line see figure X. The area can now be calculated by integrating for the absolute values of the curve.

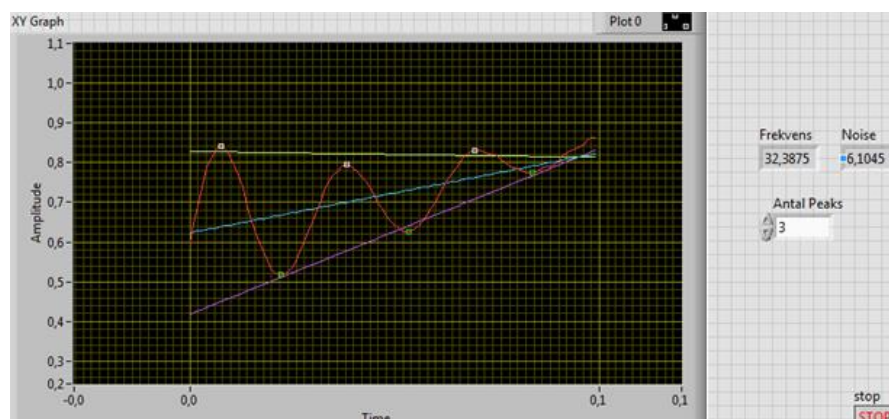


Figure 92 - Isolated fluctuations in start systole

Method for isolating the area of interest

For each dataset the area can be calculated simply by evaluating the number of peaks that represent the area of interest. By integrating pressure with respect to time, the unit of the noise is [Pa*s] which is also the unit for absolute/dynamic viscosity.

When deciding the number of peaks to be included for calculation of the area beneath the curve should include as many peaks as possible as long as the period remains constant, the rest of the curve can be considered to be random and should not be included. In figure 93, the circled area represents the range of the calculation. The calculated frequency is grossly misrepresented; therefore another method is used to calculate frequency.

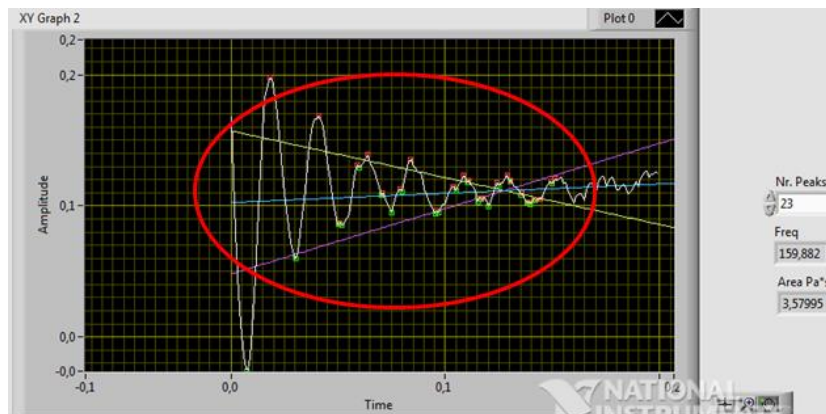


Figure 93 - Fluctuations during start diatole isolated with Labview

Method for isolating frequency of interest

The number of peaks included in the calculations will have to be evaluated manually for each curve, to make sure the calculations are comparable. The frequency is calculated by measuring the distance between the peaks and valleys. Peaks are represented with red points and valleys with green points. In figure 94 it is seen that the point do not mark the distance between what can be considered to be a period. By reducing the number of peaks, the program will choose only the extreme peaks and valleys and thereby obtaining a correct frequency value.

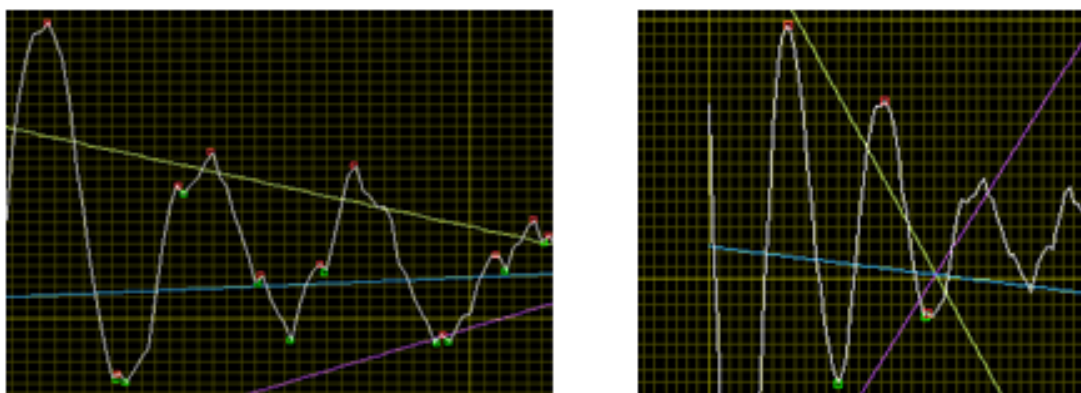


Figure 94 - Noise curve 23 peaks (left) and 3 peaks (right)

The program does not discriminate between peaks in the constant systemic noise and random noise, therefore this also needs to be evaluated manually. In figure 95 the program has chosen accurate peaks for the systemic noise, but it has also chosen peaks in the area of random fluctuations. In this case it would be necessary to reduce the number of peaks from 5 to 3.

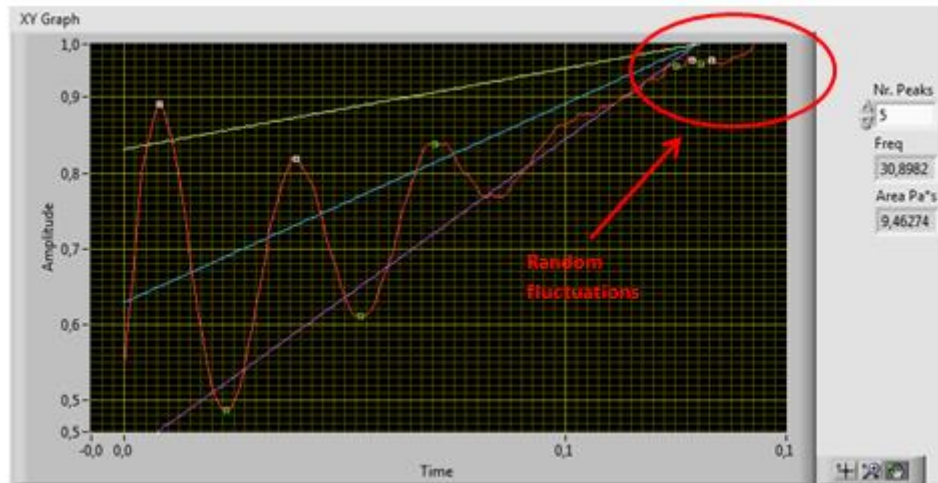


Figure 95 - Fluctuations in start systole isolated in labview

Spectral analysis

²⁸ Fourier transform is a mathematical tool for transforming signals in the time domain to the spectral domain.

The cardiac cycle is the sum of sinus of different frequencies. If our curve only consisted of a single sinus the spectral image of it would be a straight line in the frequency domain.

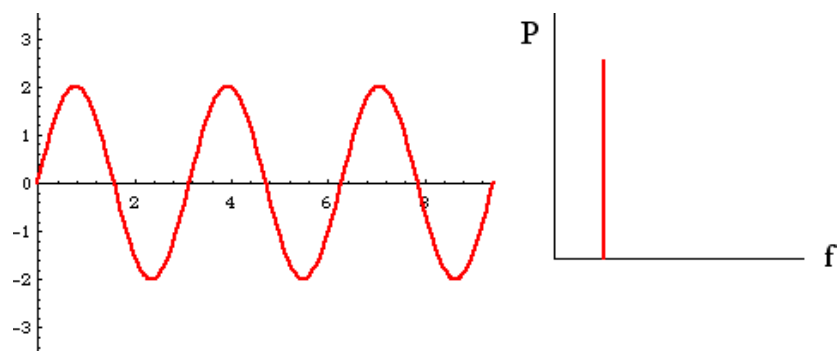


Figure 96 - Spectral analysis for one frequency

²⁸ <http://classes.yale.edu/fractals/CA/OneOverF/PowerSpectrum/PowerSpectrum.html>

The cardiac cycle is the sum of sinus with different frequencies, if the cycle consisted of the green and red line the blue curve in figure 97 would be the cardiac cycle. The spectral analysis would then show that the red has a lower frequency and higher amplitude, than the green sinus.

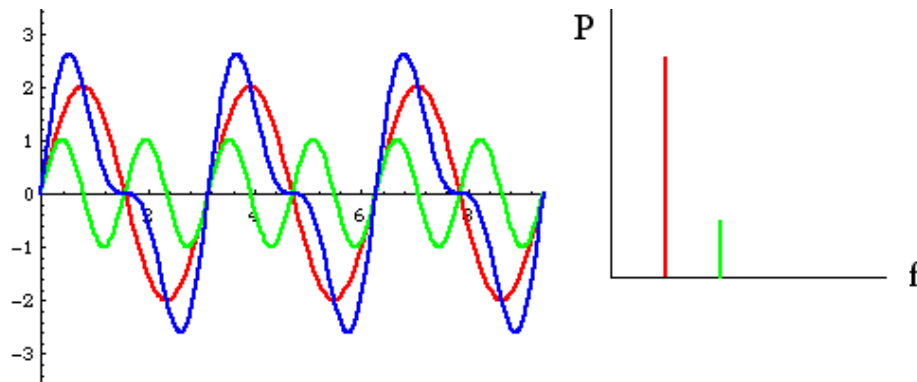


Figure 97 - Spectral analysis for more than one frequency

The components of sinus displayed in figure 98 (left), shows that the cardiac cycle consists of every single frequency of sine from 0-500 [Hz], with various amplitudes. However many of the frequencies are due to noise, by considering the spectral analysis of the mean cardiac cycle, some of the frequencies are eliminated figure 98 (right). There are peaks around 200,300 and 400 [Hz] which suggests that there is something in the in vitro system that vibrates with these frequencies. These frequencies are very high and will affect the shape of the cardiac cycle. The cardiac cycle from old and the new model will be compared to determine if these signals have been eliminated, and to make sure a different set of frequencies does not occur in the new model. However the sources of the frequencies are unidentified and no active step has been made in the development of the new model, and should therefore be investigated further. Some suggested methods for locating source of high frequencies are Solid works frequency study or by the usage of accelerometers.

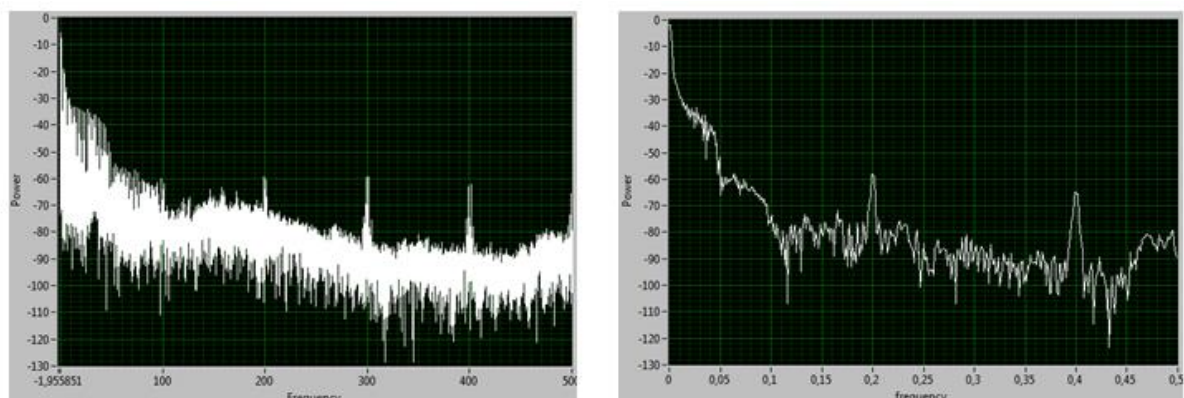


Figure 98 - Spectral domain – cardiac cycle

As the noise seen has a similar shape compared to a step response, a method for recreating the step response has been proposed. The idea is shown in the figure 99. The way to recreate it is by closing a chamber with a glove (or a similar object) and add compliance. Once it is fulfilled, break it with a needle or a lighter in order to change the state as fast as possible obtaining the graph seen below.

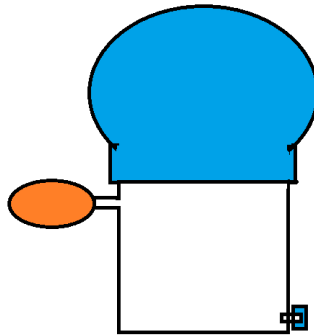


Figure 99 - System to recreate the step response

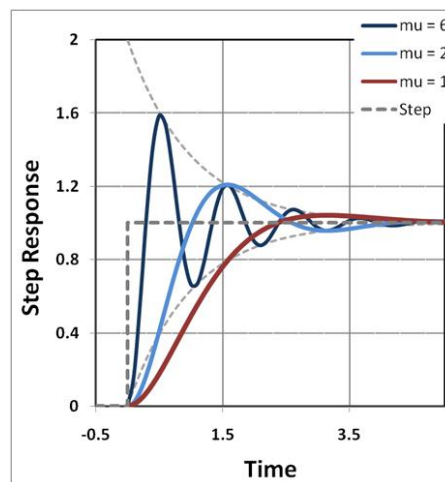


Figure 100 - Step response

19.3. Test description and results

Equipment used

The equipment used for the test is named following:

- New In Vitro model (Atrium, compliance chamber and ventricle chamber)
- Silicone bag with 3 layers of silicone (if required)
- Pump
- Millar Catheters (pressure sensors)
- Flow meter
- Peripheral resistance
- TAVI valve no. 3
- Terminal for adding compressed air to the compliance chamber.
- Equipment for collecting the data

Data set for the different tests carried out

Discussion of the waveforms

This analysis has been done with the new ventricle chamber without bag and the square compliance chamber.

In this test an analysis of all the waveforms has been done in order to determine if waveforms have a significant influence on the way the results are being evaluated. It has been seen that the results will vary depending on the chosen waveform but nothing conclusive, see figure 101. For this reason all the tests will be performed with all the waveforms.

Waveform B seems to behave better for diastole noise while waveform D behaves better for systole. However, irregular tendency with cardiac output increase has been seen for these waveforms as well. Hence, further tests will be performed with all the waveforms to conclude if the tendency is normal or is a matter of unsuitable measurements.

The frequency is not dependant on the waveform as similar values have been achieved for the four waveforms. See figure 102.

Noise	New model – VC without bag and square CC			
Systole noise	A	B	C	D
CO 1-2	5.27305	7.32741	3.2661	6.9317
CO 2-3	6.16017	5.80488	4.5494	4.13645
CO 3-4	8.28195	10.9551	6.9317	4.935
CO 4-5	11.0607	10.5316	6.9317	4.59364
Average	7.6939675	8.6547475	5.419725	5.1491975
Diastole noise	A	B	C	D
CO 1-2	2.16871	1.60103	2.55628	5.16281
CO 2-3	2.52883	1.76866	2.84054	5.24442
CO 3-4	2.88751	3.21079	5.16281	5.6498
CO 4-5	4.84071	4.37133	5.16281	6.23477
Average	3.10644	2.7379525	3.93061	5.57295

Figure 101 - Systole and diastole noise. Waveforms A, B, C and D

Frequency	New model – VC without bag and square CC			
Systole frequency	A	B	C	D
CO 1-2	38.2627	36.4651	37.324	39.713
CO 2-3	39.7486	37.0199	38.2597	38.0869
CO 3-4	39.1001	36.7049	38.873	38.6228
CO 4-5	38.2527	38.5784	38.873	38.5825
Average	38.841025	37.192075	38.332425	38.7513
Diastole frequency	A	B	C	D
CO 1-2	40.8022	44.8462	40.9105	41.999
CO 2-3	41.8146	40.6696	41.9404	42.166
CO 3-4	41.4954	41.2609	41.4841	43.1013
CO 4-5	42.8827	43.9037	41.8441	42.9482
Average	41.748725	42.6701	41.544775	42.553625

Figure 102 - Systole and diastole frequency. Waveforms A, B, C and D

The waveform from the following test with the bag was also analysed in order to determine if the tendency seen before remained.

This test was performed with ventricle chamber with the bag and squared compliance chamber. The results vary with the waveforms; again it is observed that waveform D behaves best for systole noise while waveform B is best for diastole. The normal tendency is for the noise to increase with the cardiac output but with some anomalies. These irregularities seem to reoccur for waveforms B and D, same behaviour as seen in the test without the bag. Again is seen that the frequency is fairly constant.

Noise	New model – VC with bag and square CC			
Systole noise	A	B	C	D
CO 1-2	9.50493	7.74308	7.54304	4.53959
CO 2-3	11.7904	9.41204	9.17174	3.83601
CO 3-4	12.8533	12.2057	9.09903	3.16448
CO 4-5	12.4849	9.78726	10.1701	6.08805
CO 5+	17.5863	15.9889	9.97306	8.28016
Average	12.843966	11.027396	9.191394	5.181658
Diastole noise	A	B	C	D
CO 1-2	3.99203	1.75161	3.71356	3.52167
CO 2-3	5.77231	2.66389	4.99715	5.11579
CO 3-4	4.75373	3.37348	4.77296	6.46826
CO 4-5	5.16877	3.66013	5.55667	7.33703
CO 5+	5.22591	4.71436	6.61562	8.15047
Average	4.98255	3.232694	5.131192	6.118644

Figure 103 - Systole and diastole noise. Waveforms A, B, C and D

Frequency	New model – VC with bag and square CC			
Systole frequency	A	B	C	D
CO 1-2	21.3583	27.0612	27.1455	33.6153
CO 2-3	21.6096	27.1298	27.5494	33.7924
CO 3-4	25.6599	26.6736	29.0966	33.2312
CO 4-5	26.1756	26.1099	29.9896	33.0847
CO 5+	33.9228	27.3679	31.5101	33.4117
Average	23.70085	26.743625	28.445275	33.4309
Diastole frequency	A	B	C	D
CO 1-2	29.5407	35.236	36.3596	42.1129
CO 2-3	29.9689	37.1337	36.6945	43.3881
CO 3-4	34.9756	35.9982	39.093	42.9314
CO 4-5	35.5012	36.768	38.9684	43.2502
CO 5+	43.7516	37.1853	41.7736	44.8123
Average	32.4966	36.283975	37.778875	42.92065

Figure 104 - Systole and diastole frequency. Waveforms A, B, C and D

To conclude what can be said for the waveform analysis is that the waveform D is better for systole and waveform B is better for diastole.

Further tests with the trapezoidal chamber with and without bag indicated that the waveform analysis was consistent with what was previously observed.

Comparison between the old model and the new model (the ventricle chamber is without bag and the two available new compliance chambers)

This test was performed to determine if any of the new chambers behaves better in the new model without bag in comparison to the old model the following was found:

- The model with trapezoidal chamber has a smaller area of noise than the model with square chamber in systole and diastole.
- The old model has less area of noise compared to the new model regardless of the compliance chamber in diastole.
- Frequency for the new model was generally higher compared to the old in systole
- In diastole the model with square chamber has the same frequencies as the old.
- Because of the irregular frequencies recorded for the trapezoidal chamber in diastole the data is considered invalid.

Noise	Old model	New model – without bag	
Systole noise	Old chamber	Trapezoidal chamber	Square chamber
CO 1-2	2.53	3.28482	6.9317
CO 2-3	5.35	4.56418	4.13645
CO 3-4	6.033524	6.21045	4.935
CO 4-5	8.33947	4.82717	4.59364
Average	5.5632485	4.721655	5.1491975
Diastole noise	Old chamber	Trapezoidal chamber	Square chamber
CO 1-2	1.688	3.04032	5.16281
CO 2-3	3.4758	4.01024	5.24442
CO 3-4	2.56	4.09329	5.6498
CO 4-5	3.56965	4.9726	6.23477
Average	2.8233625	4.0291125	5.57295

Figure 105 - Systole and diastole noise comparison old model and new model without bag

Frequency	Old model	New model – without bag	
Systole frequency	Old chamber	Trapezoidal chamber	Square chamber
CO 1-2	32.927	44.1247	39.713
CO 2-3	32.2672	40.3695	38.0869
CO 3-4	33.6683	38.2834	38.6228
CO 4-5	32.0948	38.7858	38.5825
Average	32.739325	40.39085	38.7513
Diastole frequency	Old chamber	Trapezoidal chamber	Square chamber
CO 1-2	44.8663	47.461	41.999
CO 2-3	45.4804	121.727	42.166
CO 3-4	45.6438	43.9603	43.1013
CO 4-5	44.2663	45.386	42.9482
Average	45.0642	64.633575	42.553625

Figure 106 - Systole and diastole frequency comparison old model and new model without bag

Comparison between the old model and the new model (the ventricle chamber is with bag and the two available new compliance chambers).

This test was performed to determine if the model with bag has an effect in the noise.

Comparing it with the old model the following was found:

- The square chamber has less systole noise than the trapezoidal new chamber and the old model.
- The old chamber has less diastole noise than the new model
- The trapezoidal chamber has a lower frequency in comparison with the other models for systole and diastole.

Noise	Old model	New model – with bag	
Systole noise	Old chamber	Trapezoidal chamber	Square chamber
CO 1-2	2.53	5.79515	4.53959
CO 2-3	5.35	7.01218	3.83601
CO 3-4	6.033524	7.37454	3.16448
CO 4-5	8.33947	5.23202	6.08805
Average	5.5632485	6.3534725	4.4070325
Diastole noise	Old chamber	Trapezoidal chamber	Square chamber
CO 1-2	1.688	3.49664	3.52167
CO 2-3	3.4758	4.75574	5.11579
CO 3-4	2.56	6.20574	6.46826
CO 4-5	3.56965	3.05462	7.33703
Average	2.8233625	4.378185	5.6106875

Figure 107 - Systole and diastole noise comparison old model and new model with bag

Frequency	Old model	New model – with bag	
Systole frequency	Old chamber	Trapezoidal chamber	Square chamber
CO 1-2	32.927	23.0417	33.6153
CO 2-3	32.2672	26.8021	33.7924
CO 3-4	33.6683	27.0973	33.2312
CO 4-5	32.0948	26.8662	33.0847
Average	32.739325	25.951825	33.4309
Diastole frequency	Old chamber	Trapezoidal chamber	Square chamber
CO 1-2	44.8663	35.5702	42.1129
CO 2-3	45.4804	35.5116	43.3881
CO 3-4	45.6438	35.7547	42.9314
CO 4-5	44.2663	36.4439	43.2502
Average	45.0642	35.8201	42.92065

Figure 108 - Systole and diastole frequency comparison old model and new model without bag

The square chamber has a bigger area of noise in systole and less area in diastole without the bag.

Noise	Square chamber	
Systole noise	With bag	Without bag
CO 1-2	4.53959	6.9317
CO 2-3	3.83601	4.13645
CO 3-4	3.16448	4.935
CO 4-5	6.08805	4.59364
Average	4.4070325	5.1491975
Diastole noise	With bag	Without bag
CO 1-2	3.52167	5.16281
CO 2-3	5.11579	5.24442
CO 3-4	6.46826	5.6498
CO 4-5	7.33703	6.23477
Average	5.6106875	5.57295

Figure 109 - Noise in the squared chamber with and without the bag

With the bag lower frequencies have been obtained in systole.

Frequency	Square chamber	
Systole frequency	With bag	Without bag
CO 1-2	33.6153	39.713
CO 2-3	33.7924	38.0869
CO 3-4	33.2312	38.6228
CO 4-5	33.0847	38.5825
Average	33.4309	38.7513
Diastole frequency	With bag	Without bag
CO 1-2	42.1129	41.999
CO 2-3	43.3881	42.166
CO 3-4	42.9314	43.1013
CO 4-5	43.2502	42.9482
Average	42.92065	42.553625

Figure 110 - Frequency in the squared chamber with and without the bag

With the trapezoidal chamber the area of noise was smaller without the bag.

Noise	Trapezoidal chamber	
Systole noise	With bag	Without bag
CO 1-2	5.79515	3.28482
CO 2-3	7.01218	4.56418
CO 3-4	7.37454	6.21045
CO 4-5	5.23202	4.82717
Average	6.3534725	4.721655
Diastole noise	With bag	Without bag
CO 1-2	3.49664	3.04032
CO 2-3	4.75574	4.01024
CO 3-4	6.20574	4.09329
CO 4-5	3.05462	4.9726
Average	4.378185	4.0291125

Figure 111 - Noise in the trapezoidal chamber with and without the bag

Lower frequencies were obtained with the bag; however some irregular frequencies were recorded in diastole so the data will be considered invalid.

Frequency	Trapezoidal chamber	
Systole frequency	With bag	Without bag
CO 1-2	23.0417	44.1247
CO 2-3	26.8021	40.3695
CO 3-4	27.0973	38.2834
CO 4-5	26.8662	38.7858
Average	25.951825	40.39085
Diastole frequency	With bag	Without bag
CO 1-2	35.5702	47.461
CO 2-3	35.5116	121.727
CO 3-4	35.7547	43.9603
CO 4-5	36.4439	45.386
Average	35.8201	64.633575

Figure 112 - Frequency in the trapezoidal chamber with and without the bag

In order to interpret the results the graphs have to be considered.

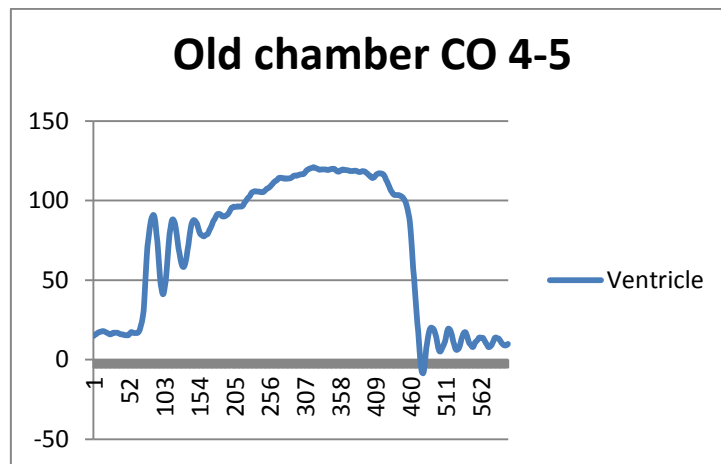


Figure 113 - Old model CO 4-5 [L/min]

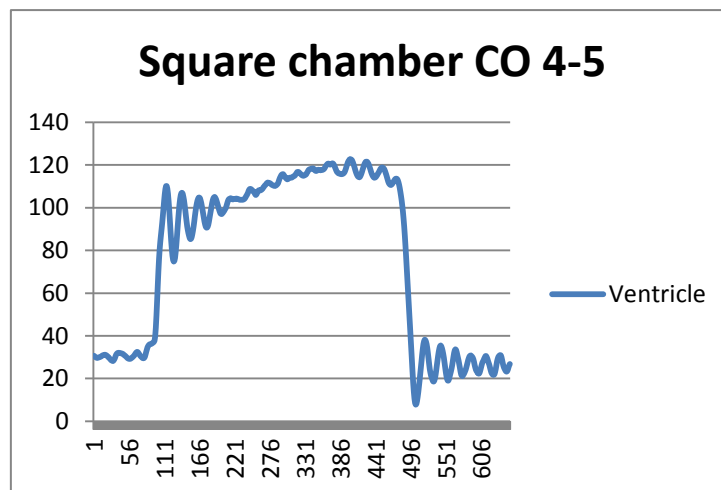


Figure 114 - New model CO 4-5 [L/min] square compliance chamber and ventricle chamber without bag

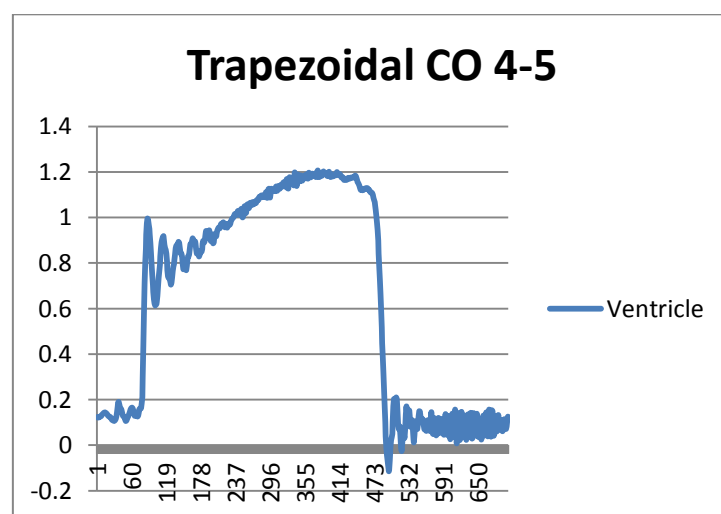


Figure 115 - New model CO 4-5 [L/min] trapezoidal compliance chamber and ventricle chamber without bag

Addition of compliance in the ventricle chamber

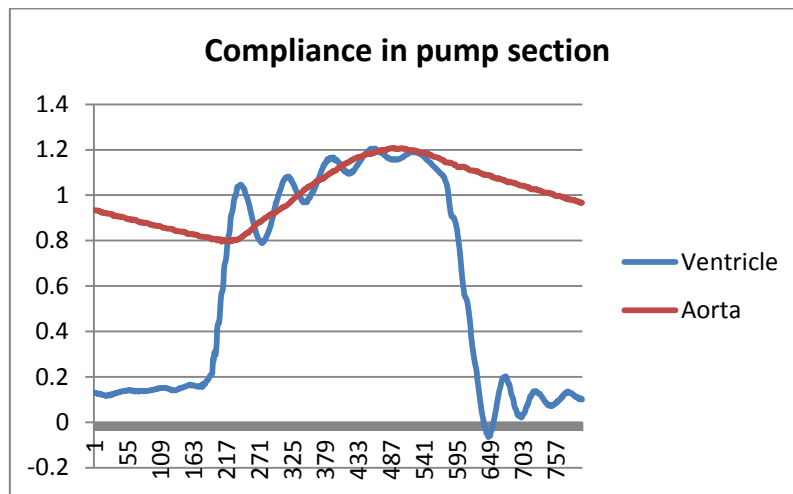


Figure 116 - Some compliance added in the pump section of the ventricle chamber

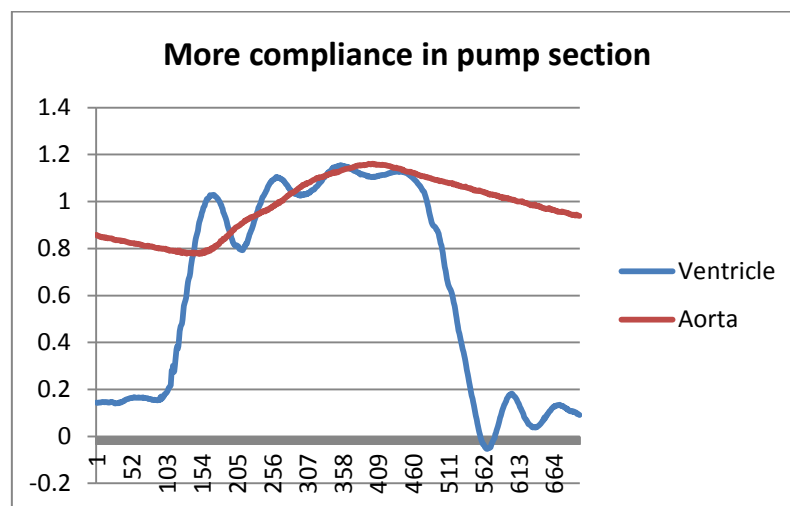


Figure 117 – More compliance added in the pump section of the ventricle chamber

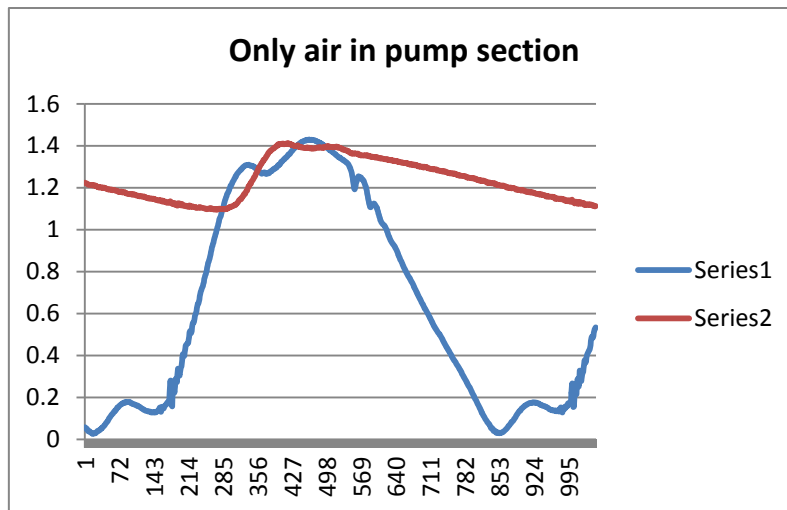


Figure 118 - All the pump section of the ventricle chamber fulfilled with air

By comparing the three curves is seen that the area of noise is reduced as the amount of air is increased. It is also noted that the addition of compliance moves the noise from start systole so it extends into mid to end systole. Too much added air cause some significant physiology loses as can be seen in figure 118.

Comparison new designed bag and old bag

Noise	New bag		Old bag	
Systole noise	A	C	A	C
CO 1-2	9.50493	7.54304	10.1349	7.93568
CO 2-3	11.7904	9.17174	11.1203	7.7537
CO 3-4	12.8533	9.09903	13.5775	9.30823
CO 4-5	12.4849	10.1701	13.613	10.4891
Average	11.65838	8.995978	12.11143	8.871678
Diastole noise	A	C	A	C
CO 1-2	3.99203	3.71356	4.31004	3.68277
CO 2-3	5.77231	4.99715	5.70192	4.91795
CO 3-4	4.75373	4.77296	6.48882	5.36877
CO 4-5	5.16877	5.55667	6.92312	6.96397
Average	4.92171	4.760085	5.855975	5.233365

Figure 119 - Systole and diastole noise from test of old and new bag

Frequency	New bag		Old bag	
Systole frequency	A	C	A	C
CO 1-2	21.3583	27.1455	26.1115	26.1586
CO 2-3	21.6096	27.5494	26.4352	26.4448
CO 3-4	25.6599	29.0966	26.1963	26.1397
CO 4-5	26.1756	29.9896	26.3719	26.1779
Average	23.70085	28.44528	26.27873	26.23025
Diastole frequency	A	C	A	C
CO 1-2	29.5407	36.3596	34.543	34.2615
CO 2-3	29.9689	36.6945	34.771	33.8944
CO 3-4	34.9756	39.093	34.9583	34.5833
CO 4-5	35.5012	38.9684	35.6234	34.9018
Average	32.4966	37.77888	34.97393	34.41025

Figure 120 - Systole and diastole frequency from test of old and new bag

High cardiac output possible to achieved

The aim of developing the model has been to achieve physiological pressure readings during high cardiac outputs. Even though the new model obtained a pressure curve with a lot of noise, especially in diastole, it had more physiological properties than what was obtained with the old model as can be seen in the graphs.

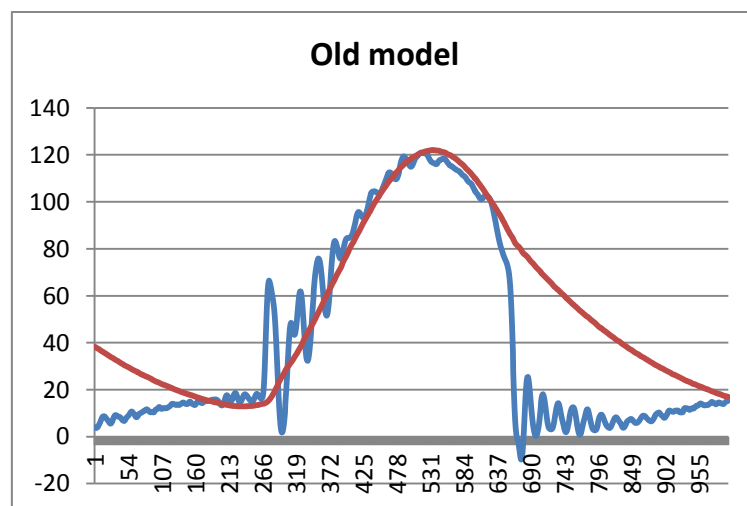


Figure 121 - Old model running with high CO

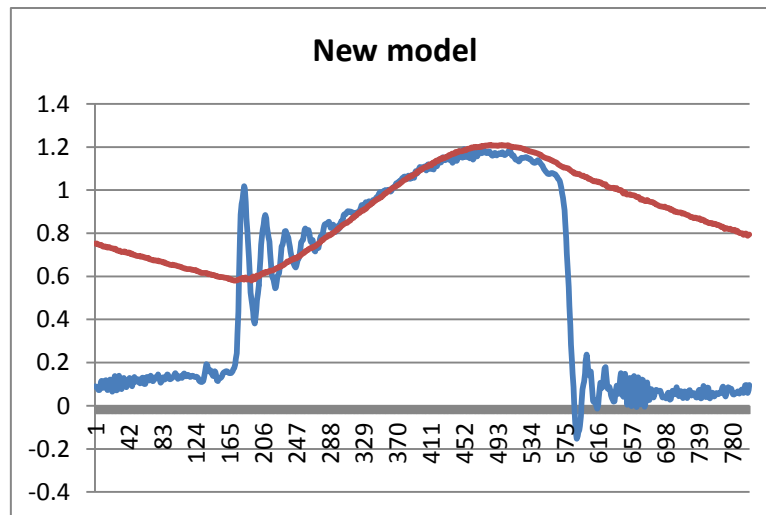


Figure 122 - New model running with high CO

20- Project management planning's tools. FMEA and Fishbone analysis

²⁹ Quality planning is part of the project quality management. In this stage is where the relevant standards are going to be clarified and the decision of how are going to be fulfilled will be made. In order to prepare a good quality management plan, some tools have to be carried on, for instance: brainstorming, FMEA or Fishbone analysis.

In this section is going to be described the two tools that have been developed at the begging of the project in order to clarify, organize and decide which problems should be resolved and how.

20.1. FMEA

FMEA explanation

³⁰ FMEA is the acronym for Failure Mode and Effect Analysis. It is a method used to analyse potential failures in a system determined by gravity or effect of failures. With this method all the possible stages of failure are analysed. Applying the equations (explained after) is possible to achieve which of them has the biggest risk and therefore be able to focus on it.

FMEA worksheet

Following are presented the different parts in the model which are going to be taken into account in the analysis. There are also listed and rated all the potential failures. The result of that rating will show in which component are the highest risks and how it is possible to solve the problem.

- Overall model
 - o Connections between parts and chambers
 - o Drainage
- Compliance chamber
 - o Maintain pressure
 - o ARAMIS
- Ventricular chamber
 - o Silicone bag
 - o Connections module between Mitral and Aortic valve
- Atrium chamber
 - o Pressure
 - o Dimensions/Volume
- Aortic root
 - o Measurements
 - o Flow (Smaller root, silicone root)
 - o Pressure
 - o Ultrasonic transducer
 - o Longer root

²⁹ Kousholt, Bjarne (2012). *Project Management. Theory and Practice*, 2. ed. Nyt Teknisk Forlag

³⁰ This analysis is done towards the M7BACH14 group

- Tests
 - Equipment failure
 - Pump failure
 - Lack of knowledge
 - Problems procedure
 - Problems with the model
 - Verifying the model

Risk level calculation

The rating of the components will be made by using the following rating schedules. Therefore, it is possible to find which of the components has the highest risks. The risk level is found by multiplying the probability (P) with the severity (S).

- *Risk level: (P x S) and (D)*: It is a combination of the End Effect, Probability and Severity.

Probability/Severity	I	II	III	IV	V	VI
A	Low	Low	Low	Low	Moderate	High
B	Low	Low	Low	Moderate	High	Unacceptable
C	Low	Low	Moderate	Moderate	High	Unacceptable
D	Low	Moderate	Moderate	High	Unacceptable	Unacceptable
E	Moderate	Moderate	High	Unacceptable	Unacceptable	Unacceptable

Table 15 - Risk level (P x S) and (D)

- *Probability (P)*: It is necessary to look at the cause of a failure mode and the likelihood of occurrence.

Rating	Meaning
1	Extremely Unlikely (Virtually impossible or No known occurrences on similar products or processes, with many running hours.
2	Remote (relatively few failures)
3	Occasional (occasional failures)
4	Reasonably Possible (repeated failures)
5	Frequent (failure is almost inevitable)

Table 16 - Probability (P)

- *Severity (S)*: Determine the severity for the worst case scenario adverse the effect.

Rating	Meaning
I	No relevant effect on reliability or safety
II	Very minor, no damage, no injuries, only results in a maintenance action (only noticed by discriminating customers)
III	Minor, low damage, light injuries
IV	Moderate, moderate damage, injuries possible.
V	Critical
VI	Catastrophe

Table 17 - Severity (S)

- *Detection (D)*: Determine the likelihood for detect a failure mode.

Rating	Meaning
1	Certain – fault will be caught on test
2	Almost certain
3	High
4	Moderate
5	Low
6	Fault is undetected by Operators or Maintainers

Table 18 - Detection (D)

Conclusions

Watching at the FMEA table is possible to know that the construction failures are the biggest predictable problems. The problems with higher risk level are the ones related with the connections' section, especially problems due to leakage and rust in the connections in the design and assembly phases. There is also a big issue related with the silicone bag design in the ventricle chamber.

Therefore, construction failures can be mitigated by doing exhaustive work in the design phase; however there is a deadline for finishing the models. So it will be prioritized finishing the model over having the best possible one.

FMEA table

Below is the table of the FMEA model.

<u>Item</u>	<u>Potential failure mode</u>	<u>Potential causes</u>
Overall model		
- Connections between Parts and chambers	Leakage Leakage Leakage Difficult to assemble Rust in metal parts Fracture Wrong fitting Unable to empty chambers fully	Bad fitting Bad fitting Bad fitting Complicated design Salt water/moist Overload High strain in a small area Height/dimensions Placement of drainage
¹ - Drainage		
Compliance chamber		
- Maintain pressure - ARAMIS	Unable to maintain correct pressure Unable to use ARAMIS in 3D	Cracks - Transparency - Dimensions of the plate
Ventricular chamber		
- Silicone bag	Bag tears Bag tears Mount to the chamber Design process taking too long	Stresses, rifts, nonuniform thickness Stresses, rifts, nonuniform thickness Complicated geometry Complicated geometry
¹ - Connection module between Mitral and Aortic valve		
Atrium chamber		
¹ - Pressure - Dimensions / volume	The Water height Increased surface area doesn't have any effect	faulty diamensions Too low a volume in the chamber
Aortic Root		
- Measurements - Flow - Smaller root - Silicone root	Difficult to fix Leakage	Another dimension than the old roots. Unable to seal or fit it right.
- Ultrasonic transducer - Longer root - Longer root	Leakage Large pressure drop	Another dimension than the old roots. Bigger pressure because of the long root
Tests		
¹ - Equipment failure - Flow probe - Pump failure - Miller catheter - Verifying the model - Verifying the model	Inaccurate flow measurements No flow Fracture Leakage Inaccurate pressure measurements No consistency in the measurements No consistency in the measurements	Bad fitting Non functioning pumpe High strain in a small area Bad fitting Wrong possision, Recordings based on different settings in the pump Leakage of air in compliance chamber
- Unable to get a finished model	No finished drawings Delays in the shop Unforeseen complications	Bad planning Bad planning (FMEA)

<u>Project phase</u>	<u>Local effect of failure</u>	<u>Next higher level effect</u>	<u>System level end effect</u>
Design phase			
Assembly phase			
Test phase	Difficult to assemble	Invalid pressure measurements	Difficult to validate the results the model provides
Design phase		Invalid pressure measurements	Difficult to validate the results the model provides
Operating phase	Model will look unappealing	Time consuming	Wasted time on assembly
Assembly phase	Cracks	Difficult to assemble and disassemble	Will affect future projects working with the model
Operating phase	Cracks	Invalid pressure measurements	Difficult to validate the results the model provides
Design phase	Unable to connect to chambers	Can't run the tests	Difficult to validate the results the model provides
Design phase	Water remains in the chambers	Algae formation in chambers	Wasted time to redesign chamber
Operating / Testing phase			Extended maintenance
Design phase	Leakage of air / water	Bogus pressure readings, dawg	Difficult to validate the results the model provides
Design phase		Unable to obtain 3D strain	Unable to use aramis at all
Design phase		Unable to obtain 3D strain	Limited to 2D strain
Design phase			
Testing phase	Destroyed bag	ruined testing run	Waste of time due to redesigning the bag
Design phase	Destroyed bag	ruined testing run	Waste of time due to redesigning the bag
Design phase	Unable to mount to chamber	ruined testing run	Waste of time due to redesigning the bag
Design phase	Delayed manufacturing	delayed testing	Delayed conclusion
Design phase			
Design phase	constant open mitral valv	Ventricular chamber unable to build pressure	Non functional model
Design phase	vortex in the atrium	Air in the system	Fluxations and pressure graphs
Design phase			
Design phase			
Design phase	Leakage	Difficult in getting both new and old root to fit on model	Difficult to validate the results the model provides
Design phase	Leakage of water	Invalid test results	Difficult to validate the results the model provides
Design phase			
Test phase	Leakage	Difficult in getting both new and old root to fit on model	Difficult to validate the results the model provides
Test phase	Inaccurate pressure measurements	Invalid test results	Difficult to validate the results the model provides
Operating phase			
Testing phase	Invalid results		
Operating phase		No results	Non functional model
Testing phase	Cracks	Invalid test results	Difficult to validate the results the model provides
Testing phase	Non functioning sealing	Invalid test results	Difficult to validate the results the model provides
Testing phase	Inaccurate pressure measurements	Invalid test results	Difficult to validate the results the model provides
Test phase	Different stroke on the pump	Invalid results	Difficult to validate the results the model provides
Test phase	Difficult to maintain pressures for 22 [s]	Invalid results	Difficult to validate the results the model provides
Design phase			
Project management	No results from new model	Not able to compare new and old model	Unable to verify the requirements
Project management	No results from new model	Not able to compare new and old model	Unable to verify the requirements
Project management	No results from new model	Not able to compare new and old model	Unable to verify the requirements

Probability estimate	Severity	Detection	Risk level P's	Actions for further (plan b)	Mitigation / Requirements (Plan A)
5	2	2	12	Redesign the fitting	Evaluate in 3D model
4	5	1	21	Patch the leakage, brute force	Make sure that the 2D drawings to the shop is accurate
4	5	1	21	Patch the leakage, brute force	Make snug fittings
5	1	1	6	Ignore the error	Think assembly in to the design
5	3	5	20	Change metal parts frequently	Maintain the model, keep connections from liquid
4	4	1	17	Patch the leakage	Design sturdy, thicker plates in affected areas
4	4	1	17	Patch the leakage	Avoid using screws in acrylic, or use Helicoils to distribute the load
2	3	1	7	Redesign the chamber	Thoroughly measure the connection specs.
3	3	1	10	Shake that thing, clean chambers	Place the drain in the bottom with inclination.
3	4	1	13	Manually regulate pressure, patching the model	Avoid screw connections in chamber
1	5	1	6	Drill holes, use xray vision	Use transparent material for the model
2	4	2	10	Obtain 2D strains, make new chamber	make muy grande surface area of the compliance chamber
3	5	5	20	Redesign bag	Assuming that Vivitro model is solid
3	5	1	16	Redesign bag	Testing with diffrent thickness
2	4	1	9		
3	4	5	17	Simplify the geometry of the model	Communication following the requirements
1	6	1	7	Redesign the atrium chamber	Make sure calculations are in order
4	3	6	18	Investigate the effect of the size of the chamber	Have as big as atrium as possible
3	5	1	16	Patch the leakage	Try another way for fitting.
3	4	1	13	Patch the leakage	Make a new fitting. maybe try another way.
3	5	1	16	Patch the leakage	Try another way for fitting.
4	3	3	15		
4	4	3	0		
4	4	3	19		
2	6	1	13	Clean pump, try again	New pump.
3	4	2	14	Patch leakage	Design sturdy, thicker plates in affected areas
4	4	1	17	Replace the o-ring	Redesign the fitting
3	5	3	18	Make another kalibration	Replacing the catheters
2	5	4	14		
4	6	1	25	Patch the leakage	Try another way for fitting.
4	2	1	9		
4	6	2	26		
4	6	1	25		

20.2. Ishikawa diagram or Fishbone analysis

Diagram explanation

The Ishikawa diagram is also known as the fishbone analysis and it is also another planning tool. This diagram resembles the skeleton of a fish, in its head is written the problem that a solution is required for and on its bone is written the causes of it. Normally this diagram is also connected with brainstorming. The problem used to solve by Fishbone analysis was the entire design of the new in-vitro model taking into account all the requirements given and the possible problems associated.

Diagram

³¹ Below is represented the fishbone analysis done.

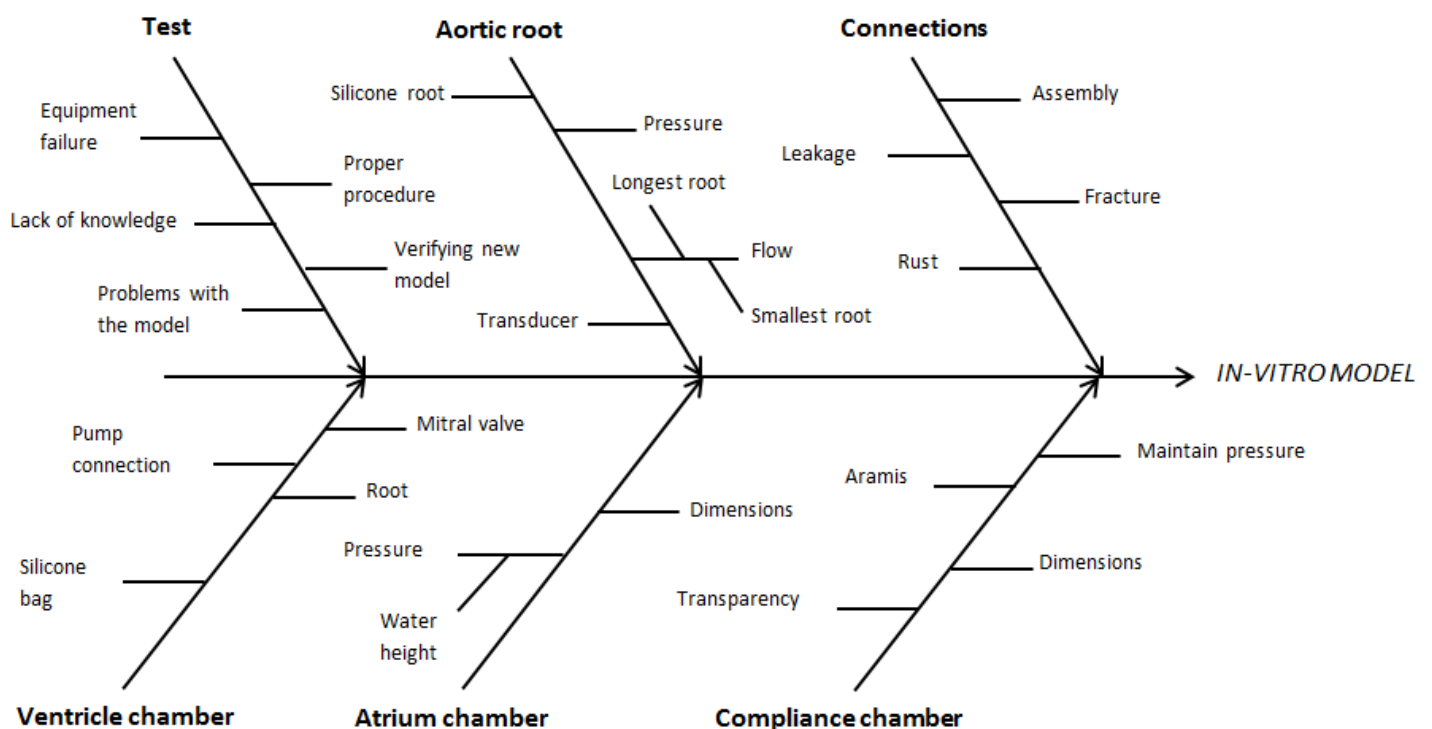


Figure 123 - Fishbone analysis

³¹ This analysis is done towards the M7BACH14 group

21- List of figures, tables and equations

Figures

Figure 1 - Isometric view – square compliance chamber (A.O.P.)	13
Figure 2 - Left and right view of the square compliance chamber (A.O.P.)	14
Figure 3 - Front view of the square compliance chamber (A.O.P.)	14
Figure 4 - Top view of the square compliance chamber (A.O.P.)	15
Figure 5 - Initial square compliance chamber (A.O.P.)	15
Figure 6 - O-ring connection (left) and silicone ring connection (right) (A.O.P.)	16
Figure 7 - Almost final square compliance chamber design – without corner cut (A.O.P.)	16
Figure 8 - Isometric view – trapezoidal compliance chamber (A.O.P.)	17
Figure 9 - Left and right side of the trapezoidal compliance chamber (A.O.P.)	17
Figure 10 - Front view of the square compliance chamber (A.O.P.)	18
Figure 11 - Top view of the square compliance chamber (A.O.P.)	18
Figure 12 - Circular shaped fitting connection (A.O.P.)	19
Figure 13 - Rectangular shaped fitting connection (A.O.P.)	19
Figure 14 - O-ring connection and silicone ring connection (A.O.P.)	20
Figure 15 - Millar catheters' positions (A.O.P.)	20
Figure 16 - Aortic root assembly (A.O.P.)	20
Figure 17 - Fittings – rods changed in position (A.O.P.)	21
Figure 18 - Connector sinus of Valsalva and silicone tube – Hand drawing (A.O.P.)	21
Figure 19 - Connector sinus of Valsalva and silicone tube – Solid Works (A.O.P.)	21
Figure 20 - Previous design for the connector - Hand drawing (A.O.P.)	22
Figure 21 - Connector silicone tube and fitting – Hand drawing (A.O.P.)	22
Figure 22 - Connector silicone tube and fitting – Solid Works (A.O.P.)	22
Figure 23 - Aortic root assembly for flow calculations – front view (A.O.P.)	23
Figure 24 - Aortic root assembly for flow calculations (A.O.P.)	23
Figure 25 – Square compliance chamber assembly (A.O.P.)	24
Figure 26 - Parts of the square compliance chamber (A.O.P.)	24
Figure 27 - Trapezoidal compliance chamber assembly (A.O.P.)	25
Figure 28 - Parts of the trapezoidal compliance chamber (A.O.P.)	25
Figure 29 - Aortic root assembly (A.O.P.)	26
Figure 30 - Parts of the aortic root assembly (A.O.P.)	26
Figure 31 - Silicone ring (A.O.P.)	63
Figure 32 - Mould assembly for the silicone ring (A.O.P.)	63
Figure 33 - Female part (right) and male part (left) (A.O.P.)	63
Figure 34 - Torque wrench (A.O.P.)	64
Figure 35 - Bench Vice (A.O.P.)	64
Figure 36 - Specimens (A.O.P.)	64
Figure 37 - General assembly (A.O.P.)	65
Figure 38 - Simplified compliance chamber (A.O.P.)	68
Figure 39 - Graph of forces in the compliance chamber's back wall (A.O.P.)	70
Figure 40 - Glue connection of two plates with dimensions	71

Figure 41 - Shear stress distribution in a glue connection of two plates	71
Figure 42 - Pressure distribution in the compliance chamber (A.O.P.).....	72
Figure 43 - Top plate dimensions (A.O.P.).....	73
Figure 44 - Pressure distribution in the top plate (A.O.P.).....	73
Figure 45 - Side plate dimensions (A.O.P.).....	74
Figure 46 - Pressure distribution in the side plate (A.O.P.).....	74
Figure 47 - Side plate dimensions (A.O.P.).....	75
Figure 48 - Pressure distribution in the side plate (A.O.P.).....	76
Figure 49 - Forces in the screws/Old chamber (A.O.P.)	77
Figure 50 - Stresses in the screws/Old chamber (A.O.P.)	77
Figure 51 - Top plate dimensions (A.O.P.).....	78
Figure 52 - Pressure distribution in the top plate (A.O.P.).....	78
Figure 53 - Forces in the screws (A.O.P.).....	79
Figure 54 - Stresses in the screws (A.O.P.).....	79
Figure 55 - Pressure distribution and fixtures (A.O.P.)	80
Figure 56 - Stress/Top plate old model (A.O.P.).....	81
Figure 57 - Displacements/Top plate old model (A.O.P.).....	81
Figure 58 - Strain/Top plate old model (A.O.P.).....	81
Figure 59 - Pressure distribution and fixtures/Top plate old model (A.O.P.)	82
Figure 60 - Stress/Top plate old model (A.O.P.).....	82
Figure 61 - Displacements/Top plate old model (A.O.P.).....	82
Figure 62 - Strain/Top plate old model (A.O.P.).....	82
Figure 63 - Pressure distribution and fixtures/Side plate old model (A.O.P.).....	83
Figure 64 - Stress/Side plate old model (A.O.P.).....	84
Figure 65 - Displacements/Side plate old model (A.O.P.)	84
Figure 66 - Strain/Side plate old model (A.O.P.)	84
Figure 67 - Pressure distribution and fixtures/Top plate old model (A.O.P.)	85
Figure 68 - Stress/Front plate old model (A.O.P.)	86
Figure 69 - Displacements/Front plate old model (A.O.P.)	86
Figure 70 - Strain/Front plate old model (A.O.P.)	86
Figure 71 - Stress distribution in the holes of the old model's back plate	87
Figure 72 - Pressure distribution and fixtures/Top plate new model (A.O.P.).....	88
Figure 73 - Stress/Top plate new model (A.O.P.).....	88
Figure 74 - Displacements (A.O.P.).....	89
Figure 75 - Strain/Top plate new model (A.O.P.)	89
Figure 76 - Short aortic root relevant dimensions (A.O.P.).....	92
Figure 77 - Long aortic root relevant dimensions (A.O.P.).....	92
Figure 78 - Table result for the short aortic root with CO of 5 [L/min]	93
Figure 79 - Table result for the short aortic root with CO of 11 [L/min]	93
Figure 80 - Table result for the long aortic root with CO of 5 [L/min]	94
Figure 81 - Table result for the long aortic root with CO of 11 [L/min]	94
Figure 82 - Bend loss coefficient calculation graph	97
Figure 83 - Ventricle chamber with the two valves' connection (A.O.P.)	98
Figure 84 - Ventricle chamber bent one (A.O.P.).....	99

Figure 85 - Ventricle chamber bent two (A.O.P.)	99
Figure 86 - Chemical reaction of the silicone (A.O.P.).....	101
Figure 87 - Chemical reaction of the Styrene (A.O.P.)	102
Figure 88 - Different options for gluing materials.....	108
Figure 89 Explanation of the number in Figure 72.....	109
Figure 90 - Noise reducing in the cardiac cycle curve	110
Figure 91 - Noise in the cardiac output to be eliminated	111
Figure 92 - Isolated fluctuations in start systole	111
Figure 93 - Fluctuations during start diastole isolated with Labview	112
Figure 94 - Noise curve 23 peaks (left) and 3 peaks (right).....	112
Figure 95 - Fluctuations in start systole isolated in labview	113
Figure 96 - Spectral analysis for one frequency.....	113
Figure 97 - Spectral analysis for more than one frequency	114
Figure 98 - Spectral domain – cardiac cycle	114
Figure 99 - System to recreate the step response	115
Figure 100 - Step response.....	115
Figure 101 - Systole and diastole noise. Waveforms A, B, C and D.....	117
Figure 102 - Systole and diastole frequency. Waveforms A, B, C and D	117
Figure 103 - Systole and diastole noise. Waveforms A, B, C and D.....	118
Figure 104 - Systole and diastole frequency. Waveforms A, B, C and D	118
Figure 105 - Systole and diastole noise comparison old model and new model without bag .	119
Figure 106 - Systole and diastole frequency comparison old model and new model without bag	119
Figure 107 - Systole and diastole noise comparison old model and new model with bag	120
Figure 108 - Systole and diastole frequency comparison old model and new model without bag	120
Figure 109 - Noise in the squared chamber with and without the bag	121
Figure 110 - Frequency in the squared chamber with and without the bag	121
Figure 111 - Noise in the trapezoidal chamber with and without the bag	122
Figure 112 - Frequency in the trapezoidal chamber with and without the bag	122
Figure 113 - Old model CO 4-5 [L/min]	123
Figure 114 - New model CO 4-5 [L/min] square compliance chamber and ventricle chamber without bag	123
Figure 115 - New model CO 4-5 [L/min] trapezoidal compliance chamber and ventricle chamber without bag	123
Figure 116 - Some compliance added in the pump section of the ventricle chamber	124
Figure 117 – More compliance added in the pump section of the ventricle chamber	124
Figure 118 - All the pump section of the ventricle chamber fulfilled with air	125
Figure 119 - Systole and diastole noise from test of old and new bag	125
Figure 120 - Systole and diastole frequency from test of old and new bag	126
Figure 121 - Old model running with high CO.....	126
Figure 122 - New model running with high CO.....	127
Figure 123 - Fishbone analysis	134

Tables

Table 1 - List of parts in the square compliance chamber assembly (A.O.P.)	24
Table 2- List of parts in the trapezoidal compliance chamber assembly (A.O.P.).....	25
Table 3 List of parts in the aortic root assembly (A.O.P.).....	26
Table 4 - Forces calculation Graph in the compliance chamber's back wall because of air and water (A.O.P.).....	70
Table 5 - Simulation's results/Top plate old model (A.O.P.)	83
Table 6 - Simulation's results/Side plate old model (A.O.P.)	85
Table 7 Simulation's results/Front plate old model (A.O.P.).....	87
Table 8 Simulation's results/Top plate new model (A.O.P.)	89
Table 9 - Reynolds number in the aortic root (A.O.P.).....	90
Table 10 - Velocity in the aortic root (A.O.P.)	91
Table 11 - Summary of the pressure drops in the aortic root due to length (A.O.P.).....	95
Table 12 - Pressure drops due to cross section changes for CO = 5L/min (A.O.P.).....	95
Table 13 - Pressure drops due to cross section changes for CO = 11L/min (A.O.P.).....	96
Table 14 - Pressure drops due to bend in the ventricle chamber (A.O.P.)	99
Table 15 - Risk level (P x S) and (D)	129
Table 16 - Probability (P)	129
Table 17 - Severity (S).....	130
Table 18 - Detection (D)	130

Equations

Equation 1 - Force balance in 'y' direction.....	66
Equation 2 - Force balance in 'x' direction.....	66
Equation 3 - Force balance in 'z' direction	66
Equation 4 - Mechanical energy equation	67
Equation 5 - Derivate of the mechanical energy equation	67
Equation 6 - Bernoulli equation	67
Equation 7 - Bernoulli equation applied in this problem	68
Equation 8 - Solution to the Bernoulli equation applied in this problem (A.O.P.).....	68
Equation 9 - Pressure	69
Equation 10 – Bernoulli equation	69
Equation 11 - Volkersen's Equation	71
Equation 12 - Middle shear stress value	71
Equation 13 - Relation between force and pressure	72
Equation 14 - Bernoulli equation for Pressure drops.....	90
Equation 15 - Reynolds' number equation	90
Equation 16 - Continuity principle	91
Equation 17 - Flow.....	91
Equation 18 - Bernoulli equation (velocity)	95
Equation 19 - Bend loose equation	96
Equation 20 - Velocity calculation with a CO = 5 [L/min] in the tube (A.O.P.).....	97
Equation 21 - Reynolds number for the tube with a CO = 5 [L/min] (A.O.P.)	97

Equation 22 - Relation between the roughness and the diameter of the pipe with a CO = 5 [L/min] (A.O.P.)	97
Equation 23 - Friction factor for the tube with a CO = 5 [L/min] (A.O.P.).....	97
Equation 24 - Bend loss coefficient with a CO = 5 [L/min] (A.O.P.)	98
Equation 25 - Pressure drop calculation with a CO = 5 [L/min] due to bend (A.O.P.)	98
Equation 26 - Pressure drop calculation with a CO = 11 [L/min] due to bend (A.O.P.)	98
Equation 27 - Fluid passing through the new model calculations	100